2014

Binding and release studies of carboxylates

Christie Lynn Beck
Iowa State University

Binding and release studies of carboxylates

by

Christie Lynn Beck

A dissertation submitted to the graduate faculty

in partial fulfillment of the requirements for the degree of

DOCTOR OF PHILOSOPHY

Major: Organic Chemistry

Program of Study Committee:
Arthur H. Winter, Major Professor
Jason Chen
Malika Jeffries-EL
William Jenks
Theresa Windus

Iowa State University

Ames, Iowa

2014

TABLE OF CONTENTS

ACKNOWLEDGEMENTS

First, I would like to thank those who have served on my graduate committee throughout the years: Dr. Jason Chen, Dr. Malika Jeffries-El, Dr. William Jenks, Dr. Theresa Windus, and Dr. Nicola Pohl. Their support, availability, and opinions were greatly appreciated. I'd like to also thank Malika for serving as my Preparing Future Faculty mentor. Her words of wisdom won't be forgotten, and I cherish all of the advice that I was given. I am also grateful for Dr. George Kraus for allowing me to work in his lab the summer before starting graduate school. I wouldn't have been as successful in lab without the skills I learned that summer. I have been lucky to have had two successful collaborations during my time at ISU, and I am thankful to the Kraus group and the Petrich group for these collaborations.

I would also like to thank the graduate and undergraduate office and laboratory personnel. In particular, Lynette has always welcomed me into her office with a smile and has gladly answered all of my many questions. She has been a mother figure to me throughout graduate school, and I have always enjoyed my interactions with her. The chemical services personnel have also been integral to my success. Sarah and Shu have always been very helpful throughout the years, and the implementation of the Cloud storage made my binding data analyses run smoothly.

* * *

I feel very fortunate to have had the opportunity to work for Dr. Arthur Winter over the past 5 years. Graduate school has been a growing experience for me, both as a chemist and as a person. Art has always encouraged this growth whether it was through letting me join PFF or by letting me work on projects that I proposed. Art has always given me the freedom to explore my own ideas and design all of my own experiments. I was able to learn from my failures and solve (most) problems. I believe that the approach Art has taken as a mentor to me has made me develop into a critically-thinking, confident chemist, and I can only hope that he is proud of the person I am today.

Art has truly been a fantastic mentor. I'm sure there were times when I made him angry or when I disappointed him, but he never faltered in his encouragement of me. Art is an integral member of the ISU community and an asset to the Chemistry Department. I know he will be very successful in his future endeavors.

* * *

I am indebted to the two undergraduates I mentored, Stephen and Ryan, and to all of the Winter lab group members: Alex, Fatema, Katie, Mark, Pat, Pratik, Rita, and Toshia. I know most of you very well, and I consider you all my family. You have seen me through my best and worst times, and have always been there for me with hugs, candy, laughs, and drinks. Sometimes we may bicker like siblings, but in the end, I

know I can always turn to you for support, and I always looked forward to coming into work to see all of you. I will miss you all very much when I leave.

Fatema, you are the newest member of our family, and our time together was short, but you couldn't have joined a better group! Alex and Mark, you are like my little brothers. You have been good sports over the years when I pick on you, and you guys are a never-ending fountain of jokes and witty one-liners. When things get too stuffy, I know I can always step onto your side of lab and have a good laugh. Pratik, you are like the wise, older brother. Your positive attitude helps keep everyone in a good mood, and I hope that 'sad panda' stays with the Winter lab long after I am gone. Rita and Katie, you are two of the kindest people I know. Whenever I needed a favor, you two always had my back. I always enjoyed the girls-only chat sessions with the two of you and Toshia, and having girls' nights. Toshia, you are like the older sister. We've had some ups and downs, but I'm really happy that in the end we've become really good friends. As the little sister, I had some maturing to do before we could finally get to this point, and I'm sorry for the lost time. Pat, you are like my twin brother. You've been my partner in crime since our first year. Without having you as a friend, I would have been very lonely throughout the last five years. You've been one of the best friends I've ever had, and I'm really going to miss you. Winter lab, it's been fun, and "it's gonna take a lot to take me away from you…" in memory, at least.

I'd also like to thank my non-Winter lab friends, Andy, Adam, and Ben. After prelims, we didn't see each other as much, but these guys made the transition to graduate

school easy and our first two years full of fun with Grape Escape, 4 am infomercials, cookouts, and video games.

* * *

I would like to thank my family. They were always available to talk and give encouragement when I needed it. Without them, I would definitely not be where I am today. My parents, Judi and Dave, and sister, Aubrey, have always supported me in my endeavors, and I am very appreciative. My snuggly monkeys, Lady Bird and Roo Kitten, have given me unconditional love, snuggles, and meows over the years. No matter how rough a day was, my 'kiddens' always made it better.

Finally, I want to thank my fantastic fiancé, Ger Bear. From the first day we met in Dr. Kraus' lab, I knew you were special. You taught me all of my synthetic chemistry lab skills, and I wouldn't have been a successful chemist without your support and guidance throughout the years. We've enjoyed quite the adventure at ISU, and I look forward to many, many more adventures with you in the future.

Thank you, everyone. I know that I wouldn't be the person I am today without all of your support.

ABSTRACT

Part I. It is important to understand the factors that influence binding. Rigid molecular receptors have been widely studied, with some of these receptors being able to form stable complexes in competitive solvents such as aqueous DMSO. The scope of my research is to study both the binding of ferrocene derivatives to carboxylates in competitive solvents, and the release of these carboxylates when cucurbit[7]uril is added to the system with the aim of identifying more tightly binding hosts to carboxylates in neat water.

In Chapter 1, pincher cationic ferrocene hosts for carboxylate ion guests were synthesized and the binding constants were determined by NMR or UV-vis titrations. These (di)cationic hosts formed tight complexes with benzoate or acetate even in competitive aqueous DMSO solvent. A bis(acylguanidinium) ferrocene dication achieved a remarkable K_a of ~ 10^6 M^{-1} to acetate in 9:1 DMSO:H_2O and a K_a of 850 M^{-1} in pure D_2O, one of the highest association constants known for a mono-carboxylate complex exploiting only electrostatic interactions in pure water. Density functional theory (DFT) computations of the binding enthalpy were in good agreement with the experimentally determined association constants.

In Chapter 2, association constants of a bis(acylguanidinium) ferrocene dication to various (di)carboxylates in water were determined through UV-vis titrations. Association constant values greater than 10^4 M^{-1} were determined for both phthalate and maleate carboxylates to the bis(acylguanidinium) ferrocene salt in pure water. DFT

binding enthalpy computations of the rigid carboxylates geometrically complementary to the dication agree well with the experimentally determined association constants. Catch and release competitive binding experiments were done by NMR for the cation-carboxylate ion pair complexes with CB[7], showing dissociation of the ion pair complex upon addition of CB[7].

Part II. Heterolytic bond scission is a staple of chemical reactions. While qualitative and quantitative models exist for understanding the thermal heterolysis of carbon—leaving group (C-LG) bonds, no general models connect structure to reactivity for heterolysis in the excited state.

Time-Dependent Density Functional Theory (TD-DFT) excited-state energy calculations and Complete Active Space Self-Consistent Field (CASSCF) minimum energy crossing (conical intersection) searches were performed to investigate representative systems that undergo photoheterolysis to generate carbocations. Certain classes of unstabilized cations are found to have structurally-nearby, low-energy conical intersections, whereas stabilized cations are found to have high-energy, unfavorable conical intersections. The former systems are often favored from photochemical heterolysis. These results suggest that the frequent inversion of the substrate preferences for non-adiabatic photoheterolysis reactions arises from switching from transition-state control in thermal heterolysis reactions to conical intersection control for photochemical heterolysis reactions. The elevated ground-state surfaces resulting from generating unstabilized or destabilized cations, in conjunction with stabilized excited-state surfaces, can lead to productive conical intersections along the heterolysis reaction coordinate.

From the TD-DFT excited-state calculations, we were able to notice trends and predict if molecules have the potential for a productive conical intersection. To test this experimentally, BODIPY dyes that were shown to have small energy gaps between the ground state and excited state surfaces were synthesized. These dyes were irradiated with a xenon lamp, and the growth of the acetic acid leaving group peak was monitored by NMR over time.

INTRODUCTION FOR PART I

"Supramolecular Chemistry aims at developing highly complex chemical systems from components interacting by non-covalent intermolecular forces." [1]

– Jean-Marie Lehn

INTRODUCTION TO NON-COVALENT INTERACTIONS

Supramolecular chemistry. Since the development of the supramolecular chemistry field, many self-assembled host-guest systems have been reported, ranging from simple dimers to complex nanotubes.[2, 3] These supramolecular structures rely on non-covalent interactions for self-assembly which can include hydrogen bonding, electrostatic, ion-dipole, and hydrophobic interactions.[2, 4] As a mark of this field's impact, in 1987 Donald J. Cram, Jean-Marie Lehn, and Charles J. Pedersen were jointly awarded the Nobel Prize in chemistry 'for their development and use of molecules with structure-specific interactions of high selectivity.'[5-7] Pedersen is best known for synthesizing crown ethers while working for DuPont.[6, 8, 9] Lehn and Cram developed cryptands, hemicarcerands, spherands etc. as expansions of the crown ether work by Pedersen.[5, 6, 10-12]

The strength of non-covalent interactions depends significantly on external factors such as solvent polarity, pH, and temperature, and these factors can give rise to external control of self-assembly.[2] Non-covalent interactions are thermodynamically controlled and reversible, which is exploited in the recent development of self-healing materials.[2] This reversibility of non-covalent bonds, while attractive for self-healing

materials, is also the main weakness of artificial self-assembled structures, especially those relying heavily on hydrogen bonding interactions, because protic solvents can dramatically decrease the strength of hydrogen bonds.[2, 7]

Hydrogen-bonded assemblies. Hydrogen bonding is a Coulombic interaction between a polar donor bond ($D^{\delta-}$ - $H^{\delta+}$) and an acceptor atom ($:A^{\delta-}$).[3,13] The majority of self-assembled structures studied rely on hydrogen bonds, which are attractive due to their complementarity and directionality.[2,4,14] For example, in 1993 Rebek, et al, was able to make a synthetic 'tennis ball' dimer that formed through self-complementary hydrogen bonds in chloroform.[15] Recent focus in supramolecular chemistry, however, has been on developing receptors that can achieve self-assembly in water, which is important for the recognition of biologically important guests.[4,14] While hydrogen bonds persist in aprotic or nonpolar solvents, competitive solvation in polar and protic solvents, such as water, leads to dissociation of most assemblies.[2,4]

In 1987, Maguire and co-workers intended to design receptors that recognized uric acid (Figure 1A, B).[16] The lack of solubility of the uric acid derivatives in neutral organic solvents precluded binding studies, so the authors changed their guest to a pyrazolo-[3,4-*d*]pyrimidone system.[16] It was discovered that in 1:1 (v/v) dichloromethane/ toluene mixtures, their receptor bound the pyrazolo-[3,4-*d*]pyrimidone derivative with $K_a = 9.1 \times 10^5\ M^{-1}$.[16]

In 1991, Hamilton's group efficiently synthesized a range of barbiturate receptors in only two steps (Figure 1C).[17] These receptors showed relatively strong binding to barbitals through hydrogen bond interactions in non-polar solvents.[17] Fluorescence

binding titrations in dichloromethane indicated an association between the barbital and receptor as high as 2.5 x 10^5 M^{-1}.[17]

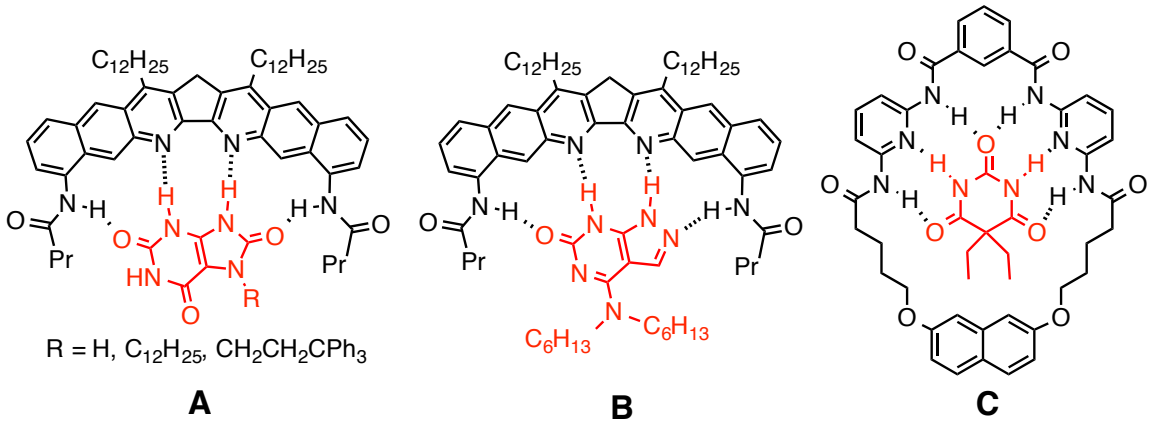

Figure 1. Maguire (**A, B**) and Hamilton's (**C**) hydrogen-bond driven receptors

The hydrogen bonding strength of the receptors in Figure 1 can be attributed to the (non)polarity of the solvents, the preorganization of the host and guest, and the complementary binding sites of the host and guest.

In 2005, Zimmerman et al wanted to study hydrogen-bonded networks in more polar solvents. They introduced a ureido-naphthyridine dimer with eight self-complementary donor and acceptor hydrogen bonding sites (Figure 2).[18]

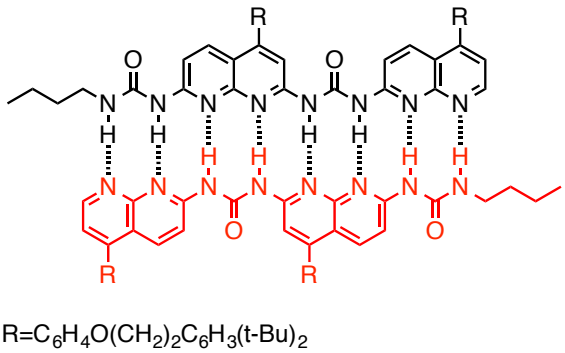

Figure 2. Zimmerman's ureido-naphthyridine dimer

It was found that this ureido-naphthyridine dimer had an association constant as high as 4.5 x 10^5 M^{-1} in 10% DMSO/chloroform, but that the association constant dropped to only 40 M^{-1} when the amount of DMSO was raised to 20%.[18] In neat DMSO, or in protic solvents like water or methanol, no dimerization was observed.[18] Therefore, in order to achieve self-assembly in polar solvents like water, additional non-covalent interactions, such as electrostatic interactions, must be exploited.[2]

Electrostatic interactions. Electrostatic interactions are Coulombic attractions or repulsions between charges or partial charges.[3] There are many types of electrostatic interactions including ion pairs, salt bridges, and ion-dipole interactions.[3] Electrostatic interactions between two charged species, or ion pairs, are more stable than hydrogen bonds, but like hydrogen bonds, they are also solvent-dependent.[2] While ion pairs persist in non-polar solvents, they are much weaker in polar or aqueous solvents due to the dielectric of the solvent that shields the charges from one another. Because ion pairs lack directionality, they are usually paired with hydrogen bonds to achieve substrate specificity.[3] Simple point charge ion pair interactions are very weak, even when they are paired with hydrogen bonds.[3]

In 2000, Schmuck and coworkers studied the binding interactions between various guanidinium-bearing receptors.[19] There was no observed complexation between the N-acetyl alanyl carboxylate **1** and guanidinium hydrochloride **2** in 60% DMSO/ water solutions (Figure 3).[19]

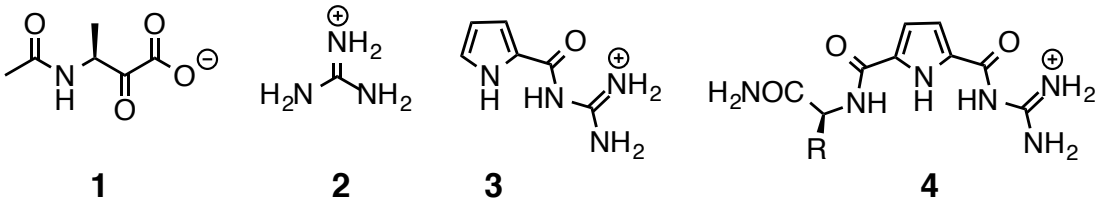

Figure 3. Carboxylate **1** and guanidinium-bearing cations studied by Schmuck in competitive solvent.

Remarkably, however, with the recruitment of just one additional hydrogen bond, the guanidiniocarbonyl pyrrole **3** was able to bind to the N-acetyl alanyl carboxylate **1** under the same solvent conditions with an association constant of 130 M^{-1}.[19] It should be noted that the carbonyl next to the guanidine makes the guanidine hydrogens more acidic (increased δ+), which helps favor hydrogen-bond formation.[2] Compound **4**, which was able to form four hydrogen bonds with the carboxylate, had an association constant of 1610 M^{-1}.[19]

In 1997, Anslyn's group synthesized a receptor that his group used as an indicator-displacement assay with a 5-carboxyfluorescein indicator to bind ATP, citrate, and numerous other tri-carboxylates in buffered water (Figure 4).[20] According to Anslyn, this tri-cationic "pinwheel" receptor was a by-product of a reaction in which the group was trying to design a phosphate-ester hydrolysis catalyst.[20, 21] While drinking a can of Fresca, which contains citrate, Anslyn decided to use this tri-cationic byproduct to try to selectively bind citrate.[20]

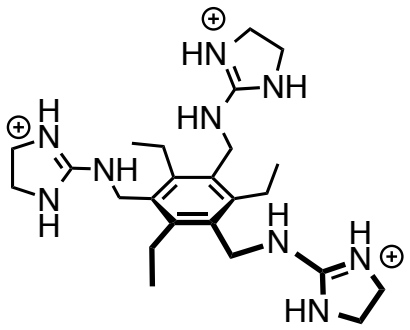

Figure 4. Anslyn's citrate and ATP receptor

By NMR binding titrations, Anslyn et al found that the pinwheel receptor was able to bind citrate as high as 6.9 x 10^3 M^{-1} in pH 7.4 buffered D_2O,[22] and was able to bind ATP with an association of 1.2 x 10^3 M^{-1} under the same conditions.[21] Since the development of this pinwheel receptor, many other pinwheel-like receptors have been studied. For example, Schmuck and coworkers have also created a "molecular flytrap" that could selectively bind citrate and other tri-carboxylates in water (Figure 5).[23] This flytrap receptor, which was based both on Anslyn's pinwheel and on Schmuck's guanidiniocarbonyl pyrrole receptors, bound citrate as high as 1.6 x 10^5 M^{-1} in pure water and 8.6 x 10^4 M^{-1} in buffered water.[23] An explanation for the increased binding affinity of Schmuck's flytrap versus Anslyn's pinwheel for citrate is that Schmuck's flytrap guanidine hydrogens are more acidic due to the proximal carbonyl.

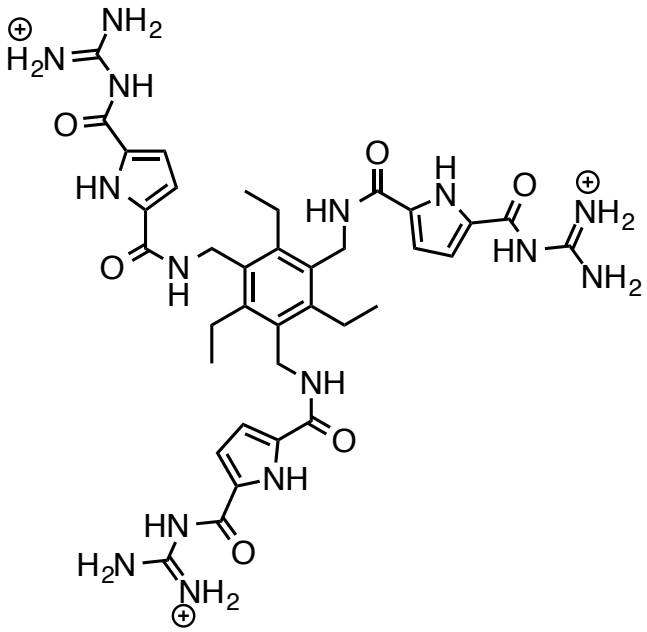

Figure 5. Schmuck's molecular flytrap receptor

These examples of the work done by Schmuck and Anslyn illustrate the importance of recruiting additional non-covalent interactions (electrostatic and hydrogen bonding) to form stable aggregates in polar or aqueous solvents.

Hydrophobic interactions. A type of non-covalent interaction that is rather stable in water is the hydrophobic interaction; however, unlike hydrogen bonds, these are neither specific nor directional.[14] Hydrophobic interactions are often entropy driven.[24, 25] For example, if there are two hydrocarbon molecules in water that are separated by a distance, water molecules must reorient themselves around both of the hydrocarbons, leading to an ordering of the water molecules, which is entropically disfavored.[24] When the two hydrocarbons aggregate, there are less water molecules that must reorient themselves.[3] While aggregation of the two hydrocarbons is entropically disfavored,

decreasing the amount of water molecules that must reorient themselves is greatly favored.[3] Therefore, overall it is more entropically favorable for the hydrocarbons to aggregate rather than not.[3]

Hydrophobic properties can be exploited for host-guest chemistry. For example, cyclodextrins, cucurbit[n]urils, and cyclophanes all have a hydrophobic cavity. Cyclodextrins (CD) are cyclic oligosaccharides made up of 6, 7, or 8 glucose units (α, β, γ respectfully).[26] The hydroxyl groups of cyclodextrins are easily modified, which allows for the change of the depth of the CD cavity as well as solubility properties (Figure 6).[27] The ability to modify the CD cavity depth and its good solubility in water make CDs attractive potential hosts for drug delivery.

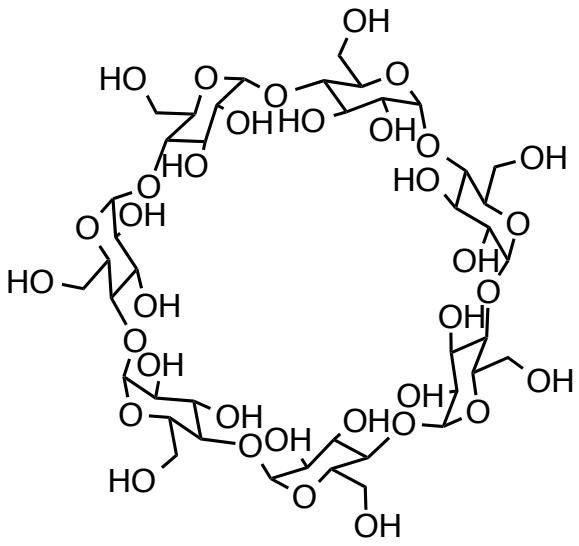

Figure 6. β-Cyclodextrin

In 2012, Qi et al studied the solubilizing ability of a modified β-cyclodextrin with curcumin (Figure 7).[27] Curcumin, which is a spice used in many Asian countries, has

been shown to have pharmaceutical potential for the treatment of cancer, cystic fibrosis, Alzheimer's disease, and Parkinson's disease.[27] However, due to its hydrophobic poly-phenol structure, it is not very soluble in aqueous solvents, making direct oral bioavailability very low.[27] Qi's group showed that the modified CD and curcumin could form a complex in water at many pH ranges.[27] They also found that due to the solubilizing ability of the CD, after oral administration in rats the bioavailability of the curcumin significantly improved.[27]

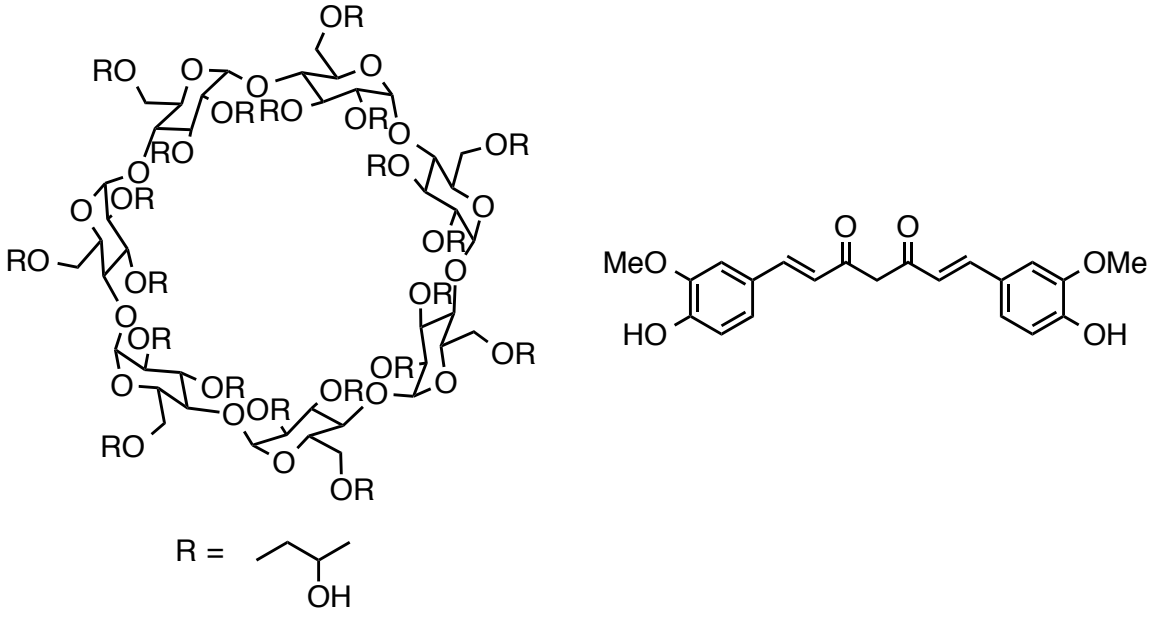

Figure 7. Qi's modified cyclodextrin studied with curcumin

While cyclodextrins have potential applications in medicine due to their ability to solublize drugs, the association constants of CDs with their guests in water are smaller than those for cucurbit[n]urils or cyclophanes.[28] For example, in 1983, Laufer and coworkers studied the complexation of α- and β-CDs with various modified

adamantanes in water (Figure 8).[29] They found that β-cyclodextrin formed a complex with the adamantylammonium with an association of 8 x 10^3 M^{-1} in water.[29] A similar study of the complex between the same substituted adamantine and cucurbit[7]uril (CB[7]) in water showed that a complex with an association of 4.2 x 10^{12} M^{-1} was formed.[30]

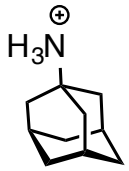

Figure 8. Adamantylammonium studied by Laufer

Cucurbit[n]urils, which are highly symmetrical, rigid cyclic oligomers of bis(methylene)-bridged glycourils, have also been found to form stable complexes with methylviologen ($K_a > 10^6$ M^{-1}) and many other ammonium compounds in water (Figure 9).[31-33] Cucurbit[7]uril will be discussed in detail later in the **Cyclodextrin and Cucurbit[7]uril as Ferrocene Hosts** section.

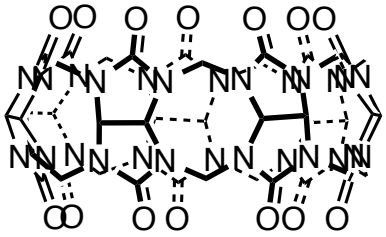

Figure 9. Cucurbit[7]uril

In 1984, Jean-Marie Lehn's group synthesized a speleand, which is a type of cavitand and cyclophane hybrid containing both ether and aromatic groups (Figure

10).[3,34] They found that this speleand was able to bind substituted ammonium ions, and that the complexes formed were more stable than those formed with 18-crown-6.[34] Methylviologen formed a strong complex with the speleand, and it was determined to have a binding constant greater than 10^6 M^{-1} in water.[34]

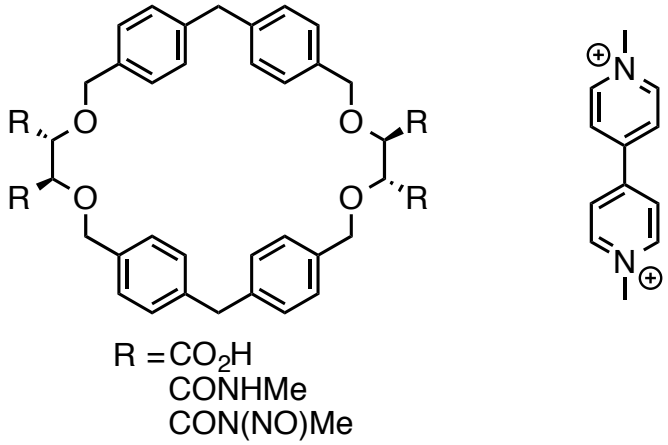

Figure 10. Speleand receptor and methylviologen studied by Lehn

One limitation of CDs, cucurbit[n]urils, and cyclophanes is the size of the hydrophobic cavity. The cavity size, both height and diameter, limits the size of the guest that may be encapsulated. It is also possible to have favorable or unfavorable ion-dipole interactions between the host and the guest (See **Cyclodextrin and cucurbit[7]uril as ferrocene hosts** section).[4] Therefore, when designing artificial receptors, there are many factors that must be taken into account (size, shape, rigidity, hydrogen bonding interactions, ion-pair interactions, etc.). According to Andrew J. Wilson, there are three general principles for the elaboration of any artificial receptor: (i) the host and guest should have as many non-covalent interactions as possible, (ii) the

host and guest should have complementary shapes, and (iii) the host and guest should be preorganized for binding.[4]

Complementarity, preorganization, and induced-fit. In 1894, Emil Fischer described a lock-and-key model for enzyme recognition.[35] The concepts of complementarity and preorganization are similar to the lock-and-key model, which indicates that the high specificity of an enzyme-substrate complex is due to the enzyme being rigid and the substrate being complementary to the enzyme binding pocket (Figure 11).[3, 35] For supramolecular chemistry, Cram has said that "the more highly hosts and guests are organized for binding… the more stable will be their complexes."[35, 36]

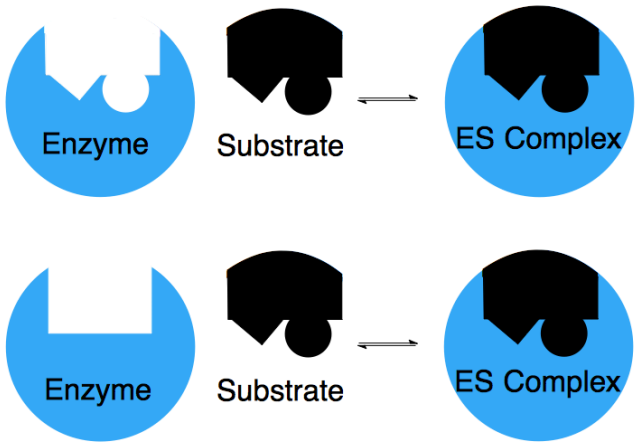

Figure 11. Lock-and-key (top) versus induced fit (bottom)

Umezawa et al synthesized receptors that were preorganized to bind specific guests (Figure 12).[37] Their hosts were based on the thiourea moiety connected to a xanthene spacer. The rigid backbone of their receptor, paired with directional hydrogen bonds proved to be an excellent design for the binding of phosphate.[37]

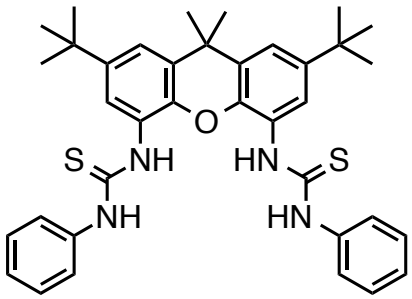

Figure 12. Umezawa's xanthene thiourea receptor

The xanthene thiourea receptor was bound to chloride, phosphate, and acetate in neat DMSO. While chloride only bound with an association of 1 x 10^3 M^{-1}, phosphate had a K_a of nearly 2 x 10^5 M^{-1}, and the association to acetate was too large to determine by NMR titrations.[37] It was determined that these large associations to phosphate and acetate were due to the complementarity and preorganization of the host.

Unlike Umezawa's receptor, many synthetic hosts are not completely preorganized for binding and may require conformational changes in order to become complementary to their guest. This is similar to the induced fit model proposed by Koshland, which states that "the substrate may cause an appreciable change in… the active site."[35] Figure 11 shows both the lock-and-key and the induced fit models proposed by Fischer and Koshland. In the event that a host or guest is not preorganized for binding, energetic costs, both entropic and enthalpic, associated with the molecule restricting itself to a specific conformation reduces the overall binding association.[35, 38] Therefore, rigid, preorganized hosts, like cucurbit[n]urils, have very strong binding associations with their guests, provided that the guests are the appropriate size to fit into the cucurbit[n]uril binding cavity.

Examples of induced fit anion binding receptors mentioned previously are Anslyn's 'pinwheel' (Figure 4) and Schmuck's 'molecular flytrap' (Figure 5) citrate receptors. These receptors had a flexible connectivity to a benzene ring and rigid arms that were able to clasp onto the citrate, much like a Venus flytrap. Both of these receptors were able to bind citrate with an association up to 10^5 M^{-1} in water because they exploited many types of non-covalent interactions, and they had a host that was preorganized to bind citrate.[20, 23] Most artificial receptors use many different types of non-covalent interactions to achieve stable self-assembly, and most receptors are designed to be complementary and preorganized to bind a specific guest.

ARTIFICIAL RECEPTOR DESIGN

Introduction. In order to form stable aggregates, it is often the case that many non-covalent forces must be combined. These non-covalent interactions must contain a directional aspect in order to form defined structures.[14] In water, multiple interactions are often combined in order to form stable aggregates. In supramolecular chemistry, combining multiple (weak) interactions to form stable aggregates is referred to as the Gulliver principle,[2,14] referring to the book Gulliver's Travels by Jonathan Swift, wherein the Lilliputians were able to tie Gulliver to the floor with a large number of weak ropes.[39] In chemistry, many combined weak interactions can lead to strong aggregates. To understand just how important these weak interactions are to complexation, Boger et al synthesized different peptide substrate analogues to bind to vancomycin with specifically

altered binding sites,[40] and Schmuck' group performed knock-out analogue studies on guanidiniocarbonyl pyrroles.[41]

Non-covalent interactions in medicine. Gram-positive bacteria, which get their name from the ability for stains to adhere to their cell walls, are common causes of infections in hospitalized patients.[42, 43] Over the last decade, there has been a large increase in antibiotic resistance to gram-positive bacteria. Methicillin-resistant *Staphylococcus aureus* (MRSA) and vancomycin-resistant enterococci (VRE) have become great concerns.[43] As of 2006, sixty percent of the staph infections in the US were caused by MRSA.[43]

Unfortunately, antibiotic resistance is a recurring theme in medicine. In the early 1940's, virtually all *S aureus* strains were susceptible to penicillin, but by 1944 there were already reports of penicillin resistance.[43] Penicillin resistance occurred due to the acquisition of genes that encode penicillinase enzymes, which are drug-inactivating enzymes.[43] Methicillin, which is a penicillinase-resistant variant of penicillin was introduced in 1959.[43] By 1961, there were already reports of methicillin resistance in bacteria.[43] To cope with the methicillin resistance, vancomycin was developed.

Vancomycin is a last resort antibiotic for the treatment of MRSA that binds to a specific N-Acyl-D-Ala-D-Ala sequence that is found on the surface of gram-positive bacteria cell walls.[7,44] When vancomycin binds to the peptide sequence, it sterically blocks the enzyme needed for the bacteria cell wall maturation.[40] With more frequent use of antibiotics, vancomycin-resistant gram-positive bacteria have emerged. The

resistant gram-positive bacteria have N-Acyl-D-Ala-D-Lac peptidoglycan termini (Figure 13).[45, 46]

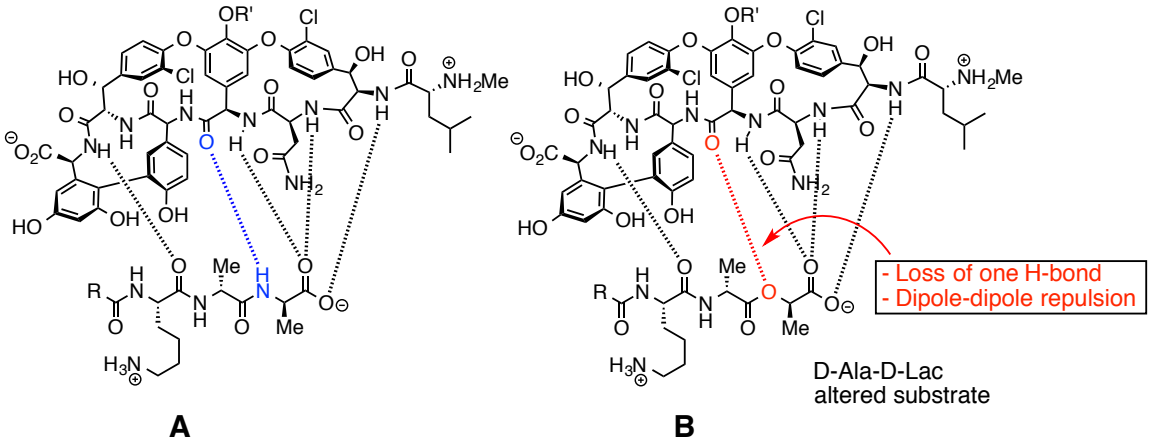

Figure 13. Vancomycin bound to peptide sequence of bacteria (**A**) and vancomycin bound to resistant strain of bacteria (**B**)

Replacement of the D-Ala by D-Lac renders the antibiotic ineffective against the bacteria, due to the unfavorable dipole-dipole interaction between the vancomycin carbonyl and the lactic acid ester.[7,40] This unfavorable interaction is highlighted in red in Figure 13.

To understand just how the change in peptide sequence alters the binding affinity of vancomycin to the bacteria, Boger et al synthesized the bacteria peptide sequence of interest and systematically altered the Ala residue (Figure 14).[40] Then they looked at the binding affinity of these altered residues to vancomycin and found that changing the amide NH to a CH_2 resulted in a 10-fold decrease in complex stability.[40] Changing the amide NH to an O resulted in a 1000-fold decrease in complex stability.[40]

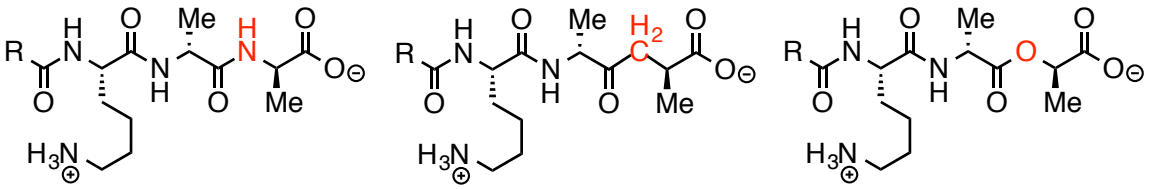

Figure 14. Peptide sequences studied by Boger

This is a fascinating example of the importance of pre-organization in supramolecular chemistry. Even a subtle change in one structure can have huge effects on the complex stability. Intrigued by Boger's studies, Schmuck decided to make artificial receptors and computationally test "knock-out" analogues to determine the importance of the various non-covalent interactions and their interplay.[41]

Schmuck's "knock-out" analogues. To understand the importance of individual non-covalent interactions, Schmuck et al experimentally and computationally studied different guanidiniocarbonyl pyrrole derivatives (Figure 15).[41] Compounds **1** and **2** were synthesized and their binding constants were determined (Figure 15).[47-49] In pure DMSO, compound **1** had a $K_a > 10^4$ M^{-1}. In pure water, **1** still formed stable complexes with an association constant of 170 M^{-1}.[41] Compound **2** was able to dimerize in chloroform with an association greater than 10^4 M^{-1}, but when even 5% DMSO was added, there was disruption of the dimers due to competitive solvation.[41] From the experimental data, it could not be determined the exact reason behind the disparity in complex stability, so Schmuck proceeded with the computational "knock-out" studies where he systematically knocked out non-covalent binding interactions to determine the destabilization of losing these interactions. Geometry optimizations were computed at

the BLYP/TZVPP level of theory, and solvent calculations were performed with COSMO.[41] The highlighted areas in red in Figure 15 indicate the areas in the complexes where non-covalent interactions have been knocked out.

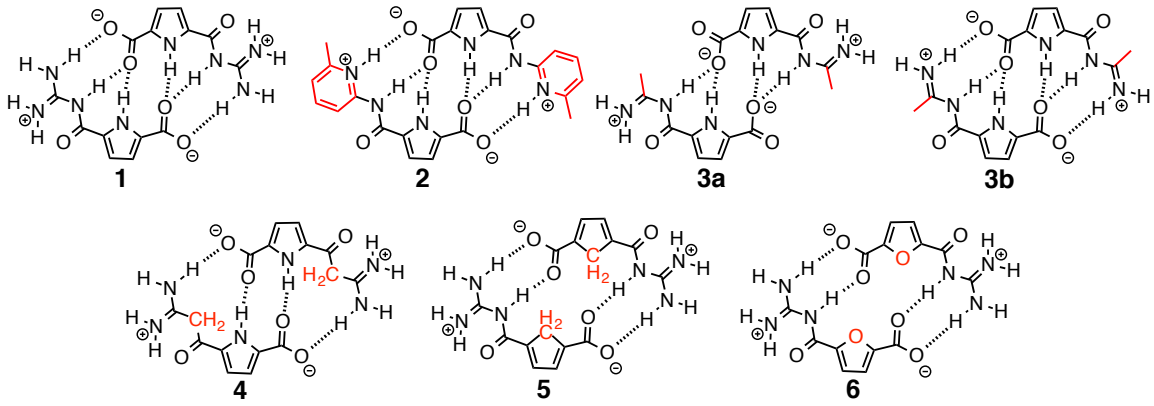

Figure 15. Schmuck's "knock-out" analogues studied computationally

Complexes **3a** and **3b,** which included two different rotamers of the same compound, have replaced a guanidine NH_2 with a methylene group. Complex **4** has replaced an amide NH with a methylene group. Complexes **5** and **6** have replaced the pyrrole NH with methylene and oxygen, respectively. Due to tautomerization and conformational instability, compounds **3a-6** were not studied experimentally.[41]

Computed dissociation energies of the dimers going to two zwitterionic monomers showed the following trend: ΔE **3b > 1** > **3a** ~ **5** > **4** > **6** > **2**. The dimerization of complex **3b** was calculated to be the most energetically favorable, which was surprising to Schmuck, since **1** had an additional internal hydrogen bond, making it more rigid and therefore better pre-organized for binding. These simple models show the difficulty in predicting the stability of complexes. Schmuck was able to conclude that

four interactions seem to be important: (i) charge interactions with ionic hydrogen binding networks are more stable than simple point charges (ii) additional hydrogen bonds are good, but ionic ones are better, (iii) solvation affects hydrogen bonds differently depending on their accessibility, and (iv) secondary electrostatic interactions help stability.[41] The difficulties that Schmuck had in predicting complex stability is not limited to his dimers, but to artificial receptors in general, in which both the host and the guest need to be designed to have an optimum number of non-covalent binding interactions.

Guanidinium-oxoanion receptors. Schmuck's guanidiniocarbonyl pyrrole and many other artificial receptors have one moiety in common – guanidinium. The guanidinium group is a common structural motif found in nature to coordinate to many types of anions, it is found in the side chain of arginine, and it can form strong ion-pairs with oxoanions (carboxylates and phosphates) found in enzymes.[50] The guanidinium moiety is attractive for artificial receptors and molecular recognition because it is rigid, planar, has directional hydrogens, and has a high pK_a of 12-13, which ensures protonation over a wide pH range.[50, 51]

Artificial receptors already mentioned that bear the guanidinium moiety include Schmuck's guanidiniocarbonyl pyrrole (Figures 3 and 15), Schmuck's 'molecular flytrap' (Figure 5), and Anslyn's 'pinwheel' (Figure 4), but there are many other receptors that utilize the guanidinium moiety. In 1992, Hamilton et al developed a bis-acylguanidinium benzene that was able to bind phosphodiesters in acetonitrile (Figure 16A).[52-54] Proton and phosphorous NMR titrations indicated that Hamilton's receptor

bound tetrabutylammonium diphenylphosphate with a $K_a = 4.6 \times 10^4\ M^{-1}$.[54] In the same year, Anslyn's group developed a bis-guanidinium cleft that was also able to bind phosphodiesters (Figure 16B).[55] A series of investigations were carried out in aqueous DMSO, which indicated that even in competitive solvents (2:1 DMSO-d_6:D_2O), Anslyn's receptor was able to form complexes with dibenzyl phosphate with an association of $7 \times 10^2\ M^{-1}$.[55]

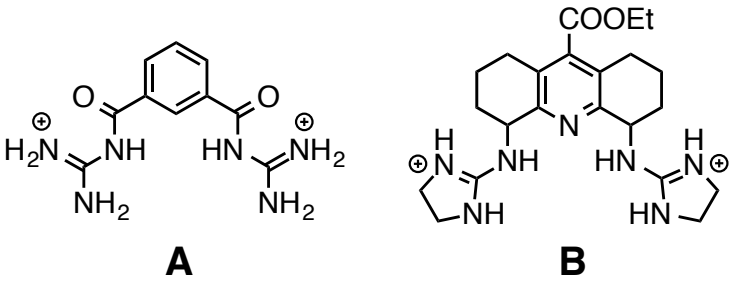

Figure 16. Hamilton (**A**) and Anslyn's (**B**) guanidinium-based receptors

Over the years, Hamilton's group continued to design artificial receptors based on his original design shown in Figure 16A, with the ultimate goal of forming stable complexes in water. In 2001, they designed bis-guanidinium receptors that bound dicarboxylates in aqueous methanol (Figure 17).[56] NMR titration experiments in different ratios of CD_3OD:D_2O were done with receptors **A** and **B** with both glutarate and 5-nitroisophthalate as guests.[56]

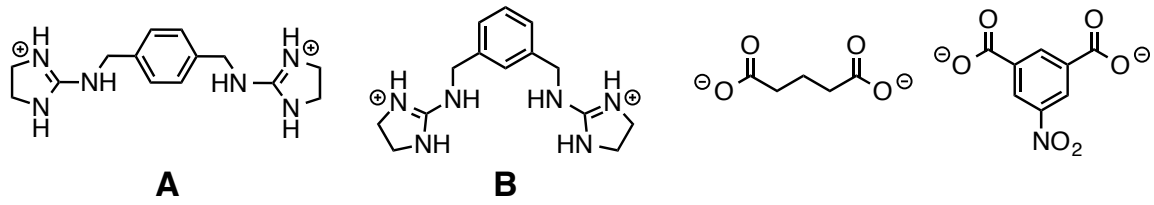

Figure 17. Hamilton's bis-guanidinium receptors, glutarate, and 5-nitroisophthalate

Receptor **B** showed stronger complexation than receptor **A** with glutarate and 5-nitroisophthalate in all ratios of aqueous methanol solutions tested, which indicate the importance of designing a host that is geometrically matched to its substrate.[56] Both receptors bound the rigid 5-nitroisophthalate with a higher association than the flexible glutarate, which indicates the importance of preorganization. Even in 75% D_2O, receptor **B** was able to bind 5-nitroisophthalate with an association of 3.2×10^2 M^{-1}.[56]

It has been shown that guanidinium-based receptors have the ability to form stable complexes even in competitive solvents. While many of these artificial receptors contain a benzene or pyrrole backbone, a guanidinium-bearing ferrocene artificial receptor has also been developed.[50] In 1997, Beer et al developed a ferrocene receptor that formed complexes with pyrophosphate with a 2:1 binding stoichiometry (Figure 18).[57] Aqueous methanol NMR titrations indicated that even with 50% D_2O, the complex formed with an association of 4.6×10^3 M^{-2}.[57]

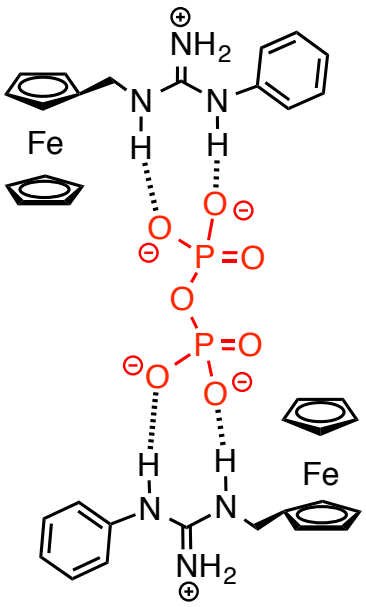

Figure 18. Beer's guanidinium-based ferrocene receptor

Beer's receptor was one of the first reported artificial receptors bearing the ferrocene backbone. Since his work, there have only been a handful of ferrocene receptors reported that were not used specifically as electrochemical sensors.[58-60]

Ferrocene receptors. The presence of the redox active subunit make ferrocenes attractive as electrochemical sensors for ions.[50] While there has been extensive work devoted to using ferrocenes as sensors,[61-73] there has been little work done toward studying ferrocenes as artificial receptors for oxoanion binding.[57-60] The semi-flexible nature of the ferrocene backbone also makes 1,1'-bis-substituted ferrocenes attractive as hosts. Much like induced fit, this semi-flexible backbone allows for some rotation so that the ferrocene host may conform better to its guest.

In 2001, Tucker and coworkers designed three 1,3-bis-substituted ferrocene receptors that bound urea derivatives in chloroform through complementary hydrogen bonds (Figure 19).[58] NMR titration experiments with a variety of ureas showed that barbital was able to bind to the ferrocene derivative shown with the highest affinity of 3.2×10^3 M^{-1}.[58] This particular ferrocene derivative was able to form the most hydrogen bonds with its guest, attributing to the strength of the complex.[58]

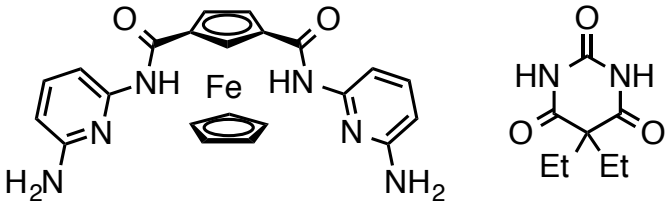

Figure 19. Tucker's bis-substituted ferrocene and barbital

In 2005, Roy's group developed a 1,1'-bis-substituted ferrocene that was able to bind many different unprotected amino acids in aqueous acetonitrile (Figure 20).[59] Due to the redox-active ferrocene unit, binding could be determined through many methods, and this group studied binding through UV-vis, NMR, isothermal titration calorimetry (ITC), and even cyclic voltammetry (CV).[59] A 1:1 binding stoichiometry was determined for the ferrocene receptor and the amino acids.[59] ITC studies in 1:1 acetonitrile:water showed that the ferrocene receptor was able to bind glutamate with a strong association of nearly 4.4×10^4 M^{-1}.[59]

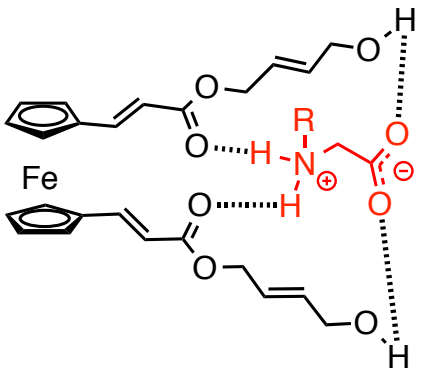

Figure 20. Roy's 1,1'-bis-substitited ferrocene binds amino acids

A ferrocene receptor that showed high selectivity for acetate in DMSO was developed by Lin et al in 2009 (Figure 21).[60] A series of UV-vis and NMR investigations were carried out to monitor the binding of their 1,1'-bis-substituted ferrocene receptor to tetrabutylammonium salts of halogens, acetate, hydroxide, and phosphate. Fluoride, hydroxide, and phosphate anions were all able to bind with a $K_a > 10^3$ M^{-1}, but acetate showed a larger binding affinity of 3.9×10^4 M^{-1} (chloride, bromide, and iodide showed no significant interactions).[60]

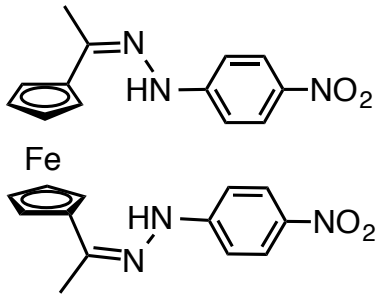

Figure 21. Lin's acetate-selective ferrocene receptor

A unique bis-ferrocene receptor was developed by Felix et al in 2005 (Figure 22).[64] Dicarboxylates phthalate, isophthalate, dipiccolinate, and 4-nitrobenzoate were bound to this bis-ferrocene receptor.[64] NMR titration experiments in CD_3OD indicated a 1:2 stoichiometry of host:guest and that phthalate bound the strongest with an association of 1.25 x 10^6 M^{-1}.[64] X-ray analysis showed that instead of the carboxylates being encapsulated by the guest, they instead bound on the outside of the host to the amino hydrogens.[64]

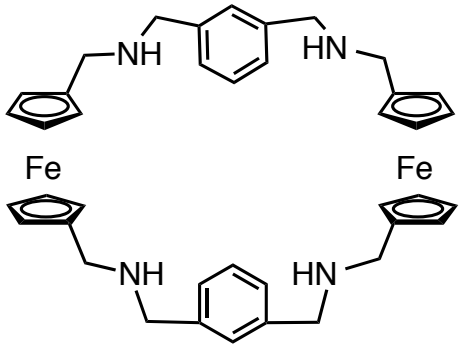

Figure 22. Felix's bis-ferrocene receptor binds dicarboxylates

In the examples above, ferrocene has been shown to be a promising backbone for artificial receptor design. However, these studies have failed to exploit many different types of the non-covalent interactions that are useful for binding in water. They have also overlooked the usefulness of the guanidinium moiety, which has proven to be an attractive feature of many other artificial receptors already mentioned. In Chapters 1 and 2, charged 1,1'-bis-substituted ferrocene receptors bearing the guanidinium moiety and their binding to carboxylates in competitive solvent will be discussed in more detail.[74]

Finally, while ferrocenes can be great hosts, they may also be excellent guests. Studies have shown that ferrocenes bind tightly to cyclodextrins and cucurbit[n]urils in water.

Cyclodextrin and cucurbit[7]uril as ferrocene hosts. As previously mentioned, both cyclodextrins and cucurbit[n]urils have a hydrophobic binding pocket and are able to encapsulate guests. Cucurbit[7]uril and β-cyclodextrin (Figure 23) have similar cavity sizes, so their binding to various guests are often compared.[75] In most cases, cucurbit[n]urils bind their guests more strongly than cyclodextrins.[26, 30, 31, 33, 75-79] This strength is partially attributed to the favorable ion-dipole interactions that are possible with the carbonyls at the portal of CB[7].[75] The hydroxyl groups lining the CD opening do not appear to have such strong favorable interactions with guests.[75]

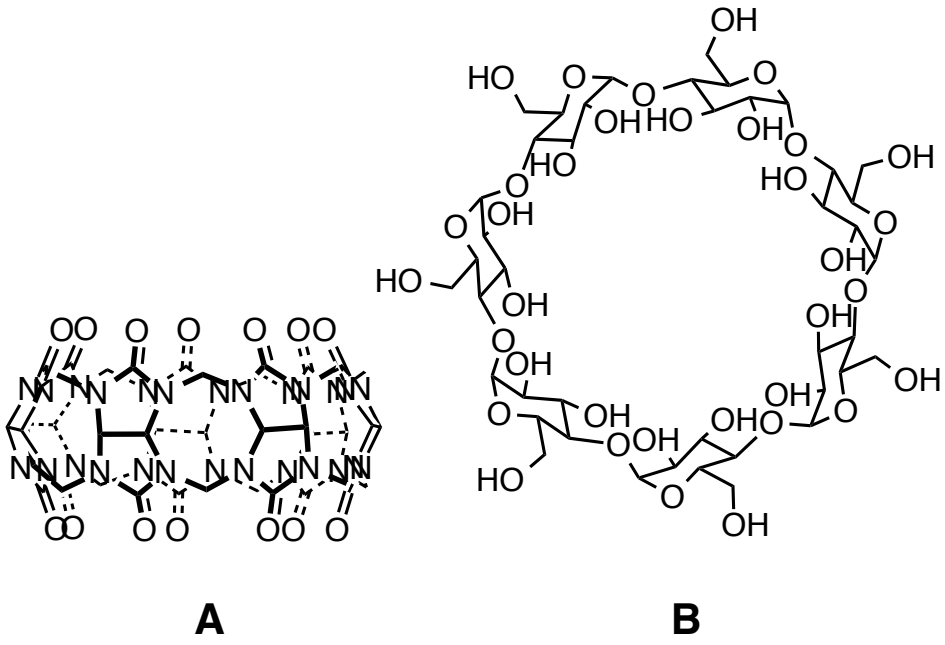

Figure 23. Cucurbit[7]uril (**A**) and β-cyclodextrin (**B**)

In 2000, Gobetto et al studied the strength of complexation of many substituted ferrocenes with β-cyclodextrin (Figure 24A and B).[26] In 95% water: acetonitrile solutions, hydroxymethyl ferrocene **A** bound to β-CD with an association greater than 2 x 10^3 M^{-1}.[26] (Ferrocenylmethyl)trimethylammonium ion **B** bound with an association of 4.2 x 10^3 M^{-1}.[26] Binding studies by Kaifer and Kim showed that in pure water, ferrocenes **A** and **B** bound to CB[7] with association constants of 3 x 10^9 M^{-1} and 4 x 10^{12} M^{-1}, respectively.[30, 31, 75]

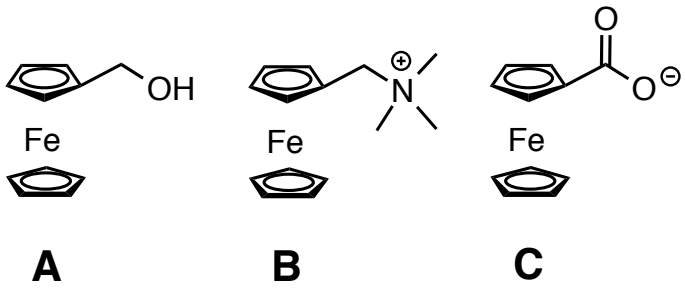

Figure 24. Substituted ferrocene guests of β-CD and CB[7]

At this point, it may tempting to say that all ferrocene compounds bind to CB[7] several orders of magnitude stronger than they bind to CDs; however, Kaifer and Kim noticed that ferrocene carboxylate did not bind to CB[7] (Figure 24C). [30, 31, 75] In contrast to this finding, compound **C** did indeed bind to β-CD with an association greater than 10^3 M^{-1}.[30, 31, 75] This inability of **C** to bind to CB[7] is attributed to the unfavorable ion-dipole interactions of the ferrocene carboxylate with the portal carbonyls of the CB[7].[75] The β-CD portal hydroxyl groups clearly do not influence binding as much as the CB[7] portal carbonyls.

Exploiting the favorable ion-dipole interactions between CB[7] and its guest, Kaifer and Kim developed a guest that formed stable inclusion complexes with CB[7] with associations as strong as 3 x 10^{15} M^{-1}, which is the highest reported K_a for a synthetic receptor (Figure 25A).[30, 76-78] To understand the importance of this ion-dipole interaction on the complex stability, Kaifer and Kim synthesized compounds **C** and **D**, which are structurally similar to compound **B** (which has a K_a of 4 x 10^{12} M^{-1}), but with a different number of methylene groups (Figure 25).[79]

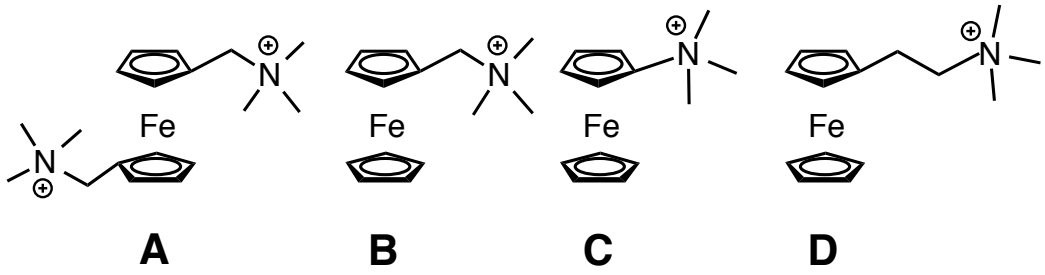

Figure 25. Kaifer's bis-substituted ferrocene guests of CB[7]

It was found that compounds **C** and **D** bound to CB[7] in water with associations of 3.6 x 10^{10} M^{-1} and 7.3 x 10^{10} M^{-1}, respectively.[79] Cleary, since there was a 2-order of magnitude decrease in complex stability for compounds **C** and **D** compared to **B**, the number of methylene groups was important to the complex stability. The studies by Kaifer and Kim (Figures 24 and 25) have shown that hydrophobic interactions paired with favorable ion-dipole interactions can have a large impact on complex stability.

REFERENCES

1. J. M. Lehn, *Science*, 2002, **295**, 2400-2403.

2. T. Rehm and C. Schmuck, *Chem. Commun.*, 2008, 801-813.

3. E. V. Anslyn and D. A. Dougherty, *Modern Physical Organic Chemistry*, University Science Books, Sausalito, CA, 2006.

4. A. Wilson, Wilson, J. Steed and P. Gale, *Hydrogen-Bonding Receptors for Molecular Guests. Supramolecular chemistry: from molecules to nanomaterials*, 2012.

5. J. W. Steed, J. L. Atwood and P. A. Gale, in *Supramol. Chem.*, John Wiley & Sons, Ltd, 2012.

6. Nobelprize.org, Nobel Media AB, 1987, vol. 2014.

7. C. Schmuck, *Synlett*, 2011, 1798-1815.

8. C. J. Pedersen, *Scientist*, 1989, **3**, 11-11.

9. C. J. Pedersen, *Science*, 1988, **241**, 536-540.

10. E. P. Kyba, R. C. Helgeson, K. Madan, G. W. Gokel, T. L. Tarnowski, S. S. Moore and D. J. Cram, *J. Am. Chem. Soc.*, 1977, **99**, 2564-2571.

11. D. J. Cram, *Science*, 1988, **240**, 760-767.

12. J. M. Lehn, *Pure Appl. Chem.*, 1994, **66**, 1961-1966.

13. J. Emsley, *Chem. Soc. Rev.*, 1980, **9**, 91-124.

14. T. H. Rehm and C. Schmuck, *Chem. Soc. Rev.*, 2010, **39**, 3597-3611.

15. R. Wyler, J. Demendoza and J. Rebek, *Angew. Chem. Int. Ed.*, 1993, **32**, 1699-1701.

16. T. R. Kelly and M. P. Maguire, *J. Am. Chem. Soc.*, 1987, **109**, 6549-6551.

17. S. K. Chang, D. Vanengen, E. Fan and A. D. Hamilton, *J. Am. Chem. Soc.*, 1991, **113**, 7640-7645.

18. M. F. Mayer, S. Nakashima and S. C. Zimmerman, *Org. Lett.*, 2005, **7**, 3005-3008.

19. C. Schmuck, *Chem. Eur. J.*, 2000, **6**, 709-718.

20. E. V. Anslyn, *J. Org. Chem.*, 2007, **72**, 687-699.

21. A. E. Hargrove, S. Nieto, T. Zhang, J. L. Sessler and E. V. Anslyn, *Chem. Rev.*, 2011, **111**, 6603-6782.

22. A. Metzger, V. M. Lynch and E. V. Anslyn, *Angew. Chem. Int. Ed.*, 1997, **36**, 862-865.

23. C. Schmuck and M. Schwegmann, *J. Am. Chem. Soc.*, 2005, **127**, 3373-3379.

24. W. Blokzijl and J. Engberts, *Angew. Chem. Int. Ed.*, 1993, **32**, 1545-1579.

25. E. E. Meyer, K. J. Rosenberg and J. Israelachvili, *Proc. Natl. Acad. Sci. USA*, 2006, **103**, 15739-15746.

26. D. Osella, A. Carretta, C. Nervi, M. Ravera and R. Gobetto, *Organometallics*, 2000, **19**, 2791-2797.

27. H.-Z. Ouyang, L. Fang, L. Zhu, L. Zhang, X.-L. Ren, J. He and A.-D. Qi, *J. Inclusion Phenom. Macro. Chem.*, 2012, **73**, 423-433.

28. I. W. Wyman and D. H. Macartney, *Org. Biomol. Chem.*, 2008, **6**, 1796-1801.

29. R. Gelb, L. M. Gelb, D. Schwartz and R. Laufer, *Life Sci.*, 1983, **33**, 83-85.

30. Y. H. Ko, I. Hwang, D.-W. Lee and K. Kim, *Isr. J. Chem.*, 2011, **51**, 506-514.

31. A. E. Kaifer, W. Li and S. Yi, *Isr. J. Chem.*, 2011, **51**, 496-505.

32. A. R. Urbach and V. Ramalingam, *Isr. J. Chem.*, 2011, **51**, 664-678.

33. W. M. Nau, M. Florea and K. I. Assaf, *Isr. J. Chem.*, 2011, **51**, 559-577.

34. M. Dhaenens, L. Lacombe, J. M. Lehn and J. P. Vigneron, *Chem. Commun.*, 1984, 1097-1099.

35. J. Wittenberg, L. Wittenberg, J. Isaacs, J. Steed and P. Gale, *Complementarity and Preorganization; Supramolecular chemistry: from molecules to nanomaterials*, 2012.

36. D. J. Cram and J. M. Cram, *Monographs in Supramolecular Chemistry, No. 4. Container molecules and their guests*, 1994.

37. P. Buhlmann, S. Nishizawa, K. P. Xiao and Y. Umezawa, *Tetrahedron*, 1997, **53**, 1647-1654.

38. P. Gale and J. Steed, *Supramolecular Chemistry: From Molecules to Nanomaterials, Volume 3: Molecular Recognition*, 2012.

39. J. Swift, *Gulliver's Travels*, Simon & Brown, 1726.

40. C. C. McComas, B. M. Crowley and D. L. Boger, *J. Am. Chem. Soc.*, 2003, **125**, 9314-9315.

41. S. Schlund, C. Schmuck and B. Engels, *J. Am. Chem. Soc.*, 2005, **127**, 11115-11124.

42. www.digitalproteus.com, in *Bacterial Morphology*.

43. L. B. Rice, *Am. J. Med.*, 2006, **119**, S11-19; discussion S62-70.

44. S.-H. Eom, Y.-M. Kim and S.-K. Kim, *Appl. Microbiol. Biotechnol.*, 2013, **97**, 4763-4773.

45. R. C. James, J. G. Pierce, A. Okano, J. Xie and D. L. Boger, *ACS Chem. Bio.*, 2012, **7**, 797-804.

46. D. L. Boger, *Medicinal Research Reviews*, 2001, **21**, 356-381.

47. C. Schmuck, *Eur. J. Org. Chem.*, 1999, 2397-2403.

48. C. Rether and C. Schmuck, *Eur. J. Org. Chem.*, 2011, **2011**, 1459.

49. C. Schmuck, V. Bickert, M. Merschky, L. Geiger, D. Rupprecht, J. Dudaczek, P. Wich, T. Rehm and U. Machon, *Eur. J. Org. Chem.*, 2008, **2008**, 324.

50. P. Blondeau, M. Segura, R. Perez-Fernandez and J. de Mendoza, *Chem. Soc. Rev.*, 2007, **36**, 198-210.

51. M. Haj-Zaroubi and F. P. Schmidtchen, *Chemphyschem*, 2005, **6**, 1181-1186.

52. C. Schmuck, *Coord. Chem. Rev.*, 2006, **250**, 3053-3067.

53. M. D. Best, S. L. Tobey and E. V. Anslyn, *Coord. Chem. Rev.*, 2003, **240**, 3-15.

54. R. P. Dixon, S. J. Geib and A. D. Hamilton, *J. Am. Chem. Soc.*, 1992, **114**, 365-366.

55. K. Ariga and E. V. Anslyn, *J. Org. Chem.*, 1992, **57**, 417-420.

56. B. R. Linton, M. S. Goodman, E. Fan, S. A. van Arman and A. D. Hamilton, *J. Org. Chem.*, 2001, **66**, 7313-7319.

57. P. D. Beer, M. G. B. Drew and D. K. Smith, *J. Organomet. Chem.*, 1997, **543**, 259-261.

58. S. R. Collinson, T. Gelbrich, M. B. Hursthouse and J. H. R. Tucker, *Chem. Commun.*, 2001, 555-556.

59. P. Debroy, M. Banerjee, M. Prasad, S. P. Moulik and S. Roy, *Org. Lett.*, 2005, **7**, 403-406.

60. J. Li, H. Lin and H. Lin, *J. Coord. Chem.*, 2009, **62**, 1921-1927.

61. S. R. Bayly and P. D. Beer, in *Recognition of Anions*, ed. R. Vilar, 2008, vol. 129, pp. 45-94.

62. T. Moriuchi, A. Nomoto, K. Yoshida and T. Hirao, *Organometallics*, 2001, **20**, 1008-1013.

63. P. D. Beer and J. Cadman, *Coord. Chem. Rev.*, 2000, **205**, 131-155.

64. X. L. Cui, R. Delgado, H. M. Carapuca, M. G. B. Drew and V. Felix, *Dalton Trans.*, 2005, 3297-3306.

65. Y. Willener, K. A. Joly, C. J. Moody and J. H. R. Tucker, *J. Org. Chem.*, 2008, **73**, 1225-1233.

66. A. Sola, R. A. Orenes, M. A. Garcia, R. M. Claramunt, I. Alkorta, J. Elguero, A. Tarraga and P. Molina, *Inorg. Chem.*, 2011, **50**, 4212-4220.

67. A. Sola, A. Tarraga and P. Molina, *Dalton Trans.*, 2012, **41**, 8401-8409.

68. Å. Lorenzo, E. Aller and P. Molina, *Tetrahedron*, 2009, **65**, 1397-1401.

69. F. Oton, A. Espinosa, A. Tarraga, C. R. de Arellano and P. Molina, *Chem. Eur. J.*, 2007, **13**, 5742-5752.

70. F. Oton, A. Tarraga and P. Molina, *Org. Lett.*, 2006, **8**, 2107-2110.

71. B. Tomapatanaget, T. Tuntulani and O. Chailapakul, *Org. Lett.*, 2003, **5**, 1539-1542.

72. P. D. Beer, *Acc. Chem. Res.*, 1998, **31**, 71-80.

73. K. S. Wang, S. Munoz, L. T. Zhang, R. Castro, A. E. Kaifer and G. W. Gokel, *J. Am. Chem. Soc.*, 1996, **118**, 6707-6715.

74. C. L. Beck, S. A. Berg and A. H. Winter, *Org. Biomol. Chem.*, 2013, **11**, 5827-5835.

75. W. S. Jeon, K. Moon, S. H. Park, H. Chun, Y. H. Ko, J. Y. Lee, E. S. Lee, S. Samal, N. Selvapalam, M. V. Rekharsky, V. Sindelar, D. Sobransingh, Y. Inoue, A. E. Kaifer and K. Kim, *J. Am. Chem. Soc.*, 2005, **127**, 12984-12989.

76. M. V. Rekharsky, T. Mori, C. Yang, Y. H. Ko, N. Selvapalam, H. Kim, D. Sobransingh, A. E. Kaifer, S. Liu, L. Isaacs, W. Chen, S. Moghaddam, M. K. Gilson, K. Kim and Y. Inoue, *Proc. Natl. Acad. Sci. USA*, 2007, **104**, 20737-20742.

77. L. Cui, S. Gadde, W. Li and A. E. Kaifer, *Langmuir*, 2009, **25**, 13763-13769.

78. A. E. Kaifer, *Chemphyschem*, 2013, **14**, 1107-1108.

79. S. Yi, W. Li, D. Nieto, I. Cuadrado and A. E. Kaifer, *Org. Biomol. Chem.*, 2013, **11**, 287-293.

CHAPTER 1

PINCHER FERROCENE-DERIVED CATION CARBOXYLATE ION PAIRS IN AQUEOUS DMSO[1]

Taken in part from: Beck, C. L.; Berg, S. A.; Winter, A. H., *Org. Biomol. Chem.*, 2013, **11**, 5827.

INTRODUCTION

The rational synthesis of complex aggregates from simple building blocks remains an ongoing challenge in supramolecular chemistry.[2-6] The majority of self-assembled architectures reported to date rely on electrostatic interactions (ion-ion, H bonds) between building blocks.[2, 3, 7-12] While these electrostatic forces lead to aggregates in solvents such as chloroform, usually they fall apart in polar solvents such as DMSO or water where the strengths of these interactions are diminished by competitive interactions with solvent.[13-18]

In contrast to this general trend, a series of investigations have shown that aggregates containing a guanidinium-carboxylate interaction can persist even in highly polar solutions.[19-22] Experimental binding studies in combination with computational investigations have suggested that the charged nature of the host and guest is essential to understanding the stability of these guanidinium-carboxylate pairs in water.[19] The charged nature of the host and guest help with complex formation by providing an additional electrostatic interaction, by increasing the strength of the H-bonds (charge-assisted), and by improving the entropy of binding by returning ordered ion-solvating waters into the bulk when the charges are "quenched" (e.g. $\Delta S_{solvation} > 0$).[9, 13, 19, 23]

It is essential to understand how to maximize the binding of a host to a single functional group such as carboxylate to permit the design of improved self-assemblies with cooperative multivalent interactions, particularly for self-assembly in water.[24] Strong cooperative interactions are essential for the molecular recognition of biomolecules[25] such as peptides,[26-29] in the design of organocatalysts,[30, 31] and the design of complex self-assemblies in general. Towards this goal, we anticipated that recruiting additional interactions to the carboxylate could increase the strength of the complex.[23] Here we report the synthesis of several pincher bis(guanidinium) salts using a ferrocene core and the binding of these dications to benzoate. Binding studies using NMR titrations indicate that these ions form tight complexes in aqueous DMSO solutions and that additional electrostatic interactions dramatically increase the complex stability. We find that ferrocene is a potentially useful semi-flexible backbone that may allow the construction of switchable self-assemblies in water.[32-45]

RESULTS AND DISCUSSION

The (di)cationic hosts for benzoate used in this study are shown in Figure 1. With one exception, the binding constants for these hosts were determined in aqueous DMSO mixtures to benzoate. The complex of **10** with benzoate precipitates in D_2O so we bound **10** to acetate instead. Compounds **7** and **8** were unstable to hydrolysis of the acyl moiety, so association constants were not obtained for these ions. Compound **9** was used as a computational control (described *vide infra*). The binding constants and binding isotherms can be seen in Figures 2 and 3.

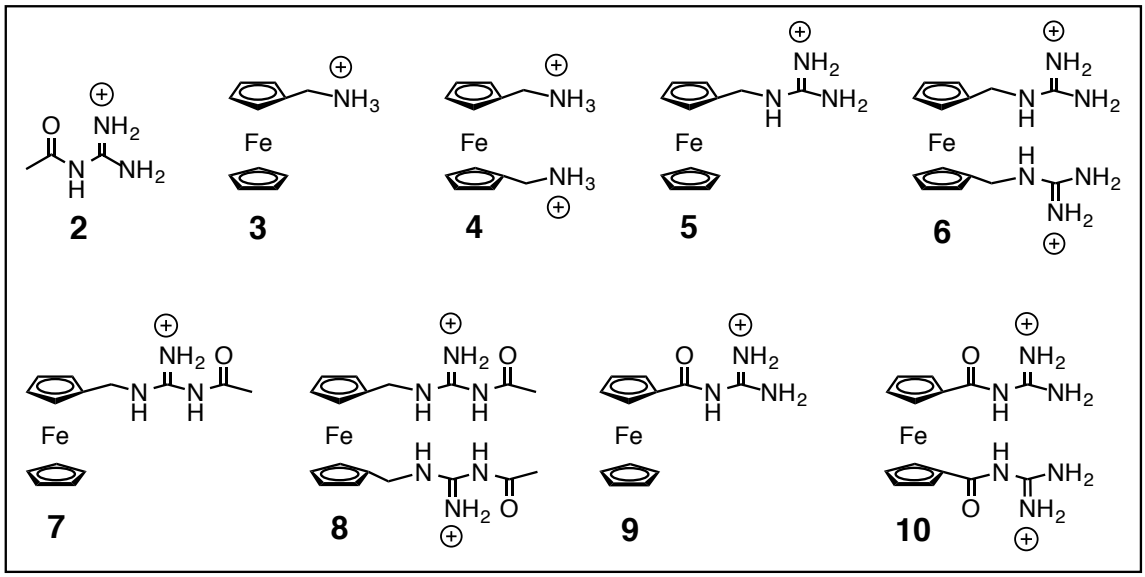

Figure 1. (Di)cationic hosts described in this study.

Effect of solvent on association constant. The binding of the acylguanidinium ion **2** to carboxylates is well known.[15, 46] Thus, we used this cation as a control to ensure that we were able to reproduce literature-reported association constants and provide a reference for the association of a carboxylate to a mono guanidinium cation. Guanidinium ion itself does not significantly bind carboxylates in aqueous DMSO solutions[46-48] but the acylguanidinium ion does due to the acyl group increasing the acidity of the H-bonding protons,[49] leading to stronger hydrogen bonds.[20] As typified from titration of the "control" compound acylguanidinium tetrafluoroborate **2**, the solvent has a dramatic effect on the binding constant to benzoate. Consistent with previous studies of this compound, while the binding constant (K_a) for **2** was 1090 M^{-1} in 9:1 DMSO:D_2O, the binding constant was negligible in 1:1 DMSO:D_2O (Figure 2). Benzoate has limited solubility in pure DMSO, which precluded study in neat DMSO. This general trend is observed for all the (di)cations, as the binding constants are much

larger in 9:1 DMSO:D_2O than in 1:1 DMSO:D_2O and much larger in 1:1 DMSO:D_2O than in neat D_2O.

Importance of cooperativity on complex stability. A comparison between the binding of the monocationic and dicationic hosts is instructive to evaluate the effect of cooperativity on the complex stability.[25] The effect of the additional cation on the association constant is dramatic in all solvent systems studied.[50-52] For instance, the mono ammonium salt **3** has a binding constant of 45 M^{-1} in 9:1 DMSO:D_2O, while the bis(ammonium) salt **4** has a binding constant of 1020 M^{-1} in the same solvent system. The bis(ammonium) dication **4** even achieves a (weak) binding constant of 30 M^{-1} in pure D_2O, which is surprising since ammonium salts are unable to form strong H-bonds in water. The mono guanidinium salt **5** has an association constant of 175 M^{-1} in 9:1 DMSO, and the bis(guanidinium) ion **6** has an association constant of 11,000 M^{-1} under the same conditions. These data demonstrate the importance of recruiting additional cooperative electrostatic interactions to achieve highly stable complexes in competitive solvents (See Figure 2 and Table 1).[53]

Binding in neat water is significant only for pincher dicationic hosts. It is challenging to achieve complexation in neat water without exploiting hydrophobic interactions.[54-57] Indeed, all of the (di)cations studied in this paper showed small or negligible binding in pure water, with the exception of bis(guanidinium) pincher **6** and the bis(acylguanidinium) derivative **10** which achieve association constants of 50 M^{-1} and 850 M^{-1} to benzoate and acetate, respectively. The larger binding constant for **10** over **6** can be attributed to the carbonyl increasing the acidity of the N-H bonds, which is

known to increase the strength of the resulting hydrogen bonds.[49] It should be noted, however, that the switch from benzoate to acetate as the counter ion hinders a direct comparison (the complex of benzoate with **10** precipitates from D_2O above 2 equivalents of benzoate, which is why we report the association constant for this dication with acetate). While making comparisons of association constants between studies can be hazardous due to small changes in conditions (salt, pH, solvent, fitting parameters, etc) leading to significant differences in association constants, it should be noted that the association constant of **10** to acetate is one of the highest reported for a host to a mono-carboxylate in neat water that relies only on electrostatic interactions.[24, 54, 58] We attribute this tight binding to the ferrocene providing a semi-flexible backbone with only a pivot joint-type of flexibility to allow the compound to find appropriately directional H-bonding, but that is otherwise rigid to minimize the entropic penalties of binding.[59, 60] The two acyl(guanidinium) ions in **10** also provide strong cooperative hydrogen bonding opportunities for the carboxylate ion.

Table 1. Binding constants of **1** with **2-6** in aqueous DMSO solutions

Substrate	% DMSO	K_a (M^{-1})
2	90	1,090
2	80	900
2	70	540
2	60	185
2	50	7
3	90	45
4	90	1,020
4	50	150
4	0	30
5	90	175
6	90	11,000
6	50	4,380
6	0	50
10[†] [‡]	90	$>10^6$
10[†]	50	39,000
10[†]	0	850

Estimated error limit in K_a < ± 25%

[†]Carboxylate is acetate instead of benzoate due to solubility problems.

[‡]UV-vis titrations were performed and the absorbance at 325 nm was measured.

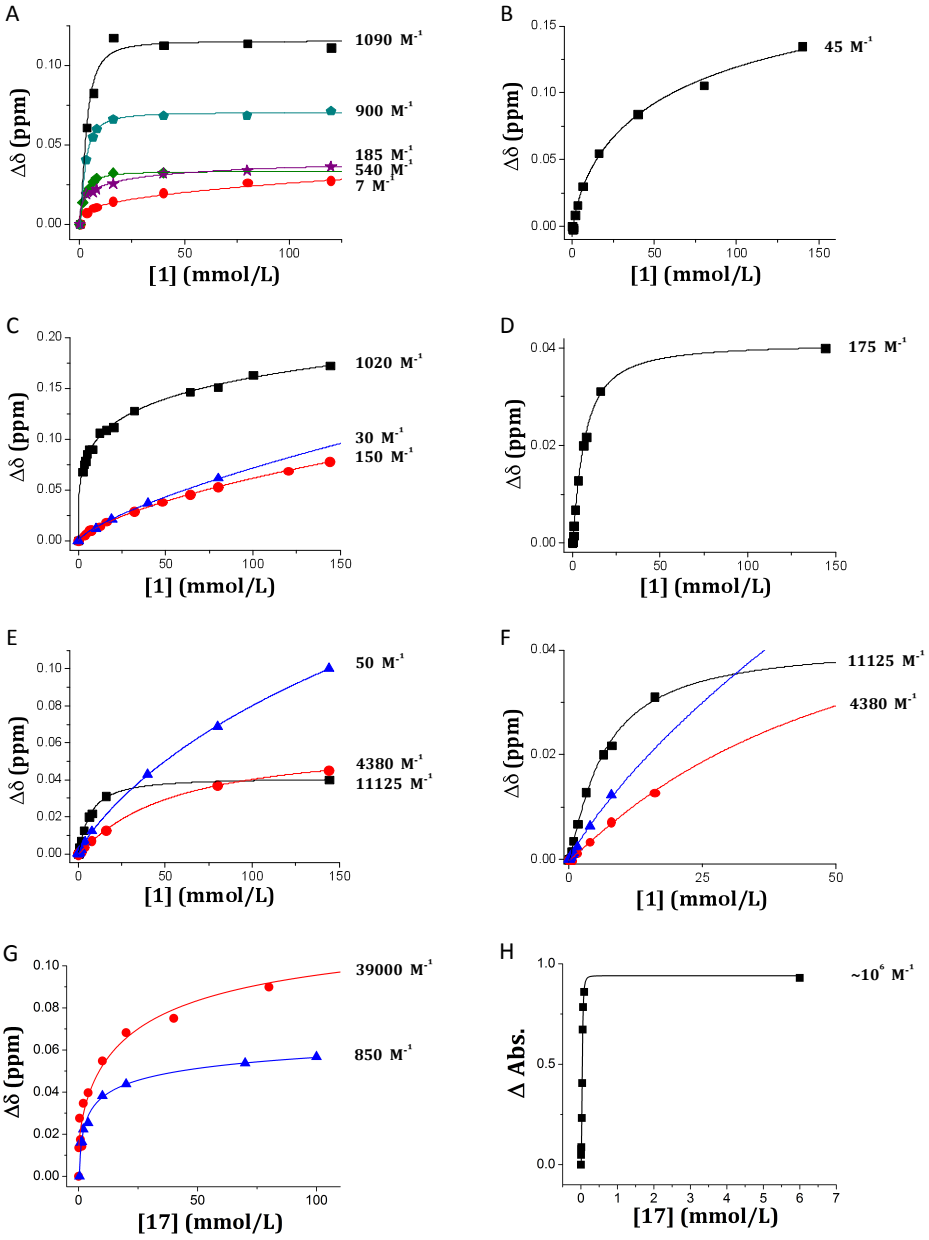

Figure 2. Binding curves and fits from titration of cations **2** (A), **3** (B), **4** (C), **5** (D), **6** (E and F), **10** (G and H) with benzoate **1** (acetate **17** for **10**) following the methyl peak in A, and the ferrocenyl proton in B-F, and in G 50% DMSO. The carboxylate's acetate proton was followed in G for pure D_2O. Percent DMSO-d_6: Black square (90), Teal pentagon (80), Green diamond (70), Purple star (60) Red circle (50), Blue triangle (0).

DFT calculations of complex enthalpy correlate well with complex association constants. DFT computations (B3LYP/6-31G(d))[61] were used to compute the geometries and binding enthalpies of complexes **2-10**. Previous studies have shown that trends in binding enthalpies for related cationic hosts match well with experimental data, even though such calculations omit entropic considerations and explicit solvent effects.[8] A considerable effort was made to find the global minima for the complex structures by optimizing numerous alternative input geometries and group orientations at a lower level of theory (B3LYP/STO-3G), which led us to find numerous local minima, particularly for the pincher complexes. The lowest minimum found at the lower level of theory was optimized with the larger basis set. A PCM water solvation model was employed.

The computed structures of the complexes are shown in Figure 3 and the binding enthalpies are shown in Table 2. As can be seen from Table 2 and the graphical depictions of the complexes (Figure 4), the computed binding enthalpies correlate well with the experimentally determined association constants (Figure 5). It is possible that the changes in entropy upon binding are similar between the complexes, which may allow the computations to correlate well with the experimental data even though they omit explicit solvents and entropy changes.[8] These data bode well for the use of computation in the design of novel tight-binding cationic hosts for carboxylate ions.

Table 2. Computed changes in binding enthalpy for carboxylate complexes of (di)cations **2-10** (B3LYP/6-31G(d)).

Complex	Δ Enthalpy (kcal/mol)
2	-30.30
3	-23.17
4	-31.74
5	-25.38
6	-32.23
7	-28.69
8	-38.38
9	-30.04
10*	-45.08

*Acetate was the carboxylate rather than benzoate.

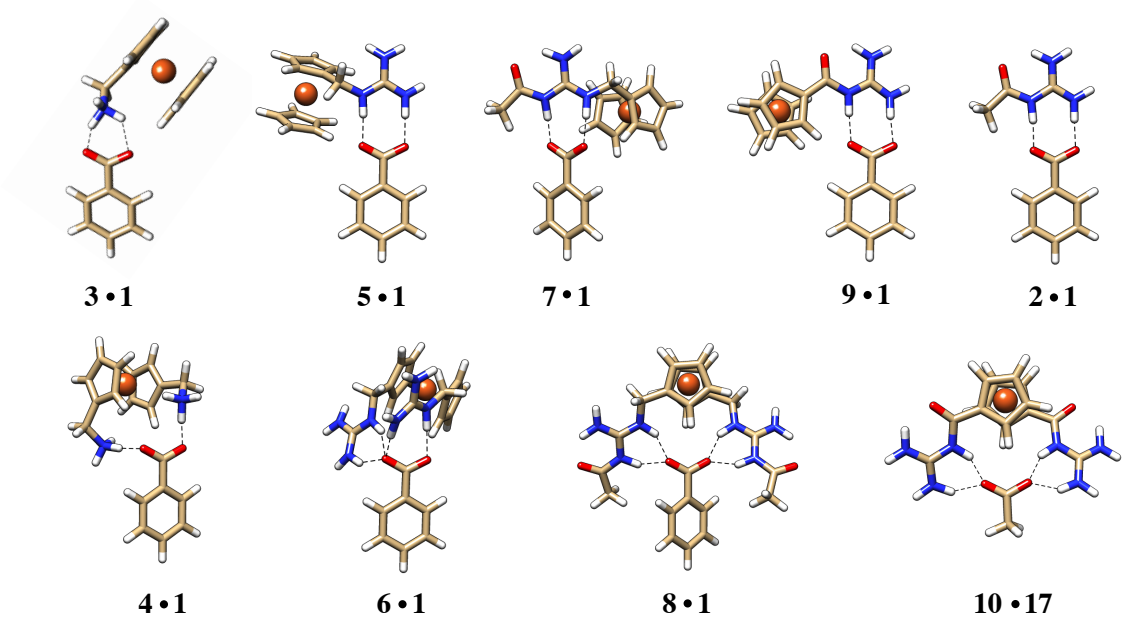

Figure 3. Computed structures of the 1:1 association complexes (B3LYP/6-31 G(d)). Lowest minima found are shown.

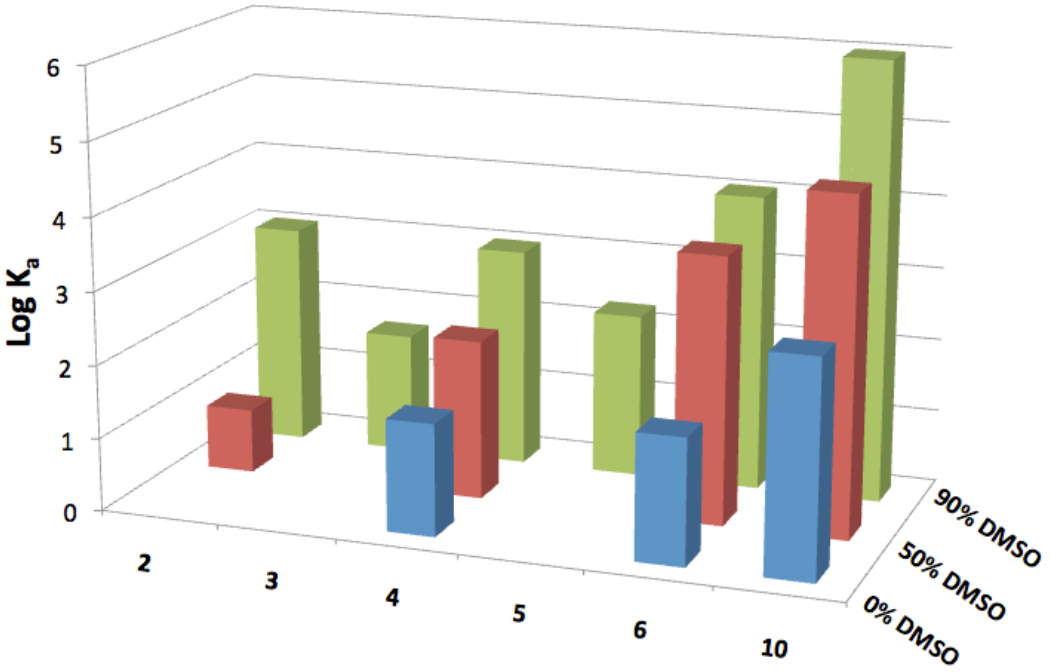

Figure 4. Graphical depiction of binding constants of compounds **2-6, 10** in aqueous DMSO solutions.

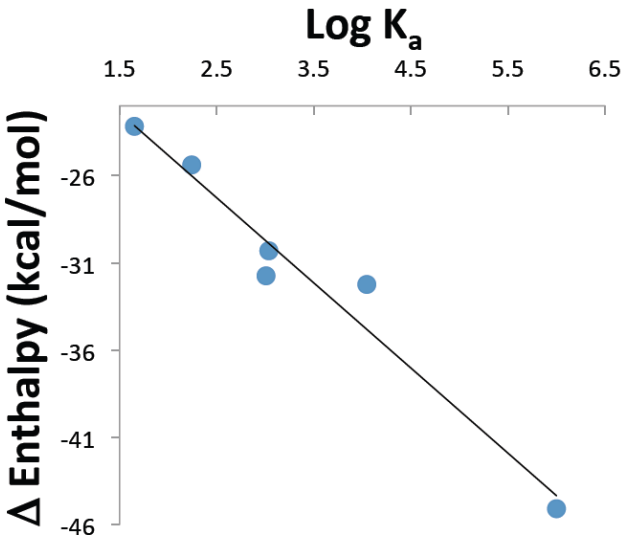

Figure 5. Plot of computed enthalpy change in binding (B3LYP/6-31G(d)) versus log K_a shows a reasonable correlation.

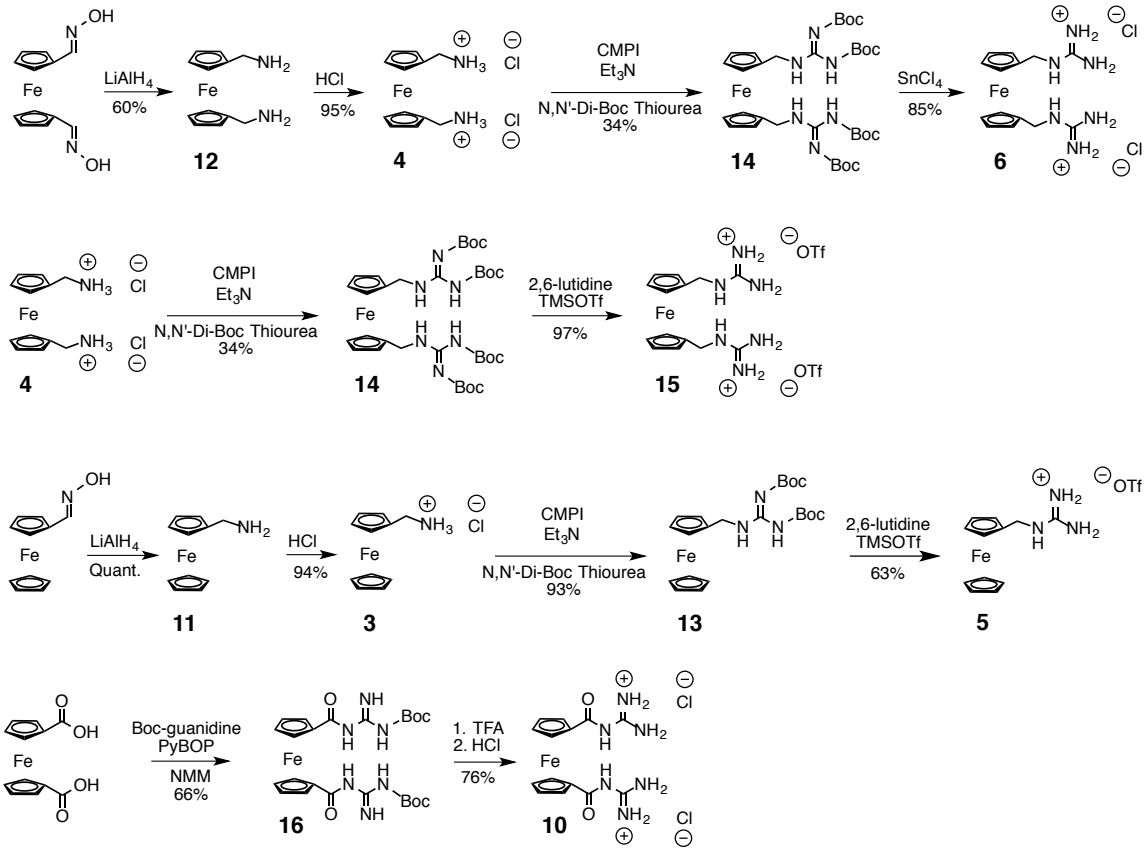

Scheme 1. Synthetic schemes for cations **3-6, 10**

EXPERIMENTAL

Materials and methods. Anhydrous solvents were purchased from Acros Organics. Ferrocene was recrystallized from ethanol prior to use. Boc anhydride was purified following a procedure from literature. [66] Ferrocene carboxaldehyde,[67, 68] Ferrocene carboxaldehyde oxime,[69, 70] Di-Boc thiourea,[71-73] 1,1'- ferrocene dicarboxaldehyde,[74] 1,1'- ferrocene dicarboxaldehyde dioxime,[69] 1,1'-diacetylferrocene,[75, 76] 1,1'-ferrocene dicarboxylic acid,[75, 76] and Boc-guanidine[77] were all synthesized following literature procedures. All spectra matched literature values. All

other chemicals were purchased from Aldrich, Fisher Scientific, or Oakwood Chemical and used without further purification.

Synthesis of (di)cation hosts. Ferrocene compound **11** was synthesized by reduction of the ferrocene carboxaldehyde oxime with lithium aluminium hydride (LAH) to form aminomethyl ferrocene **11**. Addition of dry HCl to this product afforded product **3** as the chloride salt. Compound **3** was then reacted with N,N'-di-Boc protected thiourea and Mukaiyama's reagent to form compound **13** in excellent yield.[62] Deprotection with TMSOTf afforded the desired salt **5**.[63] TMSOTf was used as the deprotection agent because typical deprotection with TFA led to *tert.* butyl alkylation product, and $SnCl_4$ caused oxidation of the ferrocene to its richly-colored ferrocenium ion.[64] Reduction of 1,1'-ferrocene dicarboxaldehyde dioxime with LAH formed the unstable amine intermediate product **12**, which was then turned into the stable 1,1'-bis(aminomethyl)ferrocene hydrochloride **4** by addition of dry HCl solution. PyBOP was used to couple ferrocene dicarboxylic acid with Boc-guanidine to yield compound **16**.[65] Compound **10** was formed after deprotection of **16** with standard TFA deprotection conditions.[14]

Reaction of compounds **3** or **4** with **18** and Mukaiyama's reagent formed the Boc-protected versions of **7** and **8**, but these compounds were unfortunately unstable to repeated attempts to purification by silica gel and alumina column chromatography and could never be isolated as pure compounds.

N-acetylguanidinium tetrafluoroborate (2). N-acetylguanidine (1.0 g, 9.89 mmol, 1 eq.) was dissolved in 5 mL MeOH. Tetrafluoroboric acid diethyl ether complex (2.69 mL, 19.78 mmol, 2 eq.) was added to the mixture, and the contents stirred overnight at rt before excess diethyl ether (125 mL) was added to the flask to precipitate the salt. The resulting solid was filtered and washed with diethyl ether to afford 1.76 g (94%) as a white solid. mp = 165-167 °C; ^{1}H NMR (CD_3OD, 400 MHz) δ = 2.67(s, 3H); ^{13}C NMR (D_2O, 100 MHz) δ = 23.7, 154.4, 174.7.

Aminomethylferrocene (11). $LiAlH_4$ (2.74g, 72.13 mmol, 5 eq.) was dissolved in 100 mL dry THF and cooled to 0 °C under argon. Ferrocene carboxaldehyde oxime, (3.30 g, 14.43 mmol, 1 eq.) dissolved in 50 mL of THF was slowly added to the flask containing $LiAlH_4$. The resulting mixture was heated to reflux, under argon, and stirred overnight before it was cooled to -40 °C and quenched slowly with water. During quenching, the rate of water addition was approximately 5 mL per 15 minutes. Prior to being fully quenched, a thick slurry formed within the flask. The compound was extracted several times with $CHCl_3$ (5 x 250mL), washed with brine, and then dried over anhydrous Na_2SO_4. The solvent was removed under reduced pressure affording the desired compound in quantitative yield as an unstable yellow oil: ^{1}H NMR (CD_3OD-d_4, 400 MHz): δ = 3.50 (s, 2H,), 4.11 (t, J = 2 Hz, 2H), 4.15 (s, 5H), 4.21 (t, J = 2 Hz, 2H); ^{13}C NMR (CD_3OD-d_4, 100 MHz) δ = 40.6, 69.9, 70.4, 70.6, 79.7; HR-MS(ESI$^+$) *m/z* = 215.0390 $(M)^+$, (calculated for $C_{11}H_{13}FeN$: 215.0397). [Note: Due to rapid decomposition, excess heat while rotovapping should be avoided. Temperatures should

not to exceed 50 °C].

Aminomethylferrocene hydrochloride (3). The unstable aminomethylferrocene **(11)** (3.10g, 14.43 mmol, 1 eq.) was dissolved in 15 mL of dry dichloromethane. 2 M dry HCl/ diethyl ether solution (10.8 mL, 21.64 mmol, 1.5 eq.) was added to the solution. The resulting mixture was allowed to stir at rt under argon for 15 min before the solid was filtered and washed with diethyl ether and dichloromethane. The goldenrod-colored solid was dried *in vacuo*, affording 3.39 g (94%) of stable product: mp = 180 °C (decomp); ^{1}H NMR (CD_3OD-d_4, 400 MHz) δ = 3.90 (s, 2H,), 4.21 (s 5H) 4.27 (t, J = 2 Hz, 2H), 4.35(t, J = 2 Hz, 2H); ^{13}C NMR (CD_3OD, 100 MHz) δ = 40.6, 69.9, 70.4, 70.6, 79.7; HR-MS(ESI$^+$) *m/z* = 215.0390 (M^+), (calculated for $C_{11}H_{13}FeN$: 215.0397).

1,1'-di(aminomethyl)ferrocene (12). $LiAlH_4$ (3.6 g, 96.5 mmol, 10.5 eq.) was dissolved in 100 mL dry THF and cooled to 0 °C under argon. 1,1'-ferrocene dicarboxaldehyde dioxime, (2.5 g, 9.2 mmol, 1 eq.) dissolved in 100 mL dry THF, was slowly added to the flask containing $LiAlH_4$. The resulting mixture was heated to reflux and stirred for 6 h before it was cooled to -40 °C and slowly quenched with water, with a rate of water addition of 5 mL per 15 min. Prior to being fully quenched, a thick slurry formed within the flask. The solution was extracted several times with $CHCl_3$ (5 x 250 mL), washed with brine, and then dried over Na_2SO_4. The solvent was removed under reduced pressure. Purification by silica gel column chromatography (40 – 60 micron mesh) with MeOH/ NH_4OH (9:1) afforded 1.32 g (60%) as an unstable yellow oil that

decomposes to a purple oil upon standing within minutes to hours: ^{1}H NMR (CD_3OD, 400 MHz) δ = 3.52 (s, 4H,), 4.12 (t, J = 2 Hz, 4H), 4.20 (t, J = 2 Hz, 4H); ^{13}C NMR (CD_3OD, 100 MHz) δ = 41.4, 69.2, 69.5, 90.1; HR-MS(ESI$^+$) *m/z* = 244.0657 (M^+), (calculated for $C_{12}H_{16}FeN_2$: 244.0663). [Note: Due to rapid decomposition, excess heat while rotovapping should be avoided. Temperatures should not to exceed 50 °C].

1,1'-di(aminomethyl)ferrocene hydrochloride (4). 1,1'-di(aminomethyl)ferrocene **(12)** (1.32 g, 5.49 mmol, 1 eq.) was dissolved in 5 mL methanol. 2 M dry HCl/ diethyl ether solution (5.50 mL, 10.98 mmol, 2 eq.) was added to the flask. The mixture was allowed to stir for 15 minutes at ambient temperature. Excess diethyl ether (200 mL) was added to the solution to fully precipitate the salt. The solid was filtered and washed with diethyl ether (125 mL) to afford 1.63 g (95%) of the desired stable product as a golden powder: mp = 205 °C (decomp); ^{1}H NMR (CD_3OD, 400 MHz) δ = 4.078 (s, 4H,), 4.44 (t, J = 2 Hz, 4H), 4.51 (t, J = 2 Hz, 4H). ^{13}C NMR (CD_3OD, 100 MHz) δ = 38.8, 70.2, 70.4, 78.8; HR-MS(ESI$^+$) *m/z* = 244.0657 (M^+), (calculated for $C_{12}H_{16}FeN_2$: 244.0663).

N, N'-*tert*-butyl carbamate guanidinylmethyl ferrocene (13). Aminomethylferrocene hydrochloride **(3)** (1.0 g, 3.98 mmol, 1 eq.), N,N'-Di-Boc-thiourea (2.20 g, 7.95 mmol, 2 eq.), and 2-chloro-1-methylpyridinium iodide (3.55 g, 7.95 mmol, 2 eq.) were dissolved in 75 mL CH_2Cl_2 at rt under argon. Et_3N (11.1 mL, 79.5 mmol, 20 eq.) was added to the

flask. The mixture was heated to reflux and stirred for 7 hours under argon before it was cooled to ambient temperature. Contents were filtered over a plug of silica gel and washed with copious amounts of hexanes/ EtOAc (7:3) (500 mL) to remove excess 2-chloro-1-methylpyridinium iodide. The filtrate was removed under reduced pressure. Purification by silica gel column chromatography with hexanes/ EtOAc (85:15) afforded 1.01 g (93%) of the desired product as a yellow powder. [Notes: Solvent is extremely important for this reaction. More polar solvents (acetonitrile) will yield no desired product. The pyridinium salt will not dissolve in dichloromethane, which allows for the slow formation of the unstable imine intermediate. As a side product of this reaction, *tert*-butyl carbamate is formed (spectra were compared to that from literature to confirm this). This impurity may be removed prior to column chromatography by doing an acid extraction with slightly acidic (pH ~ 4-5) water, making column chromatography easier, but is not required]. mp = 143-145 ˚C; ^{1}H NMR (CD_3OD, 400 MHz) δ = 1.48 (s, 9H), δ 1.55 (s, 9H) δ 4.18 (t, J = 2 Hz, 2H), 4.21 (broad s, 4H), 4.22 (s, 5H); ^{13}C NMR ($CDCl_3$, 100 MHz) δ = 28.2, 28.5, 40.6, 67.6, 68.1, 68.8, 79.5, 83.3, 84.3, 153.3, 155.7, 163.7; HR-MS(ESI$^+$) *m/z* = 458.1745 (M^+), (calculated for $C_{22}H_{32}FeN_3O_4$: 458.1742).

Guanidinylmethylferrocene Triflate (5). Compound **13** (100 mg, 0.219 mmol, 1 eq.) was dissolved in 20 mL dry dichloromethane at rt under argon. 2,6-lutidine (0.76 mL, 6.56 mmol, 30 eq.), followed by TMSOTf (1.0 mL, 5.47 mmol, 25 eq.) were added to the flask. The resulting solution refluxed for 2 days under argon with stirring, before being cooled to 0 °C and quenched with water. No extraction was performed. The

dichloromethane was removed by rotary evaporation. Excess 2,6-lutidine was removed by column chromatography in $CHCl_3$/ MeOH (95:5). Further purification by preparatory TLC plate with $CHCl_3$/ MeOH (9:1) afforded the desired product 56.3 mg (63%) as a yellow powder. [Notes: Addition of EtOAc creates a side product that is difficult to remove, so EtOAc was avoided. The first column removes most of the 2,6-lutidine, but some co-elutes with the desired product, so preparatory TLC was also used]. mp = 180 °C (decomp); ^{1}H NMR (DMSO-d_6, 400 MHz) δ = 4.05 (s, 2H), δ 4.15 (t, J = 2 Hz, 2H), 4.18 (s, 5H), 4.23 (t, J = 2 Hz, 2H); ^{13}C NMR (CD_3OD, 100 MHz) δ = 47.0, 69.4, 69.7, 69.9, 120.1, 122.1, 123.3, 157.9; ^{19}F NMR (CD_3OD, 376.05 MHz) δ = 80.18; HR-MS(ESI$^+$) *m/z* = 258.0692 $(M+H)^+$, (calculated for $C_{34}H_{52}FeN_6O_8$: 258.0694).

1,1'- ferrocenylmethyl-di-Boc guanidine (14). 1,1'-di(aminomethyl)ferrocene hydrochloride **(4)** (0.10 g, 0.319 mmol, 1 eq.), N,N'-di-Boc-thiourea (0.177 g, 0.629 mmol, 2 eq.), and 2-chloro-1-methylpyridinium iodide (0.284 g, 1.11 mmol, 3.5 eq.) were dissolved in 20 mL dry CH_2Cl_2 and 5 mL dry DMF under argon. Et_3N was added to the flask (0.66 mL, 4.78 mmol, 15 eq.). The mixture was heated to reflux and stirred for 3 h. under argon before it was cooled to rt. Following extraction several times with CH_2Cl_2 to remove DMF, the product was washed with brine and then dried over anhydrous Na_2SO_4. The solvent was removed under reduced pressure. Purification by silica gel column chromatography with hexanes/ EtOAc (7:3) afforded 0.0864 g (37%) of the desired product as a yellow powder. [Notes: Solvent is extremely important for this reaction. More polar solvents (acetonitrile) will yield no desired product. The

pyridinium salt will not dissolve in dichloromethane, which allows for the slow formation of the unstable imine intermediate. As a side product of this reaction, *t*-butyl carbamate is formed; the spectra were compared to that from literature. This impurity can be removed prior to running a column by doing an acid extraction with slightly acidic (pH = ~4-5) water]. mp = 230 °C (decomp); ^{1}H NMR (CD_3OD, 400 MHz) δ = 1.50 (s, 18H), 1.56 (s, 18H), 4.26 (s, 4H), 4.26 (t, J = 2 Hz, 4H), 4.30 (t, J = 2 Hz, 4H); ^{13}C NMR ($CDCl_3$, 100 MHz) δ = 28.2, 28.5, 40.4, 68.3, 69.1, 79.5, 83.3, 84.9, 153.3, 155.7, 163.7; HR-MS(ESI$^+$) *m/z* = 727.3243 (M^+), (calculated for $C_{34}H_{52}FeN_6O_8$: 727.3316).

1,1'-bis(guanidinylmethyl)ferrocene hydrochloride (6). 1,1'- ferrocenylmethyl- di-Boc guanidine (**14**) (0.207 g, 0.284 mmol, 1 eq.) was dissolved in 20 mL EtOAc. $SnCl_4$ (0.27 mL, 2.27 mmol, 8 eq.) was added to the flask. The mixture stirred under argon at ambient temperature for 1.5 hours before the solvent was removed by rotary evaporation without heat. The unstable salt was dissolved in 2 mL MeOH, and then precipitated by the addition of excess diethyl ether (150 mL). The solid was filtered, and then re-dissolved in MeOH for transfer to a flask. The solvent was removed *in vacuo*, without heat, affording 0.0962 g (85%) of the desired yellow salt as a film. [Notes: Typical deprotection conditions with TFA forms ferrocenium ion. Decomposition occurs when heat is used during removal of the EtOAc; this is evident with a color change from yellow to green/ blue. To ensure all removal of $SnCl_4$, the salt may need to be re-dissolved in a small amount of MeOH (less than 1mL), and then re-precipitated with

diethyl ether. Three times of repeating this process typically removes all traces of $SnCl_4$. The salt was not bench stable and was stored on a high vacuum line]. ^{1}H NMR (DMSO-d_6, 400 MHz) δ = 4.32 (s, 4H), 4.48 (t, J = 2 Hz, 4H), 4.52 (t, J = 2 Hz, 4H); ^{13}C NMR (CD_3OD, 100 MHz) δ = 42.0, 70.4, 70.7, 158.0; HR-MS(ESI$^+$) *m/z* = 327.1216 (M^+), (calculated for $C_{14}H_{20}FeN_6$: 327.1218).

1,1'-bis(guanidinylmethyl)ferrocene triflate (15). 1,1'-di(aminomethyl)ferrocene hydrochloride **(4)** (156.3 mg, 0.214 mmol, 1 eq.) was dissolved in 20 mL dry dichloromethane at rt under argon. 2,6-lutidine (1.49 mL, 12.83 mmol, 60 eq.) followed by TMSOTf (1.94 mL, 10.70 mmol, 50 eq.) were added to the flask. The resulting solution was refluxed overnight with stirring, before being cooled to rt and quenched with water and MeOH. The dichloromethane was removed under reduced pressure. Excess 2,6-lutidine was removed by column chromatography in $CHCl_3$/ MeOH (9:1). Purification by preparatory TLC plate with chloroform/ MeOH (9:1) afforded the desired product (129.3 mg, 97%) as a yellow powder. [Notes: Addition of EtOAc will create side product that is difficult to remove, so EtOAc was avoided. The first column removes most of the 2,6-lutidine, but some co-eluted with the desired product, which is why preparatory TLC was also used]. mp = 180 °C (decomp); ^{1}H NMR (DMSO-d_6, 400 MHz) δ = 4.05 (s, 4H), δ 4.19 (t, J = 2 Hz, 4H), 4.25 (t, J = 2 Hz, 4H); ^{13}C NMR (CD_3OD, 100 MHz) δ = 41.7, 70.1, 70.4, 82.3, 116.7, 119.9, 123.0, 126.2, 157.7; ^{19}F NMR (CD_3OD, 376.05 MHz) δ = 80.2; HR-MS(ESI$^+$) *m/z* = 3271216 (M^+), (calculated for $C_{14}H_{20}FeN_6$: 327.1218).

N, N'-*tert*-butyl carbamate (acetylguanidine)ferrocene (16). 1,1'-ferrocene dicarboxylic acid (1.0 g, 3.62 mmol, 1 eq.) and PyBOP (3.77 g, 7.25 mmol, 2 eq.) were dissolved in 30 mL dry DMF under argon. 4-methylmorpholine (2.39 mL, 21.74 mmol, 6 eq.) was added to the flask. The mixture was stirred under argon at rt for 30 min. before Boc-guanidine (2.31 g, 14.49 mmol, 4 eq.) was added to the flask. The contents stirred for 25 hours before the DMF was removed *in vacuo.* The organic phase was extracted several times with CH_2Cl_2 (5 x 100 mL), washed with brine, and dried over anhydrous Na_2SO_4. The solvent was removed under reduced pressure. Purification by silica gel column chromatography with hexanes/ EtOAc (1:1) afforded 1.346g (67%) of the desired product as an orange solid: mp = 85-87 °C; ^{1}H NMR (CD_3OD, 400 MHz) δ = 1.54 (s, 18H), 4.54 (t, J = 2 Hz, 4H), 4.75 (t, J = 2 Hz, 4H); ^{13}C NMR (CD_3OD, 100 MHz) δ= 28.5, 73.0, 73.8, 80.2, 82.3, 158.5, 160.1, 180.2; HR-MS(ESI$^+$) *m/z* = 557.1817 $(M+H)^+$, (calculated for $C_{24}H_{33}FeN_6O_6$: 557.1806).

1,1'-bis(acetylguanidine)ferrocene hydrochloride (10). Compound **16** (2.130 g, 3.83 mmol, 1 eq.) was dissolved in 25 mL TFA. The resulting mixture stirred for one hour at rt before the liquid was removed *in vacuo.* The remaining solid was dissolved in 15 mL MeOH and 45 mL 1.2M HCl solution in water. The mixture was stirred for 2 h before the solid was filtered, affording 1.227 g of **10** (75%) as a salmon-colored powder: mp = 210 °C (decomp); ^{1}H NMR (D_2O, 400 MHz) δ = 4.81 (t, J = 2 Hz, 4H), 5.12 (t, J = 2 Hz, 4H); ^{13}C NMR (CD_3OD, 100 MHz) δ = 72.4, 75.5, 75.9, 156.4, 172.9; HR-MS(ESI$^+$) *m/z*

= 355.0805 (M^+), (calculated for $C_{14}H_{17}FeN_6O_2$: 355.0804).

N-acyl-N'-Boc-thiourea (18). NaH (0.72 g, 18.63 mmol, 1.1 eq.) was dissolved in 20 mL dry THF at 0 °C. N-acylthiourea, (2.0 g, 16.94 mmol, 1 eq.) dissolved in 40 mL dry THF, was slowly added to the flask with NaH. The resulting mixture was allowed to react for 30 minutes before di-*tert*-butyl dicarbonate (4.435 g, 20.35 mmol, 1.2 eq.), dissolved in 20 mL dry THF, was added to the reaction flask. The resultant light green slurry was stirred for under argon from 0 °C to rt. After 24 h., the mixture was cooled to 0 °C and quenched with brine. The organic layer was extracted with EtOAc (3 x 250 mL), washed with brine, and then dried over anhydrous Na_2SO_4. The solvent was removed under reduced pressure. Purification by silica gel column chromatography with hexanes/ EtOAc (7:3) afforded 2.510 g (73%) as bright yellow/green crystals: mp = 112-114 °C; ^{1}H NMR (CD_3OD, 400 MHz) δ = 1.54 (s, 9H), 2.17 (s, 3H); ^{13}C NMR ($CDCl_3$, 100 MHz) δ = 24.8, 27.8, 83.7, 149.9, 170.9, 178.3; HR-MS(ESI$^+$) *m/z* = 241.0616 $(M+Na)^+$, (calculated for $C_8H_{14}N_2O_3S$: 241.0617).

Determination of association constants and complex stoichiometry. Binding constants were determined through NMR titration experiments and calculated using Pall Thordarson's NMR titration fitting software for Matlab.[78] Job plots[79] were used to determine the complex stoichiometry (see Figure 6). In all cases, a maxima in the Job plot corresponding to a 1:1 or 1:2 stoichiometry was observed, although in some cases a bimodal plot was obtained with maxima corresponding to both 1:1 and 1:2

(di)cation:benzoate stoichiometries. In these cases the binding isotherm was fit with 1:2 binding equations and association constants for Ka_1 and Ka_2 were determined. In all cases, Ka_1 was at least an order of magnitude larger than Ka_2 and in most cases several orders of magnitude (Figure 6).

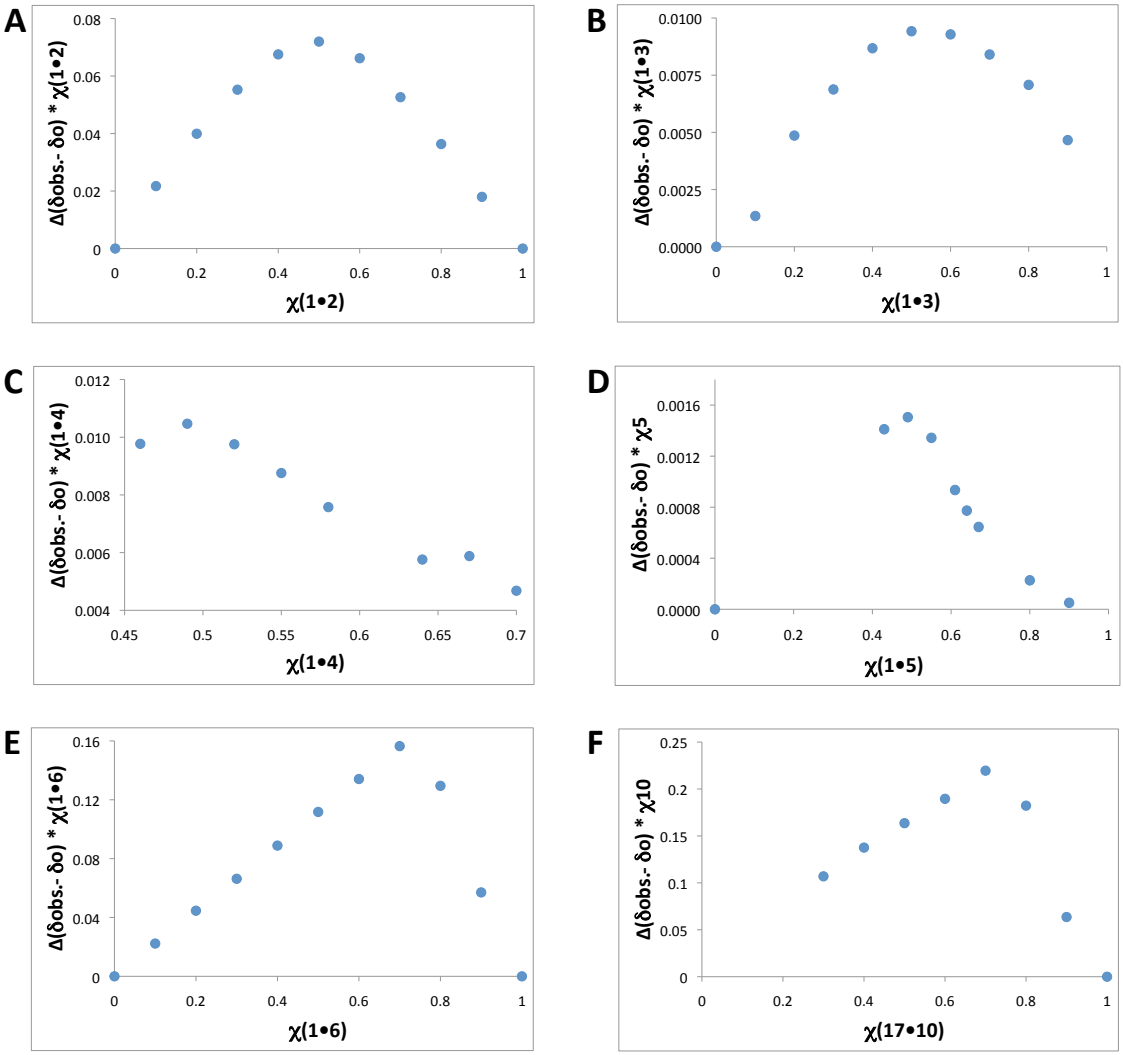

Figure 6. Job's Plots in 9:1 DMSO:D_2O (A-E) and 1:1 DMSO:D_2O (F) depicting a 1:1 stoichiometry between host and guest for cations **2**,**3**, and **5**, and depicting a 1:2 stoichiometry between host and guest for cations **4**,**6**, and **10**.

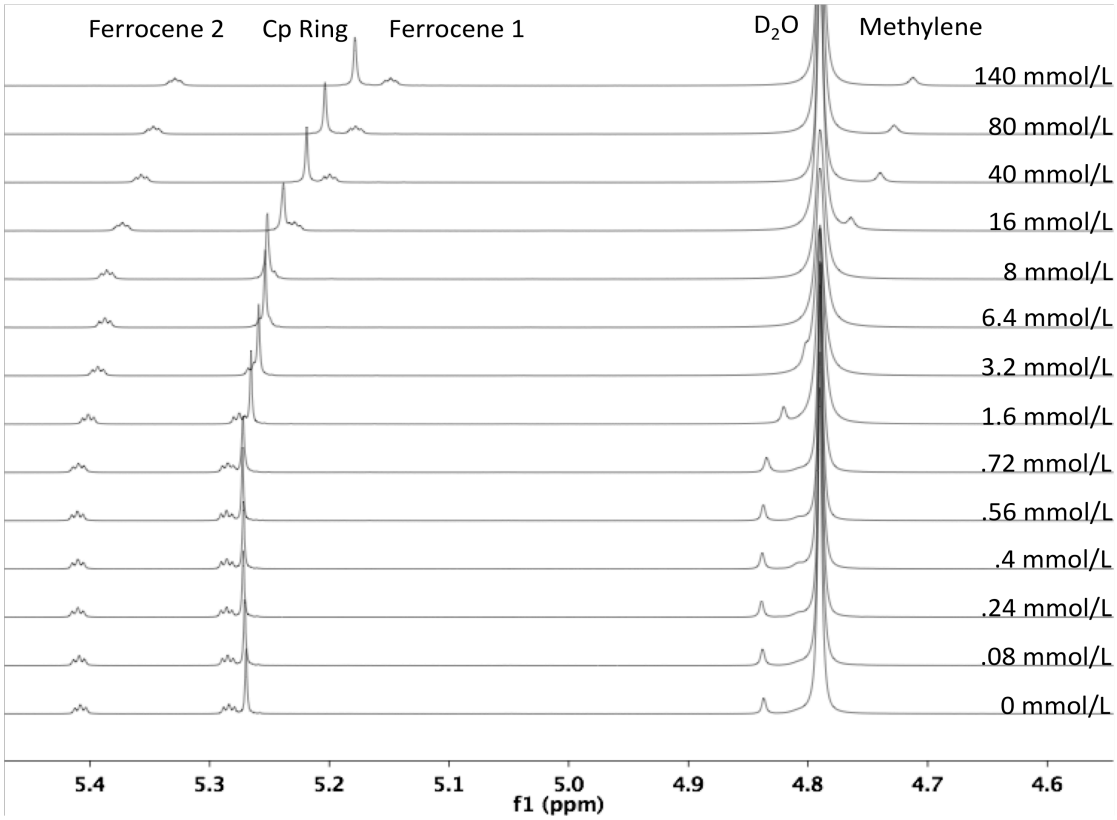

Figure 7. Stacked NMR spectra for a typical NMR titration. Stacked spectra of **3** bound to **1** show the upfield shift of ferrocenyl upon addition of benzoate **1**.

All binding constant titrations were run a minimum of three times, with the reported association constant being the average of the three runs. The NMR chemical shift of the ferrocene peaks (as well as the methylene peaks for **3-6**) were used to obtain the binding curves. See Figure 7 for a representative example. The Ka's represent the average of all the fits. Thus, a typical binding constant represents the average value of 9 different fits for cations **3-6**. In the case of **10** bound to potassium acetate, one of the ferrocene proton signals overlapped with the solvent signal, reducing the number of fits

by one set of data points. One representative fit for each cation is shown in Figure 2. Error in the K_a is estimated to be <25 percent. The binding constants to **10** by acetate were too large to obtain using ^{1}H NMR in solvents with 90% DMSO, so we switched to UV-Vis titrations to determine the association constants for this dication in 9:1 DMSO:H_2O. [24, 78] In 9:1 DMSO:H_2O the binding isotherm for **10** to acetate clearly consists of two unique binding events. These points were removed from Figure 2 for clarity. Thus, we made an estimate of the K_a by fitting only the first binding event.

CONCLUSION

In conclusion, the association constants for cationic ferrocene carboxylate complexes were determined. The effects of recruiting an additional cationic group play a major role in increasing the association constant with benzoate, and some of these dicationic hosts form strong complexes (> 10^6 M^{-1}) even in highly competitive solvents. The complex between pincher dication **10** and acetate is one of the strongest known for a carboxylate in neat water (K_a = 850 M^{-1}) that exploits only electrostatic interactions. The ferrocenyl scaffold may prove to be a useful semi-flexible backbone for switchable self-assembly processes.

REFERENCES

1. C. L. Beck, S. A. Berg and A. H. Winter, *Org. Biomol. Chem.*, 2013, **11**, 5827-5835.

2. D. R. Turner, A. Pastor, M. Alajarin and J. W. Steed, *Supramolecular Assembly Via Hydrogen Bonds I*, 2004, **108**, 97-168.

3. R. Vilar, in *Supramolecular Assembly Via Hydrogen Bonds II*, ed. D. M. P. Mingos, 2004, vol. 111, pp. 85-137.

4. P. D. Beer and P. A. Gale, *Angew. Chem. Int. Ed.*, 2001, **40**, 486-516.

5. J. W. Steed, J. L. Atwood and P. A. Gale, in *Supramol. Chem.*, John Wiley & Sons, Ltd, 2012.

6. V. S. Bryantsev and B. P. Hay, *J. Am. Chem. Soc.*, 2006, **128**, 2035-2042.

7. R. P. Dixon, S. J. Geib and A. D. Hamilton, *J. Am. Chem. Soc.*, 1992, **114**, 365-366.

8. D. Moiani, C. Cavallotti, A. Famulari and C. Schmuck, *Chem. Eur. J.*, 2008, **14**, 5207-5219.

9. L. Sebo, B. Schweizer and F. Diederich, *Helv. Chim. Acta*, 2000, **83**, 80.

10. M. Haj-Zaroubi and F. P. Schmidtchen, *Chemphyschem*, 2005, **6**, 1181-1186.

11. M. D. Best, S. L. Tobey and E. V. Anslyn, *Coord. Chem. Rev.*, 2003, **240**, 3-15.

12. N. L. Bill, D.-S. Kim, S. K. Kim, J. S. Park, V. M. Lynch, N. J. Young, B. P. Hay, Y. Yang, E. V. Anslyn and J. L. Sessler, *Supramol. Chem.*, 2012, **24**, 72-76.

13. T. Rehm and C. Schmuck, *Chem. Commun.*, 2008, 801-813.

14. C. Schmuck, *Eur. J. Org. Chem.*, 1999, 2397-2403.

15. C. Schmuck, *Chem. Eur. J.*, 2000, **6**, 709-718.

16. C. Schmuck, *Tetrahedron*, 2001, **57**, 3063-3067.

17. S. Schlund, C. Schmuck and B. Engels, *Chem. Eur. J.*, 2007, **13**, 6644.

18. R. J. Fitzmaurice, F. Gaggini, N. Srinivasan and J. D. Kilburn, *Org. Biomol. Chem.*, 2007, **5**, 1706-1714.

19. S. Schlund, C. Schmuck and B. Engels, *J. Am. Chem. Soc.*, 2005, **127**, 11115-11124.

20. D. Braga, L. Maini, M. Polito and F. Grepioni, *Supramolecular Assembly Via Hydrogen Bonds II*, 2004, **111**, 1-32.

21. G. W. Bates and P. A. Gale, in *Recognition of Anions*, ed. R. Vilar, 2008, vol. 129, pp. 1-44.

22. M. P. Conley, J. Valero and J. de Mendoza, in *Supramol. Chem.*, John Wiley & Sons, Ltd, 2012.

23. T. H. Rehm and C. Schmuck, *Chem. Soc. Rev.*, 2010, **39**, 3597-3611.

24. J. L. Sessler, P. A. Gale and W.-S. Cho, *Anion Receptor Chemistry - Introduction*, 2006.

25. S.-i. Tamaru and I. Hamachi, in *Recognition of Anions*, ed. R. Vilar, 2008, vol. 129, pp. 95-125.

26. J. S. Albert, M. S. Goodman and A. D. Hamilton, *J. Am. Chem. Soc.*, 1995, **117**, 1143-1144.

27. C. Schmuck and L. Hernandez-Folgado, *Org. Biomol. Chem.*, 2007, **5**, 2390-2394.

28. C. Schmuck and S. Graupner, *Tetrahedron Lett.*, 2005, **46**, 1295-1298.

29. G. Lancelot and C. Helene, *Proc. Natl. Acad. Sci. USA*, 1977, **74**, 4872-4875.

30. R. Gross, G. Durner and M. W. Gobel, *Liebigs Ann. Chem.*, 1994, 49-58.

31. U. Scheffer, A. Strick, V. Ludwig, S. Peter, E. Kalden and M. W. Gobel, *J. Am. Chem. Soc.*, 2005, **127**, 2211-2217.

32. S. R. Bayly and P. D. Beer, in *Recognition of Anions*, ed. R. Vilar, 2008, vol. 129, pp. 45-94.

33. T. Moriuchi, A. Nomoto, K. Yoshida and T. Hirao, *Organometallics*, 2001, **20**, 1008-1013.

34. P. D. Beer and J. Cadman, *Coord. Chem. Rev.*, 2000, **205**, 131-155.

35. X. L. Cui, R. Delgado, H. M. Carapuca, M. G. B. Drew and V. Felix, *Dalton Trans.*, 2005, 3297-3306.

36. Q.-Y. Cao, T. Pradhan, M. H. Lee, K. No and J. S. Kim, *Analyst*, 2012, **137**, 4454-4457.

37. J. Li, H. Lin and H. Lin, *J. Coord. Chem.*, 2009, **62**, 1921-1927.

38. Y. Willener, K. A. Joly, C. J. Moody and J. H. R. Tucker, *J. Org. Chem.*, 2008, **73**, 1225-1233.

39. A. Sola, R. A. Orenes, M. A. Garcia, R. M. Claramunt, I. Alkorta, J. Elguero, A. Tarraga and P. Molina, *Inorg. Chem.*, 2011, **50**, 4212-4220.

40. A. Sola, A. Tarraga and P. Molina, *Dalton Trans.*, 2012, **41**, 8401-8409.

41. Å. Lorenzo, E. Aller and P. Molina, *Tetrahedron*, 2009, **65**, 1397-1401.

42. F. Oton, A. Espinosa, A. Tarraga, C. R. de Arellano and P. Molina, *Chem. Eur. J.*, 2007, **13**, 5742-5752.

43. F. Oton, A. Tarraga and P. Molina, *Org. Lett.*, 2006, **8**, 2107-2110.

44. P. D. Beer, *Acc. Chem. Res.*, 1998, **31**, 71-80.

45. B. Tomapatanaget, T. Tuntulani and O. Chailapakul, *Org. Lett.*, 2003, **5**, 1539-1542.

46. C. Schmuck, *Synlett*, 2011, 1798-1815.

47. K. Ariga and E. V. Anslyn, *J. Org. Chem.*, 1992, **57**, 417-420.

48. B. Linton and A. D. Hamilton, *Tetrahedron*, 1999, **55**, 6027-6038.

49. C. Schmuck, *Coord. Chem. Rev.*, 2006, **250**, 3053-3067.

50. A. Ojida, S. Park, Y. Mito-oka and I. Hamachi, *Tetrahedron Lett.*, 2002, **43**, 6193-6195.

51. X. H. Sun, W. Li, P. F. Xia, H.-B. Luo, Y. Wei, M. S. Wong, Y.-K. Cheng and S. Shuang, *J. Org. Chem.*, 2007, **72**, 2419-2426.

52. T. R. Kelly and M. H. Kim, *J. Am. Chem. Soc.*, 1994, **116**, 7072-7080.

53. D. M. Perreault, X. H. Chen and E. V. Anslyn, *Tetrahedron*, 1995, **51**, 353-362.

54. P. Blondeau, M. Segura, R. Perez-Fernandez and J. de Mendoza, *Chem. Soc. Rev.*, 2007, **36**, 198-210.

55. M. Mazik and H. Cavga, *J. Org. Chem.*, 2006, **71**, 2957-2963.

56. N. Pant and A. D. Hamilton, *J. Am. Chem. Soc.*, 1988, **110**, 2002-2003.

57. C. Cruz, R. Delgado, M. G. B. Drew and V. Felix, *Org. Biomol. Chem.*, 2004, **2**, 2911-2918.

58. B. R. Linton, M. S. Goodman, E. Fan, S. A. van Arman and A. D. Hamilton, *J. Org. Chem.*, 2001, **66**, 7313-7319.

59. A. N. Leung, D. A. Degenhardt and P. Buhlmann, *Tetrahedron*, 2008, **64**, 2530-2536.

60. V. D. Jadhav and F. P. Schmidtchen, *J. Org. Chem.*, 2008, **73**, 1077-1087.

61. M. J. Frisch, G. W. Trucks, H. B. Schlegel, G. E. Scuseria, M. A. Robb, J. R. Cheeseman, G. Scalmani, V. Barone, B. Mennucci, G. A. Petersson, H. Nakatsuji, M. Caricato, X. Li, H. P. Hratchian, A. F. Izmaylov, J. Bloino, G. Zheng, J. L. Sonnenberg, M. Hada, M. Ehara, K. Toyota, R. Fukuda, J. Hasegawa, M. Ishida, T. Nakajima, Y. Honda, O. Kitao, H. Nakai, T. Vreven, J. Montgomery, J. A.; , J. E. Peralta, F. Ogliaro, M. Bearpark, J. J. Heyd, E. Brothers, K. N. Kudin, V. N. Staroverov, R. Kobayashi, J. Normand, K. Raghavachari, A. Rendell, J. C. Burant, S. S. Iyengar, J. Tomasi, M. Cossi, N. Rega, J. M. Millam, M. Klene, J. E. Knox, J. B. Cross, V. Bakken, C. Adamo, J. Jaramillo, R. Gomperts, R. E. Stratmann, O. Yazyev, A. J. Austin, R. Cammi, C. Pomelli, J. W. Ochterski, R. L. Martin, K. Morokuma, V. G. Zakrzewski, G. A. Voth, P. Salvador, J. J. Dannenberg, S. Dapprich, A. D. Daniels, Ö. Farkas, J. B. Foresman, J. V. Ortiz, J. Cioslowski and D. J. Fox, *Gaussian 09, Revision A.02*, 2009.

62. T. Mukaiyama, *Angew. Chem.*, 1979, **91**, 798.

63. H. M. M. Bastiaans, J. L. van der Baan and H. C. J. Ottenheijm, *J. Org. Chem.*, 1997, **62**, 3880-3889.

64. N. G. Connelly and W. E. Geiger, *Chem. Rev.*, 1996, **96**, 877-910.

65. K. Groger, D. Baretic, I. Piantanida, M. Marjanovic, M. Kralj, M. Grabar, S. Tomic and C. Schmuck, *Org. Biomol. Chem.*, 2011, **9**, 198-209.

66. B. M. Pope, Y. Yamamoto and D. S. Tarbell, *Organic Syntheses*, 1988, **50-9**, 418-421.

67. G. D. Broadhead, J. M. Osgerby and P. L. Pauson, *J. Chem. Soc. Res.*, 1958, 650-656.

68. A. F. Neto, J. Miller, V. F. d. Andrade, S. Y. Fujimoto, M. M. d. F. Afonso, F. C. Archanjo, V. A. Darin, M. L. A. e. Silva, Á. D. L. Borges and G. D. Ponte, *Z. Anorg. Allg. Chem.*, 2002, **628**, 209-216.

69. F. Ossola, P. Tomasin, F. Benetollo, E. Foresti and P. A. Vigato, *Inorg. Chim. Acta*, 2003, **353**, 292-300.

70. S. C. B. Gnoatto, A. Dassonville-Klimpt, S. Da Nascimento, P. Galera, K. Boumediene, G. Gosmann, P. Sonnet and S. Moslemi, *Eur. J. Med. Chem.*, 2008, **43**, 1865-1877.

71. A. Exposito, M. Fernandez-Suarez, T. Iglesias, L. Munoz and R. Riguera, *J. Org. Chem.*, 2001, **66**, 4206-4213.

72. E. Iwanowicz, M. A. Poss and J. Lin, *Synth. Commun.*, 1993, **23**, 1443.

73. Z. Ma, C. S. Day and U. Bierbach, *J. Org. Chem.*, 2007, **72**, 5387-5390.

74. A. Connell, P. J. Holliman, I. R. Butler, L. Male, S. J. Coles, P. N. Horton, M. B. Hursthouse, W. Clegg and L. Russo, *J. Organomet. Chem.*, 2009, **694**, 2020.

75. B. Gao, B. Yang, T. Li and B. Zhang, *Synth. Commun.*, 2009, **39**, 2973-2981.

76. F. Knobloch and W. H. Rauscher, *J. Polym. Sci.*, 1961, **54**, 651.

77. N. Ando and S. Terashima, *Tetrahedron*, 2010, **66**, 6224-6237.

78. P. Thordarson, *Chem. Soc. Rev.*, 2011, **40**, 1305-1323.

79. T. Ito, K. Suda, T. Kumamoto, W. Nakanishi, T. Watanabe, T. Ishikawa, H. Seki, M. Kawahata, K. Yamaguchi, Y. Ogura and K. T. Suzuki, *Mol. Divers.*, 2010, **14**, 131-145.

CHAPTER 2

NON-COVALENT CATCH AND RELEASE OF CARBOXYLATES IN WATER[1]

Taken in part from: Beck, C. L.; Winter, A. H., *J. Org. Chem.*, 2014, **79**, 3152-3158.

INTRODUCTION

The design of strong host-guest complexes from small molecules in aqueous solutions continues to be a challenge in supramolecular chemistry.[2-10] In particular, there is considerable interest in developing suitable hosts for monocarboxylates and dicarboxylates since there are numerous examples of (di)carboxylates of biological importance within living systems.[7, 11-22] Strongly-binding selective receptors to carboxylates with a reporting mechanism could find use as biological sensors.[5, 7, 17, 20, 23-30] Additionally, numerous pharmaceuticals contain carboxylate groups,[31-37] and tightly-binding receptors could eventually find use in drug delivery[38] by transporting encapsulated carboxylate pharmacophores to the site of a disease.[35-37, 39, 40]

While there have been numerous studies of receptors that can bind to carboxylates,[14, 41-47] there are fewer examples that retain strong complex affinities in water that rely on electrostatic interactions, since these interactions are diminished by competitive interactions with solvent.[19, 20, 48-50] However, rigid molecules bearing a guanidinium moiety have been shown to bind carboxylates even in polar solutions,[18, 20, 51, 52] but associations strong enough to mimic those in biology are far from realized for these particular systems.[53, 54] The self-assembly of non-covalent structures in polar solvents, such as water or DMSO, relies on electrostatic interactions between the

building blocks.[15, 18, 55-57] These electrostatic forces, coupled with hydrogen-bonding, lead to aggregates in non-polar solvents,[47, 58-64] however many of these complexes fall apart or have low association constants in polar solvents like water, due to competitive interactions with the solvent.[8, 44, 65-67]

Previous work from our lab indicated that a dicationic pincher bis-(acetylguanidinium)ferrocene salt **1** could bind to monocarboxylates in aqueous DMSO.[50] Here we show that **1** forms tight complexes to dicarboxylates in pure water and that additional electrostatic interactions, as well as the size and shape complementarity of the carboxylate to the ferrocene salt, dramatically increase the complex stability. Through NMR studies, we find that upon addition of cucurbit[7]uril (CB[7], **10**), the ferrocene cation-carboxylate complex dissociates, releasing the carboxylate to the bulk solvent demonstrating a non-covalent catch and release process.

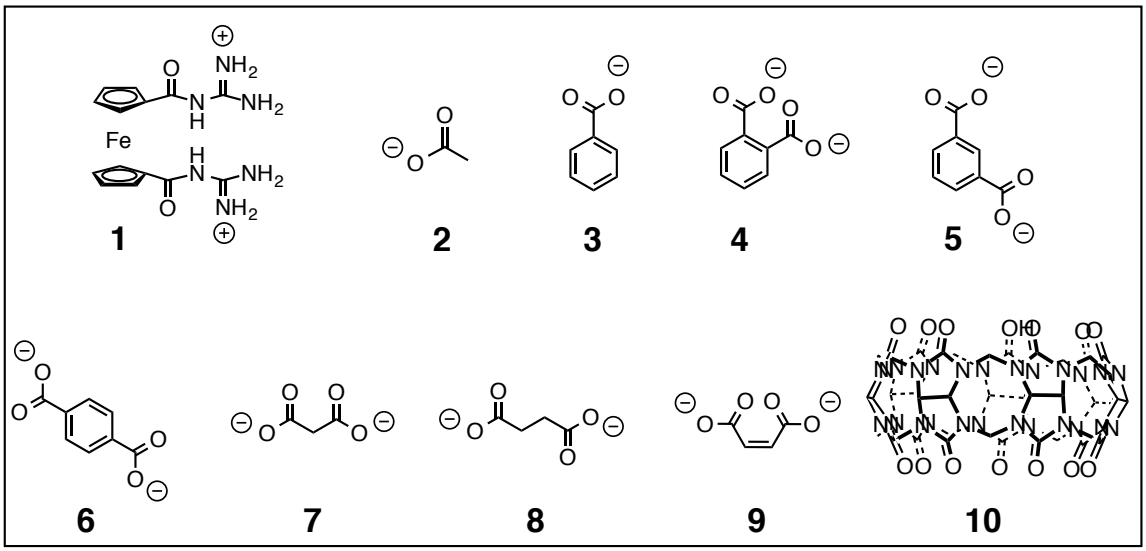

Figure 1. Compounds described in this study

RESULTS AND DISCUSSION

The (di)anionic guests used in this study are shown in Figure 1. With one exception, the binding constants for these guests were determined in neat H_2O by UV-Vis titrations. We have demonstrated the binding of **1** to monocarboxylates in water,[50] and the binding constants and stoichiometry determination of guest **2**, found via NMR titrations, were previously reported in literature.[50] The binding of bis-(acetylguanidinium)ferrocene to acetate **2** in water was used as a comparison for the carboxylates discussed in this paper. Guest **2** was found in previous studies to bind **1** as strongly as 850 M^{-1} (K_{a1}) in neat water by NMR titrations.[50] UV-Vis titrations were performed to determine the association constants of cation **1** bound to carboxylates **3-9**. A 1:1 binding stoichiometry for carboxlates **3-9** was determined from Job plots (Figure 2). Representative binding isotherms can be seen in Figure 3, and these were fit to a 1:1 binding equation.

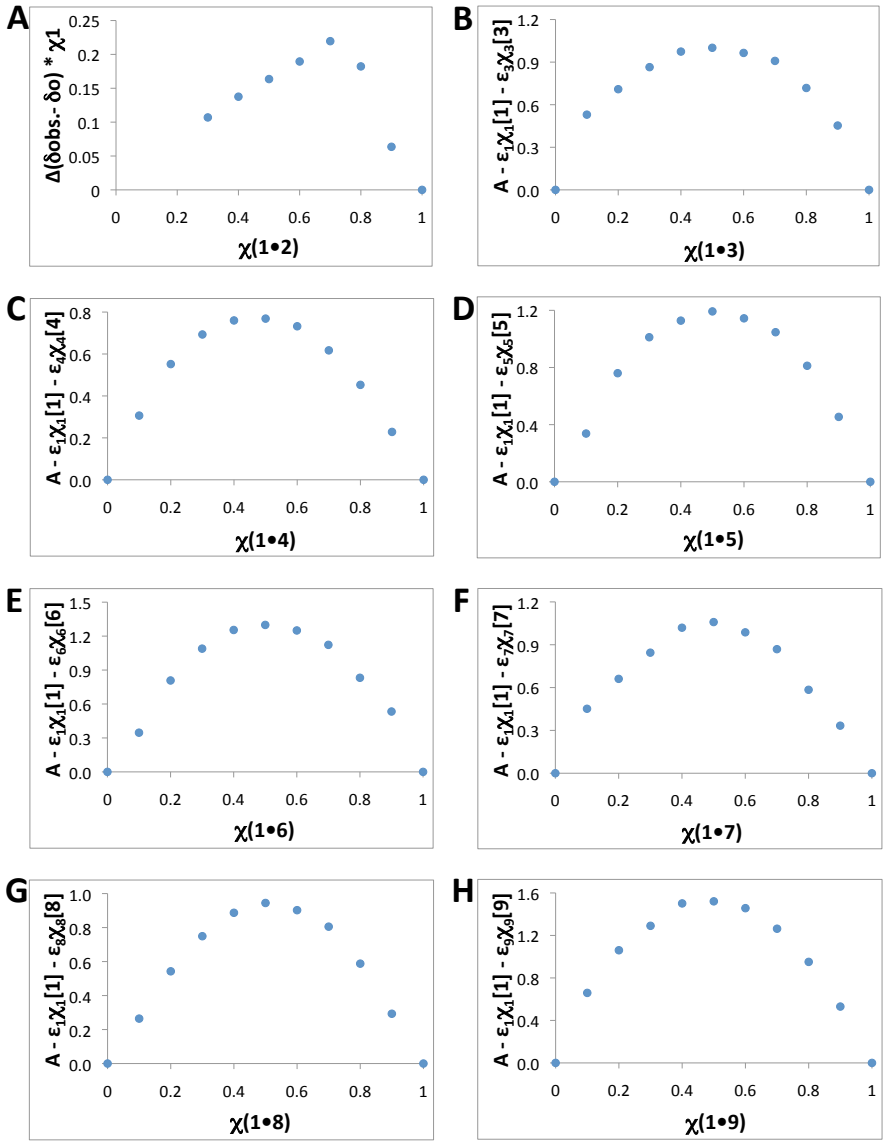

Figure 2. Determination of stoichiometry using Job's Method of Continuous Variation[68] indicating a 1:1 binding stoichiometry for complexes of cation **1** with carboxylates **3-9** at concentrations for UV-Vis titration experiments. A stoichiometry of 1:2 was determined for the complex of cation **1** with carboxylate **2** (previously reported) at concentrations for NMR titration experiments. Mole fraction in the plots above is denoted by the symbol χ.

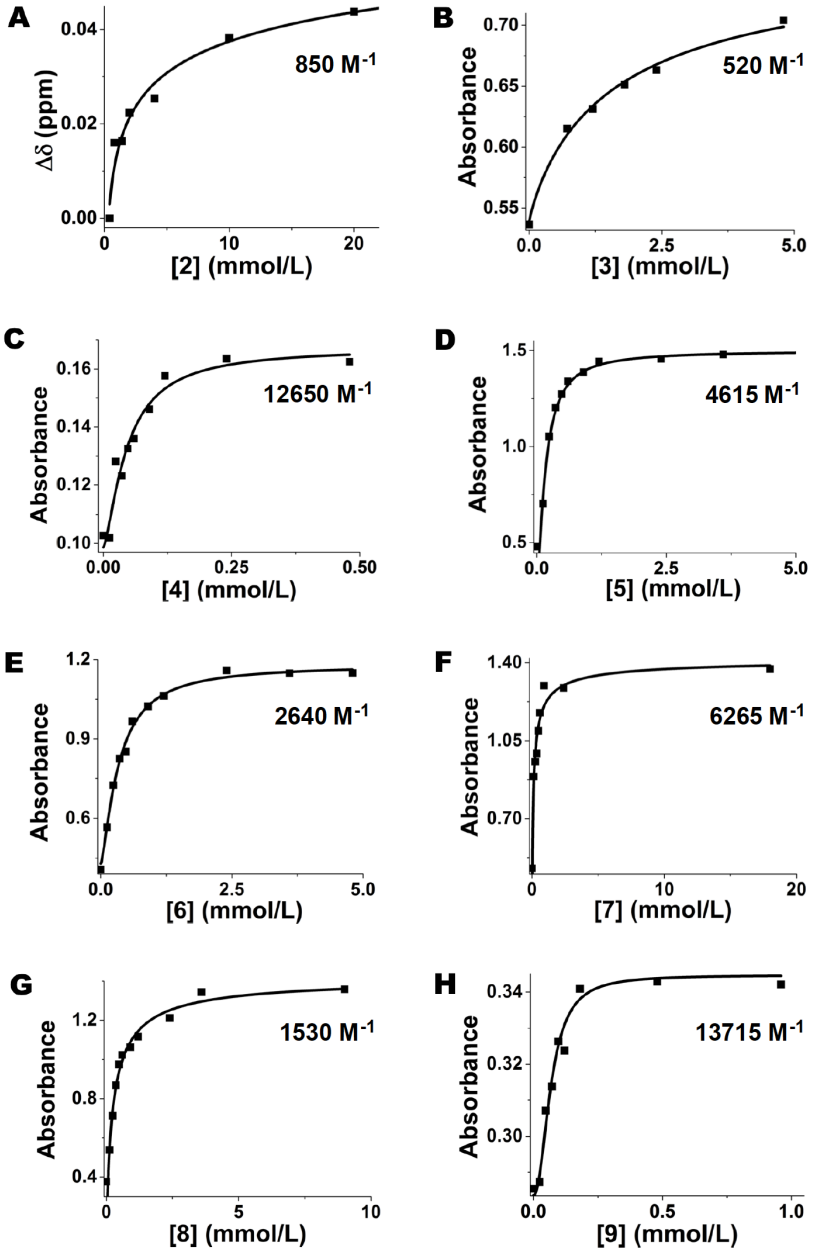

Figure 3. Representative binding isotherms for compound **1** with (di)carboxylate **2** (A), **3** (B), **4** (C), **5** (D), **6** (E), **7** (F), **8** (G) and **9** (H). All absorbances are measured at 425 nm. Data for A was previously reported.[50] Each binding titration was repeated three times and the association constant was reported as the average of the three runs.

Importance of complementary structure on association strength. The association constants for binding of **1** with (di)carboxylates **2-9** can be seen in Table 1. Not surprisingly, dicarboxylates bind the ferrocene host **1** better than monocarboxylates due to increased number of electrostatic interactions. Most remarkably, association constants greater than 10^4 M^{-1} in pure water are shown for two of the ferrocene - carboxylate complexes **1•4** and **1•9**.

Table 1 shows a summary of experimentally determined association constants and the computationally determined changes in binding enthalpy. The binding curve of the ferrocene host with (di)carboxylates, as well as the Density Functional Theory (DFT) enthalpy calculations, show that the rigid dicarboxylates with the size and shape complementary to the ferrocene host have stronger association constants. For example, **1•5** and **1•6** do not position the carboxylates ideally to allow for binding without strain and have, as a result, diminished association constants. Complexes **1•7** and **1•8** show weaker binding, presumably because of the more flexible linker connecting the dicarboxylate groups leads to a greater entropic penalty upon binding. Complementary carboxylates **1•4** and **1•9** that have the ability to exploit the maximum number of electrostatic interactions were found to have the highest associations in water (Figure 4).

Table 1. Binding constants of **1** with **2-9** in water and computed changes in binding enthalpy for complexes (B3LYP/6-31G(d)). Estimated error in Ka < ±25%

Substrate	K_a (M^{-1})	Log(K_a)	Δ Enthalpy (kcal/mol)
2	8.5×10^2	2.9	-45.1
3	5.2×10^2	2.7	-40.9
4	1.3×10^4	4.1	-62.0
5	4.6×10^3	3.7	-55.9
6	2.6×10^3	3.4	-45.9
7	6.3×10^3	3.8	-62.4
8	1.5×10^3	3.2	-66.5
9	1.4×10^4	4.1	-64.2

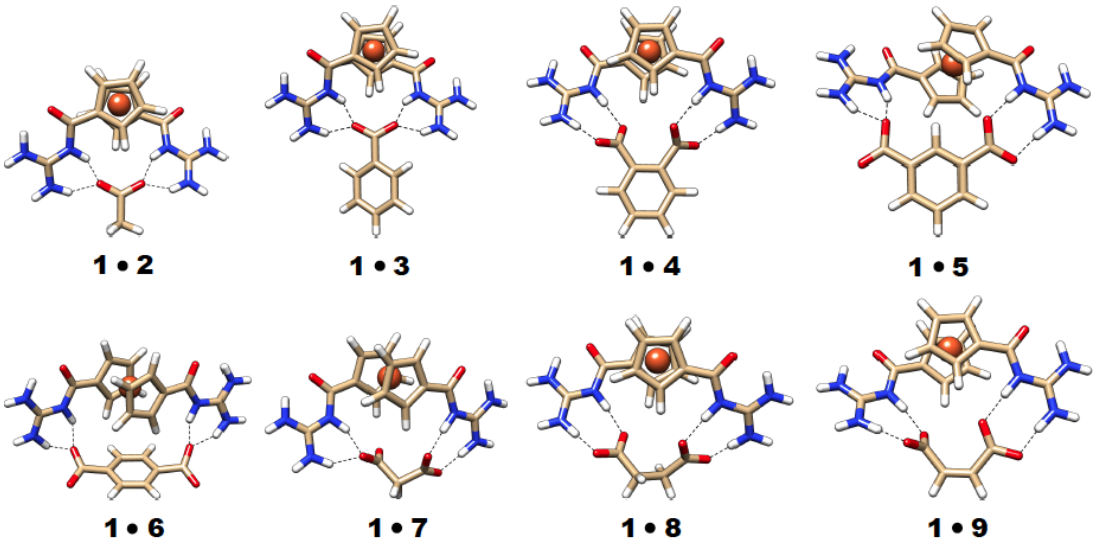

Figure 4. Computed structures of the 1:1 association complexes (B3LYP/6-31G(d)). Lowest minima found are shown.

Computational results. With the exception of the binding of **1** with **8**, the computed binding enthalpies of the cation-(di)carboxylate ion pairs (Figure 4) correlate well with experimentally determined binding constants (Figure 5). Note that these computations do not incorporate entropic effects or explicit solvent (a PCM water solvation model was employed), so they are likely only valid for noticing trends within a class of host-guest complexes, such that the errors cancel out (i.e. change in entropy of solvation).[69-71] One exception to this generally good agreement is binding of **1** to succinate ion **8**. The calculated enthalpy does not correlate well with its experimentally determined association constant. In this case, there is anticipated to be a larger entropic penalty of binding for the conformationally flexible linker than for the other hosts. Given that this entropic penalty is omitted from our computations, it is perhaps not surprising that our computations overestimate the stability of this complex relative to the other complexes.

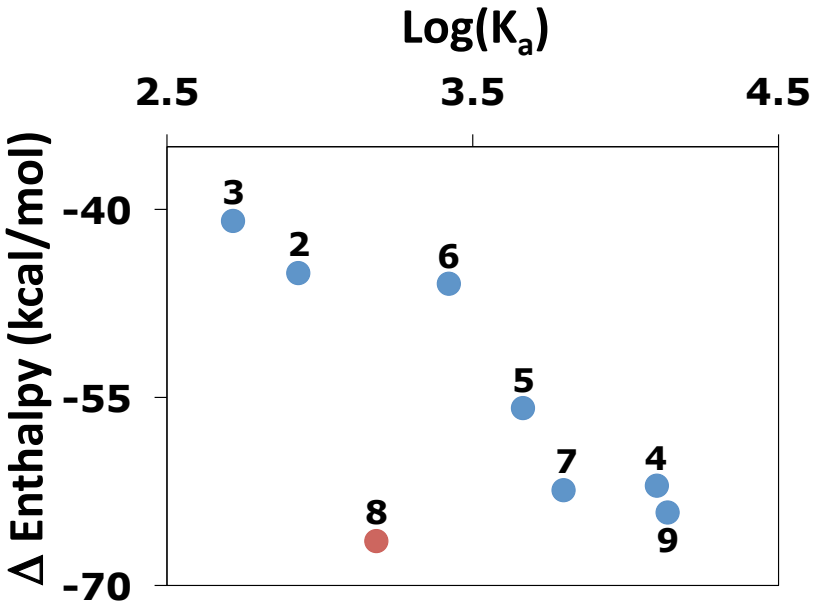

Figure 5. Plot of computed enthalpy change in binding (B3LYP/6-31G(d)) versus Log(K_a).

Catch and Release Studies. Ferrocene compounds and cucurbit[n]urils have been found to have association constants as high as 10^{15} M^{-1} in water.[53, 72-82] Therefore, we thought it might be possible to release the carboxylates from their complexes with the bis-(acetylguanidinium)ferrocene cation **1** via addition of CB[7]. It was anticipated that CB[7] would bind the ferrocene compound **1** more tightly than any of the carboxylates used in the study. We exploited the strength of the association of the ferrocene compound to CB[7] to allow us to monitor the release of the carboxylate guests via NMR. Figure 8d shows the NMR spectra of ferrocene compound **1** mixed with **10**. The large upfield shift of the ferrocene protons is indicative of binding inside the cavity of **10**.

It was a concern that the part of the guanidine substrates could potentially protrude from the CB[7] portals, thus being able to bind the carboxylate even while bis-(acetylguanidinium)ferrocene **1** and CB[7] **10** are bound. Hartree-Fock computations (RHF/ STO-3G) suggest that part of the guanidine moiety does protrude from the portal cavity (Figure 6). Thus, an NMR titration of the CB[7] - ferrocene complex to maleate **9** was done by NMR in neat D_2O to determine the extent of binding of the guanidinium substrate to the carboxylate **9** (Figure 7). The association constant determined for the interaction between the guanidine substrate and carboxylate **9** was estimated to be 185 M^{-1}, much weaker than the complexes to the unbound **1**. A possible explanation for this weak association is unfavorable ion-dipole interactions between the carboxylate anion and the carbonyl electrons at the portal of the CB[7].[72]

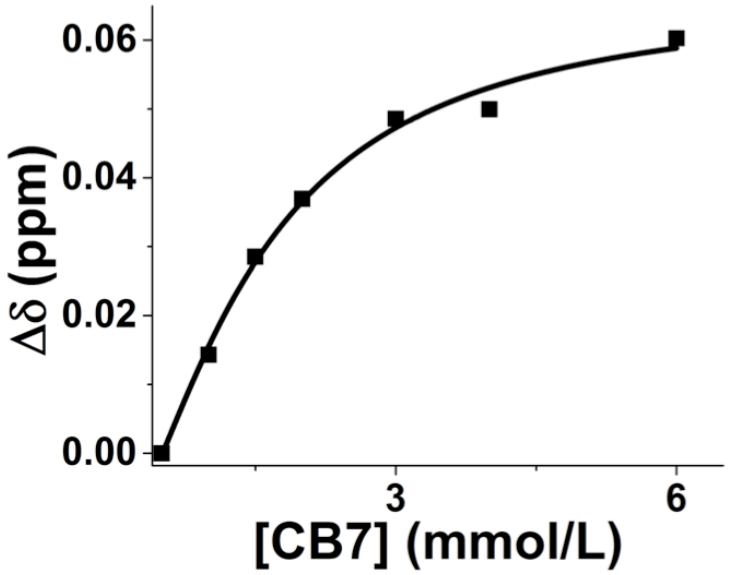

Figure 6. Binding isotherm for **1:10** complex with maleate **9** in D_2O. Estimated K_a is 185 M^{-1}.

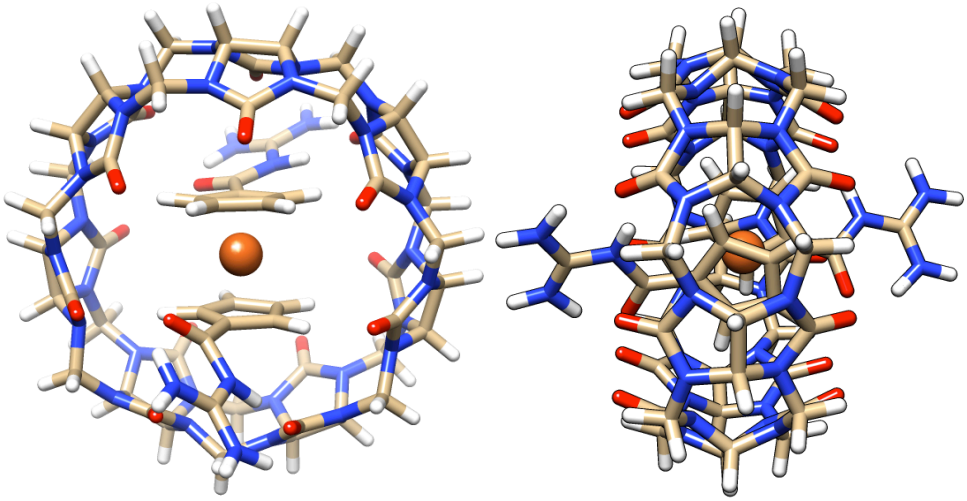

Figure 7. Top and side views of **1** bound to **10** by Hartree-Fock computations (RHF/ STO-3G).

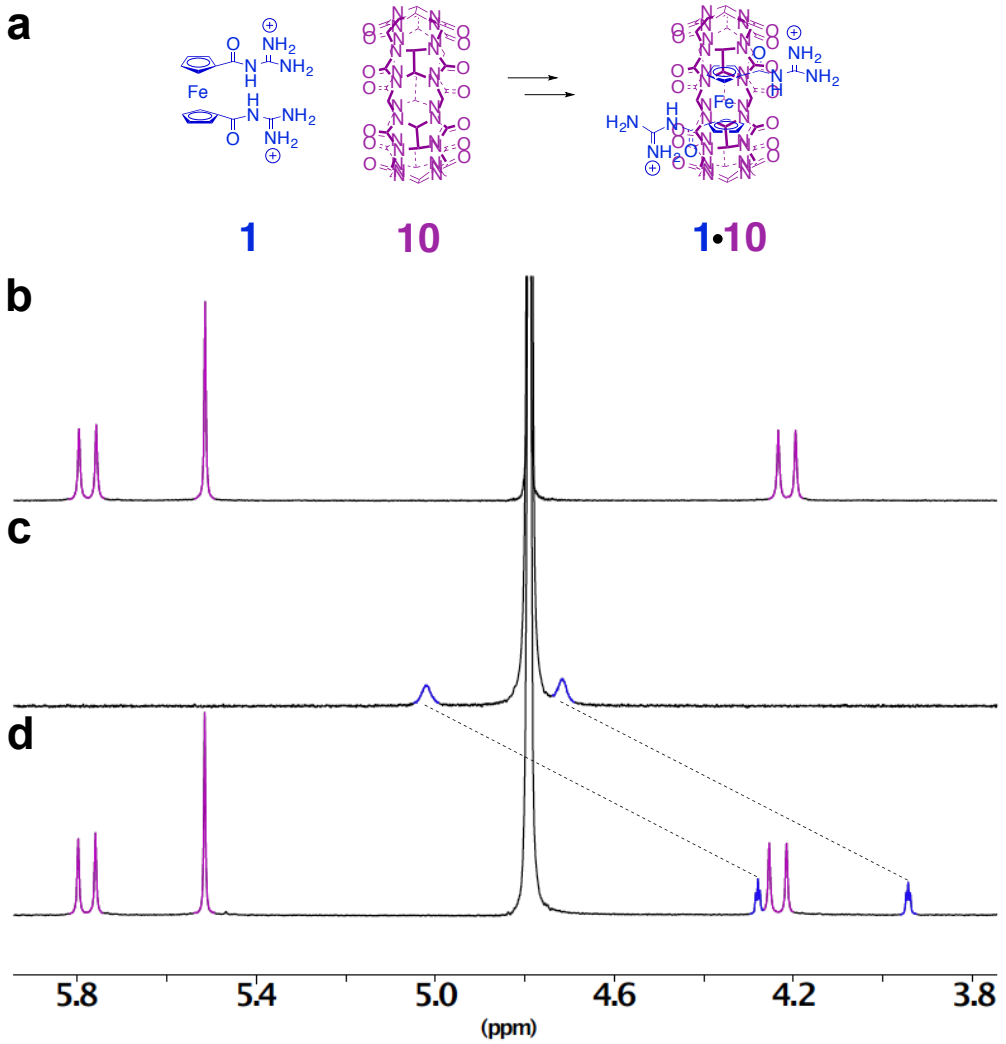

Figure 8. Stacked ^{1}H NMR spectra in D_2O (4.79 ppm) for verification of **1** binding to **10**. **1** is blue and **10** is purple (**a** shows the proposed scheme of binding, **b** is the ^{1}H NMR spectra of **10**, **c** is the spectra of **1**, and **d** is the complex of **1•10**).

The ferrocene compound **1** was mixed with one equivalent of succinate **8**. A downfield shift of the succinate protons was observed, indicating formation of the complex **1•8** (Figure 9). Upon addition of one equivalent of **10**, an upfield shift of the

succinate protons was observed, returning the NMR signal to near the unbound chemical shift, indicating release of the dicarboxylate ion. Additionally, the upfield shift of the ferrocene protons indicates incorporation of this dication within the cavity of CB[7].

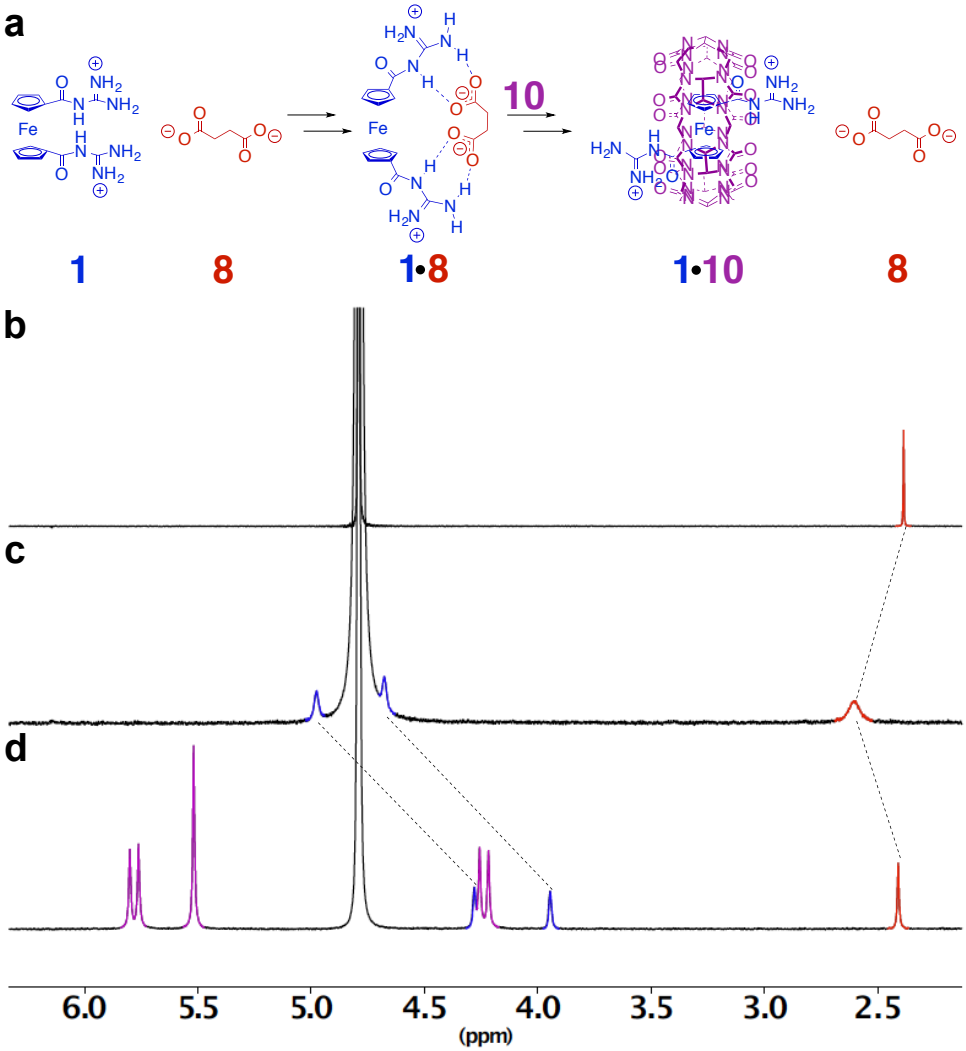

Figure 9. Stacked ^{1}H NMR spectra in D_2O (4.79 ppm) for competitive binding study of **8**. **1** is blue, **8** is red, and **10** is purple (**a** shows the proposed scheme of binding and

release, **b** is the ^{1}H NMR spectra of **8**, **c** is the spectra of the complex of **1•8**, and **d** is the complex of **1•10** showing the dissociation of **8**).

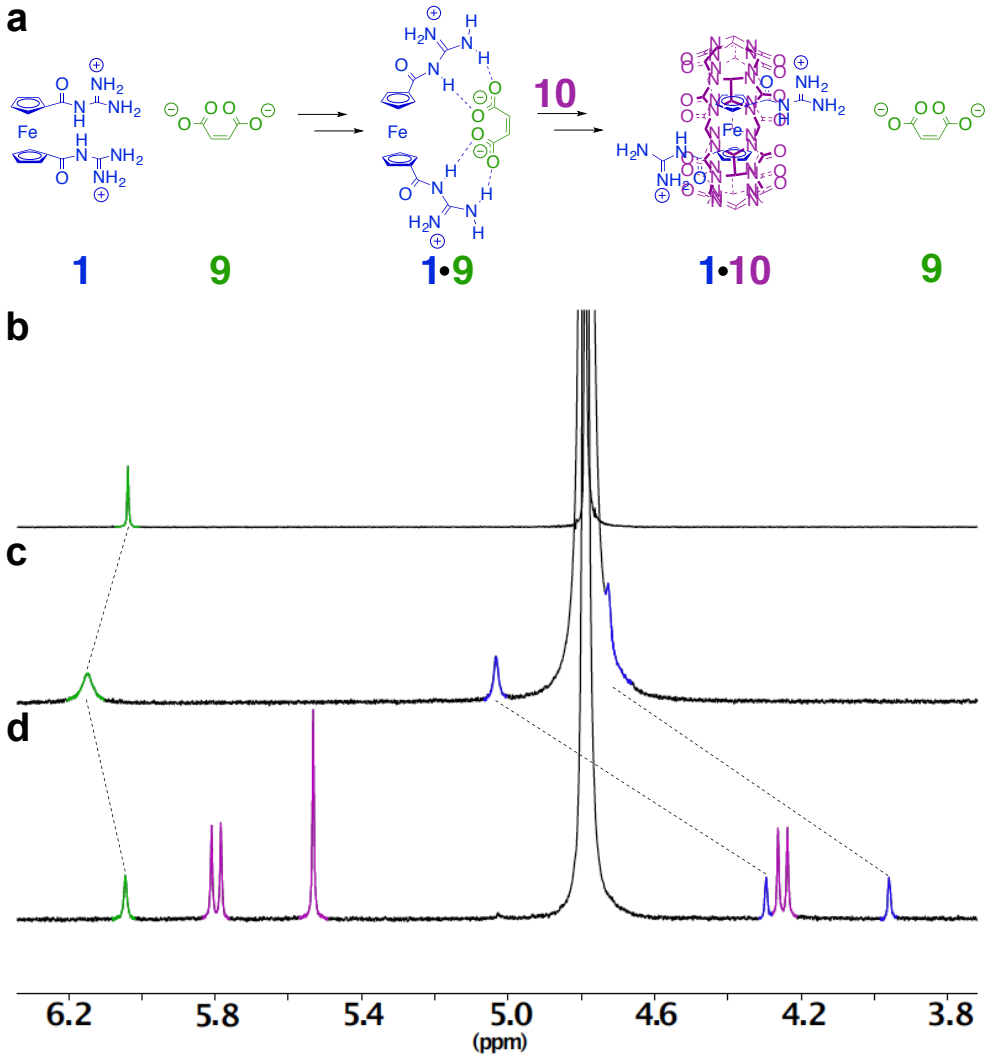

Figure 10. Stacked ^{1}H NMR spectra in D_2O (4.79 ppm) for competitive binding study of **9**. **1** is blue, **9** is green, and **10** is purple (**a** shows the proposed scheme of binding and release, **b** is the ^{1}H NMR spectra of **9**, **c** is the spectra of the complex of **1•9**, and **d** is the complex of **1•10** showing the dissociation of **9**).

Figure 10 shows ferrocene compound **1** bound to one equivalent of maleate **9**. Similar to the results found with succinate, a downfield shift was observed upon binding of **9** to **1**. Upon addition of one equivalent of CB[7], the maleate protons shift back upfield, nearly restoring its original, unbound signal shift indicating release of the dicarboxylate.

EXPERIMENTAL

Computational Methods. All of the computations were computed with Gaussian03/09.[83] For all other structures, the lowest energy molecular geometries of the complexed and non-complexed structures were all optimized using the DFT 6-31G(d) basis set with the hybrid B3LYP functional, which consists of the Becke 3-parameter exchange functional[84] with the correlation functional of Lee, Yang, and Parr.[85] All DFT geometries were found to have zero imaginary frequencies, and all of the reported enthalpies contain a correction for the zero-point energy. An effort was made to find the global minima for both the complexed and non-complexed structures by optimizing numerous input geometries. A PCM water solvation model was employed for the DFT computations.

Experimental procedures. Bis-(acetylguanidinium)ferrocene **1** was synthesized following a reported literature procedure.[50] Cucurbit[7]uril, D_2O, potassium benzoate, and dicarboxylic acids were purchased and used without further purification. Dicarboxylates were synthesized by adding two equivalents of potassium hydroxide to the dicarboxylic acid in water. Removal of the water *in vacuo* afforded the dicarboxylates as white solids. NMR competitive binding experiments for Figures

6 and 7 were performed at a field of 400 MHz. NMR competitive binding experiments for Figure 8 were performed at a field strength of 600 MHz. The catch and release was shown for both maleate **9**, which has an association constant in neat water of 1.4 x 10^4 M^{-1} and for succinate **8**, which has an association constant of 1.5 x 10^3 M^{-1}. These particular carboxylates were chosen for the catch and release study due to their complex solubility, complex strength, and the magnitude of the change in signal shift when bound and unbound. At the concentrations used for typical NMR experiments, all of the cation-carboxylate complexes, with the exception of succinate **8**, precipitate out of solution. Because of this, much less concentrated solutions were made for maleate **9**. Even at these dilute concentrations, precipitation of the complex was observed for malonate **7**. For the aromatic carboxylates **3-5**, monitoring the shift change by NMR was made difficult due to precipitation. Terephthalate **6** catch and release studies were inconclusive due to the small magnitude of change in the proton signal when bound and unbound.

Determination of association constants and complex stoichiometry. Binding constants were determined through NMR or UV-Vis titration experiments. The association constants determined through UV-Vis titrations were calculated using the global fit in Pall Thordarson's titration fitting software for Matlab, and the association constant determined through NMR titrations was calculated using the individual fit.[86] Job plots were used to determine the complex stoichiometry. For carboxylates **3-9**, a maximum in the Job plot corresponded to a 1:1 stoichiometry. With the exception of the K_a determination of maleate **9** bound to the **1•10** complex, all binding constant

titrations were run a minimum of three times, with the association constant being the average of the three runs. The K_a's shown in Table 1 represent the average value of all the fits. Thus, a typical binding constant represents the average value of at least 3 global fits consisting of 4 sets of data for each trial. One representative fit for each carboxylate is shown in Figure 2 at a 425 nm absorbance. Error in the K_a is estimated to be <25 percent.

CONCLUSION

We have shown the binding of a bis-(acetylguanidinium)ferrocene cation **1** to seven carboxylates in water by UV-Vis titrations. The effects of recruiting an additional carboxylate group play a major role in increasing the association constant. Two of these carboxylates, phthalate **4** and maleate **9**, achieve binding greater than 10^4 M^{-1} in neat water. DFT computations of the binding enthalpy of the rigid carboxylates were in good agreement with the experimentally determined association constants. We have also shown competitive binding experiments by NMR, which show that the carboxylate guest is released to the bulk solvent upon addition of cucurbit[7]uril to the system. This is due to the strong interactions between the ferrocene compound and the hydrophobic pocket of the CB[7]. Although two of the complex association constants reported are greater than 10^4 M^{-1}, their strength is still insufficient for practical biological applications; these studies may provide the basis for preparing new ligands for carboxylates that also include hydrophobic interactions to maximize binding constants.

REFERENCES

1. C. L. Beck and A. H. Winter, *J. Org. Chem.*, 2014, **79**, 3152-3158.
2. T. H. Rehm and C. Schmuck, *Chem. Soc. Rev.*, 2010, **39**, 3597-3611.
3. T. Rehm and C. Schmuck, *Chem. Commun.*, 2008, 801-813.
4. A. N. Leung, D. A. Degenhardt and P. Buhlmann, *Tetrahedron*, 2008, **64**, 2530-2536.
5. P. Gale and J. Steed, *Supramolecular Chemistry: From Molecules to Nanomaterials, Volume 3: Molecular Recognition*, 2012.
6. R. J. Fitzmaurice, G. M. Kyne, D. Douheret and J. D. Kilburn, *J. Chem. Soc. Perkin Trans.*, 2002, 841-864.
7. P. Blondeau, M. Segura, R. Perez-Fernandez and J. de Mendoza, *Chem. Soc. Rev.*, 2007, **36**, 198-210.
8. S. Carvalho, R. Delgado, M. G. B. Drew, V. Calisto and V. Felix, *Tetrahedron*, 2008, **64**, 5392-5403.
9. V. S. Bryantsev and B. P. Hay, *J. Am. Chem. Soc.*, 2006, **128**, 2035-2042.
10. C. Rether and C. Schmuck, *Eur. J. Org. Chem.*, 2011, **2011**, 1459.
11. M. Haj-Zaroubi and F. P. Schmidtchen, *Chemphyschem*, 2005, **6**, 1181-1186.
12. F. P. Schmidtchen and M. Berger, *Chem. Rev.*, 1997, **97**, 1609-1646.
13. C. Seel, A. Galan and J. Demendoza, *Supramolecular Chemistry II - Host Design and Molecular Recognition*, 1995, **175**, 101-132.
14. K. S. Jeong and Y. L. Cho, *Tetrahedron Lett.*, 1997, **38**, 3279-3282.
15. C. Schmuck and S. Graupner, *Tetrahedron Lett.*, 2005, **46**, 1295-1298.
16. M. E. Bush, N. D. Bouley and A. R. Urbach, *J. Am. Chem. Soc.*, 2005, **127**, 14511-14517.
17. M. P. Conley, J. Valero and J. de Mendoza, in *Supramol. Chem.*, John Wiley & Sons, Ltd, 2012.
18. C. Schmuck, *Coord. Chem. Rev.*, 2006, **250**, 3053-3067.
19. H. H. Zepik and S. A. Benner, *J. Org. Chem.*, 1999, **64**, 8080-8083.

20. Y. Sun, C. Zhong, R. Gong and E. Fu, *Org. Biomol. Chem.*, 2008, **6**, 3044-3047.

21. S. K. Lee and J. Kang, *Bull. Korean Chem. Soc.*, 2011, **32**, 3215-3218.

22. A. I. Vicente, J. M. Caio, J. Sardinha, C. Moiteiro, R. Delgado and V. Felix, *Tetrahedron*, 2012, **68**, 670-680.

23. A. Metzger and E. V. Anslyn, *Angew. Chem. Int. Ed.*, 1998, **37**, 649-652.

24. P. D. Beer and S. R. Bayly, in *Anion Sensing*, ed. I. Stibor, 2005, vol. 255, pp. 125-162.

25. K. Groger, D. Baretic, I. Piantanida, M. Marjanovic, M. Kralj, M. Grabar, S. Tomic and C. Schmuck, *Org. Biomol. Chem.*, 2011, **9**, 198-209.

26. X. H. Sun, W. Li, P. F. Xia, H.-B. Luo, Y. Wei, M. S. Wong, Y.-K. Cheng and S. Shuang, *J. Org. Chem.*, 2007, **72**, 2419-2426.

27. C. Schmuck and M. Schwegmann, *J. Am. Chem. Soc.*, 2005, **127**, 3373-3379.

28. C. Schmuck, *Synlett*, 2011, 1798-1815.

29. V. D. Jadhav and F. P. Schmidtchen, *J. Org. Chem.*, 2008, **73**, 1077-1087.

30. X. L. Cui, R. Delgado, H. M. Carapuca, M. G. B. Drew and V. Felix, *Dalton Trans.*, 2005, 3297-3306.

31. N. Pant and A. D. Hamilton, *J. Am. Chem. Soc.*, 1988, **110**, 2002-2003.

32. R. C. James, J. G. Pierce, A. Okano, J. Xie and D. L. Boger, *ACS Chem. Bio.*, 2012, **7**, 797-804.

33. L. B. Rice, *Am. J. Med.*, 2006, **119**, S11-19; discussion S62-70.

34. S.-H. Eom, Y.-M. Kim and S.-K. Kim, *Appl. Microbiol. Biotechnol.*, 2013, **97**, 4763-4773.

35. A. Shenderova, T. G. Burke and S. P. Schwendeman, *Pharm. Res.*, 1997, **14**, 1406-1414.

36. W. K. Tong, L. J. Wang and M. J. D'Souza, *Drug Dev. Ind. Pharm.*, 2003, **29**, 745-756.

37. A. Shenderova, T. G. Burke and S. P. Schwendeman, *Pharm. Res.*, 1999, **16**, 241-248.

38. A. Day, J. G. Day, A. Collins, J. Steed and P. Gale, *Cucurbituril Receptors and Drug Delivery. Supramolecular chemistry: from molecules to nanomaterials*, 2012.

39. S. Faulkner, A. M. Faulkner, S. Kenwright, J. Steed and P. Gale, *Supramolecular Chemistry in Medicine. Supramolecular chemistry: From molecules to nanomaterials*, 2012.

40. A. S. Abreu, E. M. S. Castanheira, M.-J. R. P. Queiroz, P. M. T. Ferreira, L. A. Vale-Silva and E. Pinto, *Nano. Res. Lett.*, 2011, **6**.

41. R. J. Fitzmaurice, F. Gaggini, N. Srinivasan and J. D. Kilburn, *Org. Biomol. Chem.*, 2007, **5**, 1706-1714.

42. A. Echavarren, A. Galan, J. M. Lehn and J. Demendoza, *J. Am. Chem. Soc.*, 1989, **111**, 4994-4995.

43. M. D. Best, S. L. Tobey and E. V. Anslyn, *Coord. Chem. Rev.*, 2003, **240**, 3-15.

44. B. R. Linton, M. S. Goodman, E. Fan, S. A. van Arman and A. D. Hamilton, *J. Org. Chem.*, 2001, **66**, 7313-7319.

45. G. Lancelot and C. Helene, *Proc. Natl. Acad. Sci. USA*, 1977, **74**, 4872-4875.

46. C. Cruz, R. Delgado, M. G. B. Drew and V. Felix, *Org. Biomol. Chem.*, 2004, **2**, 2911-2918.

47. R. P. Dixon, S. J. Geib and A. D. Hamilton, *J. Am. Chem. Soc.*, 1992, **114**, 365-366.

48. K. Ariga and E. V. Anslyn, *J. Org. Chem.*, 1992, **57**, 417-420.

49. A. Wilson, Wilson, J. Steed and P. Gale, *Hydrogen-Bonding Receptors for Molecular Guests. Supramolecular chemistry: From molecules to nanomaterials*, 2012.

50. C. L. Beck, S. A. Berg and A. H. Winter, *Org. Biomol. Chem.*, 2013, **11**, 5827-5835.

51. C. Schmuck, *Chem. Eur. J.*, 2000, **6**, 709-718.

52. C. Schmuck and W. Wienand, *J. Am. Chem. Soc.*, 2003, **125**, 452-459.

53. M. V. Rekharsky, T. Mori, C. Yang, Y. H. Ko, N. Selvapalam, H. Kim, D. Sobransingh, A. E. Kaifer, S. Liu, L. Isaacs, W. Chen, S. Moghaddam, M. K.

Gilson, K. Kim and Y. Inoue, *Proc. Natl. Acad. Sci. USA*, 2007, **104**, 20737-20742.

54. J. W. Steed, J. L. Atwood and P. A. Gale, in *Supramol. Chem.*, John Wiley & Sons, Ltd, 2012.

55. M. P. Hughes and B. D. Smith, *J. Org. Chem.*, 1997, **62**, 4492-4499.

56. C. Schmuck, *Tetrahedron*, 2001, **57**, 3063-3067.

57. W. S. Yeo and J. I. Hong, *Tetrahedron Lett.*, 1998, **39**, 8137-8140.

58. S. R. Collinson, T. Gelbrich, M. B. Hursthouse and J. H. R. Tucker, *Chem. Commun.*, 2001, 555-556.

59. N. L. Bill, D.-S. Kim, S. K. Kim, J. S. Park, V. M. Lynch, N. J. Young, B. P. Hay, Y. Yang, E. V. Anslyn and J. L. Sessler, *Supramol. Chem.*, 2012, **24**, 72-76.

60. L. Sebo, B. Schweizer and F. Diederich, *Helv. Chim. Acta*, 2000, **83**, 80.

61. J. Li, H. Lin and H. Lin, *J. Coord. Chem.*, 2009, **62**, 1921-1927.

62. T. R. Kelly and M. H. Kim, *J. Am. Chem. Soc.*, 1994, **116**, 7072-7080.

63. J. L. J. Blanco, J. M. Benito, C. O. Mellet and J. M. G. Fernandez, *Org. Lett.*, 1999, **1**, 1217-1220.

64. T. K. Chakraborty, S. Tapadar and S. K. Kumar, *Tetrahedron Lett.*, 2002, **43**, 1317-1320.

65. B. Linton and A. D. Hamilton, *Tetrahedron*, 1999, **55**, 6027-6038.

66. M. Mazik and H. Cavga, *J. Org. Chem.*, 2006, **71**, 2957-2963.

67. C. Schmuck, *Chem. Commun.*, 1999, 843-844.

68. P. Job, *Annales De Chimie France*, 1928, **9**, 113-203.

69. D. Moiani, C. Cavallotti, A. Famulari and C. Schmuck, *Chem. Eur. J.*, 2008, **14**, 5207-5219.

70. S. Schlund, C. Schmuck and B. Engels, *J. Am. Chem. Soc.*, 2005, **127**, 11115-11124.

71. S. Schlund, C. Schmuck and B. Engels, *Chem. Eur. J.*, 2007, **13**, 6644.

72. W. S. Jeon, K. Moon, S. H. Park, H. Chun, Y. H. Ko, J. Y. Lee, E. S. Lee, S. Samal, N. Selvapalam, M. V. Rekharsky, V. Sindelar, D. Sobransingh, Y. Inoue, A. E. Kaifer and K. Kim, *J. Am. Chem. Soc.*, 2005, **127**, 12984-12989.

73. L. Cui, S. Gadde, W. Li and A. E. Kaifer, *Langmuir*, 2009, **25**, 13763-13769.

74. W. M. Nau, M. Florea and K. I. Assaf, *Isr. J. Chem.*, 2011, **51**, 559-577.

75. A. E. Kaifer, W. Li and S. Yi, *Isr. J. Chem.*, 2011, **51**, 496-505.

76. Y. H. Ko, I. Hwang, D.-W. Lee and K. Kim, *Isr. J. Chem.*, 2011, **51**, 506-514.

77. S. Yi, W. Li, D. Nieto, I. Cuadrado and A. E. Kaifer, *Org. Biomol. Chem.*, 2013, **11**, 287-293.

78. A. E. Kaifer, *Chemphyschem*, 2013, **14**, 1107-1108.

79. J. Wittenberg, L. Wittenberg, J. Isaacs, J. Steed and P. Gale, *Complementarity and Preorganization; Supramolecular chemistry: from molecules to nanomaterials*, 2012.

80. Y.-M. Jeon, J. Kim, D. Whang and K. Kim, *J. Am. Chem. Soc.*, 1996, **118**, 9790-9791.

81. S. Gadde, E. K. Batchelor and A. E. Kaifer, *Aust. J. Chem.*, 2010, **63**, 184-194.

82. S. Gadde and A. E. Kaifer, *Curr. Org. Chem.*, 2011, **15**, 27-38.

83. M. J. Frisch, G. W. Trucks, H. B. Schlegel, G. E. Scuseria, M. A. Robb, J. R. Cheeseman, G. Scalmani, V. Barone, B. Mennucci, G. A. Petersson, H. Nakatsuji, M. Caricato, X. Li, H. P. Hratchian, A. F. Izmaylov, J. Bloino, G. Zheng, J. L. Sonnenberg, M. Hada, M. Ehara, K. Toyota, R. Fukuda, J. Hasegawa, M. Ishida, T. Nakajima, Y. Honda, O. Kitao, H. Nakai, T. Vreven, J. Montgomery, J. A.; , J. E. Peralta, F. Ogliaro, M. Bearpark, J. J. Heyd, E. Brothers, K. N. Kudin, V. N. Staroverov, R. Kobayashi, J. Normand, K. Raghavachari, A. Rendell, J. C. Burant, S. S. Iyengar, J. Tomasi, M. Cossi, N. Rega, J. M. Millam, M. Klene, J. E. Knox, J. B. Cross, V. Bakken, C. Adamo, J. Jaramillo, R. Gomperts, R. E. Stratmann, O. Yazyev, A. J. Austin, R. Cammi, C. Pomelli, J. W. Ochterski, R. L. Martin, K. Morokuma, V. G. Zakrzewski, G. A. Voth, P. Salvador, J. J. Dannenberg, S. Dapprich, A. D. Daniels, Ö. Farkas, J. B. Foresman, J. V. Ortiz, J. Cioslowski and D. J. Fox, *Gaussian 09, Revision A.02*, 2009.

84. A. D. Becke, *Physical Review A*, 1988, **38**, 3098-3100.

85. C. T. Lee, W. T. Yang and R. G. Parr, *Physical Review B*, 1988, **37**, 785-789.

86. P. Thordarson, *Chem. Soc. Rev.*, 2011, **40**, 1305-1323.

GENERAL CONCLUSIONS FOR PART 1

Pincher cationic ferrocene hosts for carboxylate ion guests were synthesized and the binding constants were determined by NMR or UV-vis titrations. These (di)cationic hosts formed tight complexes with benzoate or acetate even in competitive aqueous DMSO solvent. A bis(acylguanidinium) ferrocene dication achieved a K_a of ~ 10^6 M^{-1} to acetate in 9:1 DMSO:H_2O and a K_a of 850 M^{-1} in neat D_2O, which is one of the highest association constants known for a mono-carboxylate complex exploiting only electrostatic interactions in neat water.

Due to its large association constant to acetate in water, the bis(acylguanidinium) ferrocene dication was bound to various (di)carboxylates in water and their associations were determined through UV-vis titrations. Association constant values greater than 10^4 M^{-1} were determined for both phthalate and maleate carboxylates to the bis(acylguanidinium) ferrocene salt in pure water. Catch and release competitive binding experiments were done by NMR for the cation-carboxylate ion pair complexes with CB[7], showing dissociation of the ion pair complex upon addition of CB[7].

DFT computations of the binding enthalpy were in good agreement with the experimentally determined association constants, and the computations of the rigid carboxylates geometrically complementary to the dication agree well with the experimentally determined association constants.

INTRODUCTION FOR PART II

"On the arid lands there will spring up industrial colonies without smoke and without smokestacks; forests of glass tubes will extend over the plains and glass buildings will rise everywhere; inside of these will take the photochemical processes that hitherto have been the guarded secret of the plants, but that will have been mastered by human industry... And if in a distant future the supply of coal becomes completely exhausted, civilization will not be checked by that, for life and civilization will continue as long as the sun shines!"[1]

- Giacomo Luigi Ciamician

PHOTOPHYSICAL PROCESSES

Introduction. Photochemistry plays an increasingly important role in bioorganic chemistry where there is much interest in the use of "caged" molecules, dyes, and sensors for fluorescent imaging.[2] Examples of photochemistry of importance in other areas of chemistry include LEDs and luminescent materials, [2+2] and [2+4] cycloaddition reactions, and the characterization of reactive intermediates by using laser flash photolysis.[2-5]

In order to understand photochemistry, one must first consider the fundamental photophysical processes. The scope of this introduction will cover the basics of photochemical and photophysical processes, non-adiabatic photochemical reactions, and an overview of "caged" molecules.

The Jablonski diagram. In photophysical processes, the chemical structure of the molecule is not changed in the end; however, in a photochemical process, the

interaction of light with matter leads to a change in the chemical structure.[2, 6] A simplified version of a photophysical process is typically described by a Jablonski diagram (Figure 1), which is a modified version of the diagram that was proposed by Jablonski in 1933.[2, 6, 7] In the Jablonski diagram, each surface is represented by a Morse potential, where the excited-state energy surfaces are placed higher on the diagram than the ground-state surfaces.[2] After absorption of a photon (excitation), excess energy then gets released through the emission of light (fluorescence or phosphorescence), or through a radiationless decay pathway (internal conversion), which converts the energy into vibrational energy in the ground state (**IVR** in Figure 1).[8]

Absorption. After excitation of a molecule in the ground state ($\mathbf{S_0}$), absorption (**A** in Figure 1) of a photon produces an excited-state singlet ($\mathbf{S_1}$).[2, 6] In most cases, the ground states of organic molecules are closed-shell singlets, hence the exited state is also a singlet.[2]

The transition of $\mathbf{S_0}$ to $\mathbf{S_1}$ happens on the femtosecond timescale (10^{-16} - 10^{-14} s). Nuclear motions are much slower (10^{-13} – 10^{-12} s) than light absorption.[2] This leads to the Franck-Condon Principle which essentially states that the electronic transitions are most favorable, or faster, when the excited-state geometry and the ground-state geometry of the nuclei are the same (**FC** in Figure 7 shows the Franck-Condon region).[2, 6, 9, 10] After absorption, excess energy can be released either in the form of light or through radiationless decay to bring the molecule back to its ground state.

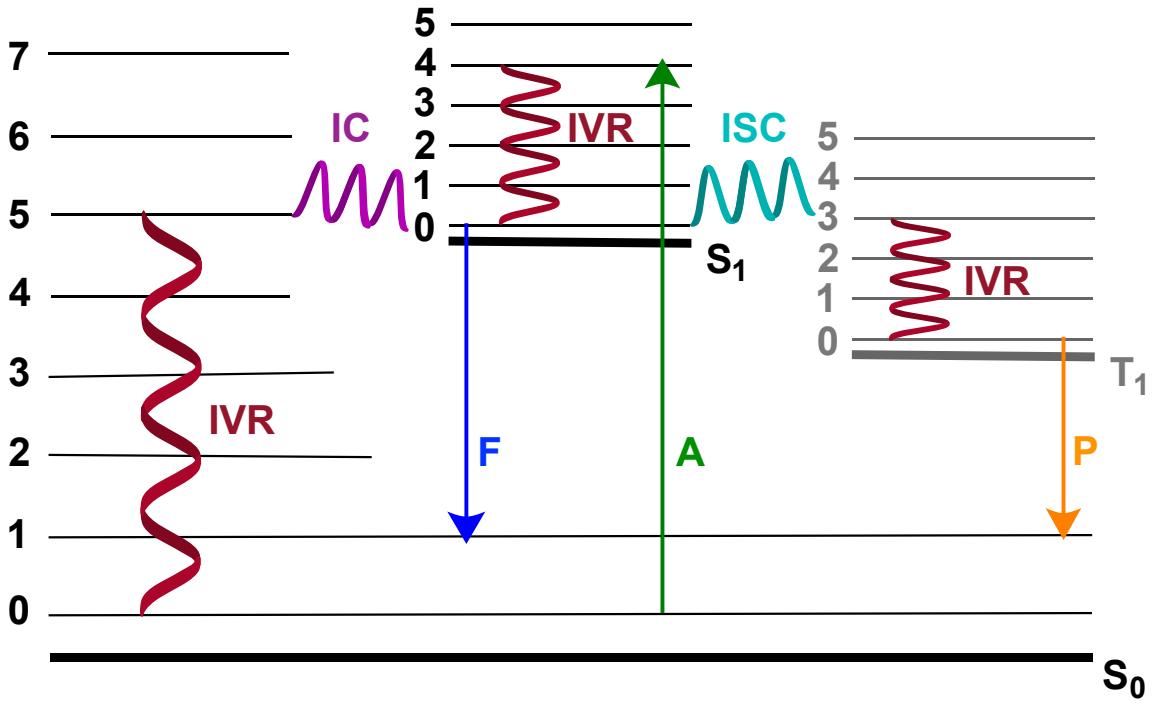

Figure 1. Jablonski diagram (**A** is absorption, **F** is fluorescence, **P** is phosphorescence, **IVR** is intramolecular vibrational redistribution, **IC** is internal conversion, and **ISC** is intersystem crossing)

Radiationless decay. Intramolecular vibrational redistribution, internal conversion, and intersystem crossing are examples of radiationless decay that can occur when excess energy is released from an excited molecule.[2, 8] In these processes, no photons are emitted during the relaxation of S_1 back to S_0. Instead, the excess energy is given off as heat in the form of vibrational energy.[2, 8]

Intramolecular vibrational redistribution, or relaxation, is the redistribution of the vibrational energy among the various vibrational modes of the molecule.[6] An example of intramolecular vibrational redistribution is the process by which a vibrationally

excited state (S_{n+1}) relaxes down to the ground vibrational state of S_1 (**IVR** in Figure 1).[2, 11] Once at the ground vibrational state of S_1, internal conversion can happen, which is a spin-allowed process (**IC** in Figure 1).[6] With internal conversion, there is no change in spin state when the molecule relaxes from S_1 to S_0.[6]

Intersystem crossing (**ISC** in Figure 1) is a general term for the interconversion of spin states to go from S_1 to a triplet excited state (T_1).[2] Note in Figure 1 that T_1 is shown to be lower in energy than S_1. This is due to Hund's rule, which results in a larger number of exchange interactions, making T_1 lower in energy than S_1.[2, 6] When S_1 is converted to T_1, the change in the spin angular momentum is often coupled, or compensated, with a change in orbital angular momentum, as is the case with the 'heavy atom effect.'[2, 9, 10] However, when there are no heavy atoms present in the molecule, El-Sayed's rule takes over.[2] This rule says that when two states being interconverted are both π, π* or n, π*, intersystem crossing is forbidden, or very slow, because spin angular momentum does not change.[2, 9, 10] However, interconverting π, π* to n, π*, or vice versa, is allowed since there is a change in orbital angular momentum.[2, 9, 10]

Fluorescence and phosphorescence. When excess energy is released in the form of light when going from S_1 to S_0, it is called fluorescence (**F** in Figure 1).[2, 6, 8] Similar to fluorescence, phosphorescence also emits a photon when relaxing to S_0 (**P** in Figure 1). Unlike fluorescence, however, intersystem crossing is required prior to phosphorescence to convert S_1 to T_1, because phosphorescence is when an excited-state triplet converts to a ground state singlet and releases a photon.[2] Because ISC is spin forbidden, the rate of phosphorescence can be on the order of seconds.[2, 11] This means

that it is possible for a sample to phosphoresce even after the source of excitation has been removed.[2]

While the Jablonski diagram in Figure 1 describes photophysical processes, which produce no net change in the material, it does not give any insight into photochemical processes.[6, 12] It has been said that photochemistry is controlled by the competition of rates.[2] The rate at which competing photochemical and photophysical processes occur will govern the observed outcome(s).[13-15]

PHOTOCHEMICAL PROCESSES

Adiabatic and hot-molecule reactions. Adiabatic and hot-molecule reactions take place on only one surface.[6, 9, 10, 16-18] In an adiabatic reaction, the conversion from reactant geometry to product geometry takes place on the excited-state surface (Figures 2 and 7).[9, 10, 13, 14, 17] Following the conversion to product geometry, the molecule relaxes back down to the ground state.[2] During the relaxation back to the ground state, a photon can be emitted, resulting in fluorescence.[2, 19]

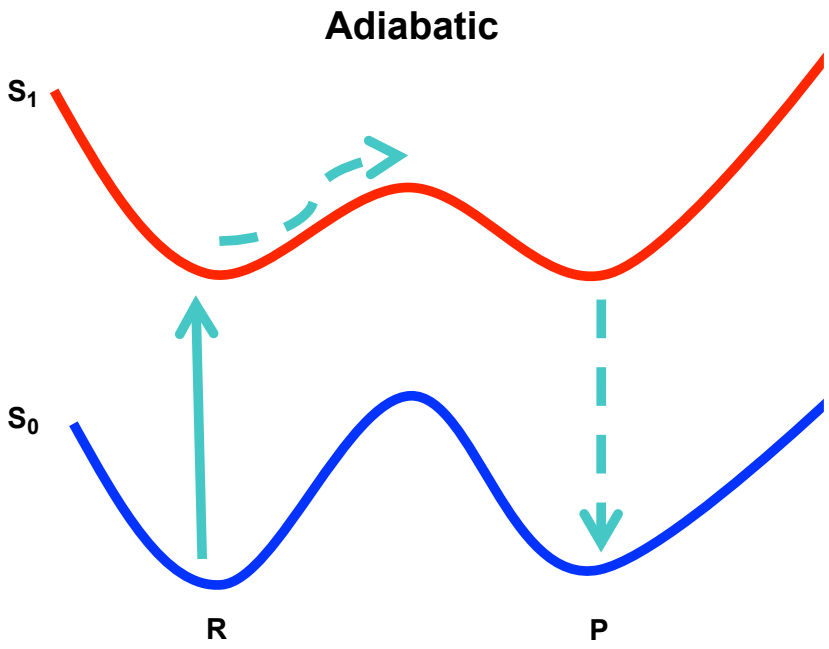

Figure 2. Adiabatic photoreaction (**R** is reactant, **P** is product)

There are numerous examples of adiabatic reactions in literature, and many of them involve cis-to-trans isomerization or photo ring-opening.[9, 10, 20] For example, Mazzucato and co-workers determined that styrylpyrene undergoes an adiabatic cis-to-trans isomerization in nonpolar solvents from the singlet excited state $\mathbf{S_1}$ (Figure 3).[20, 21]

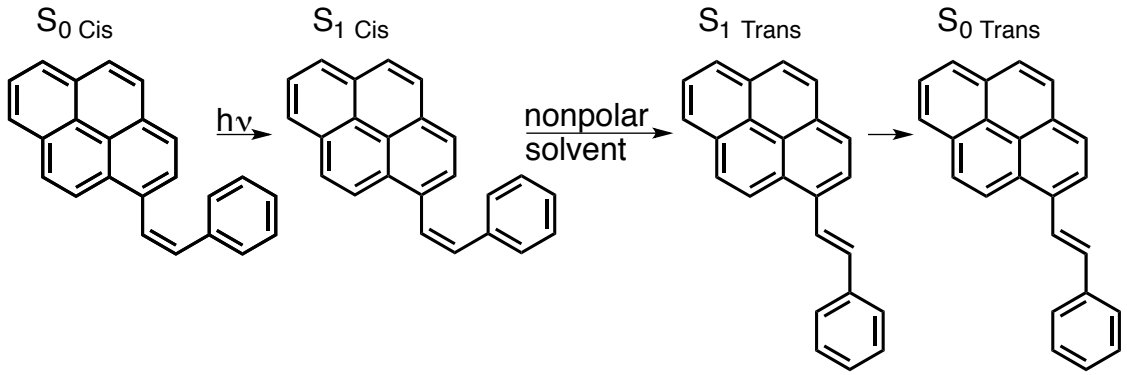

Figure 3. Styrylpyrene adiabatic cis-to-trans isomerization

Later, Tokumaru's group determined that including polar substituents on the styryl ring and using polar solvents led to cis-to-trans isomerization via a non-adiabatic route.[20, 22] (Non-adiabatic routes will be discussed in further detail later).

Photochemical studies of nephthvalene at 77 K by Turro et al revealed that it undergoes adiabatic photo ring-opening and efficiently generates a naphthalene triplet.[23] They also note that they observed phosphorescence, but no fluorescence as evidence for the observed excited-state spin-flip.[23]

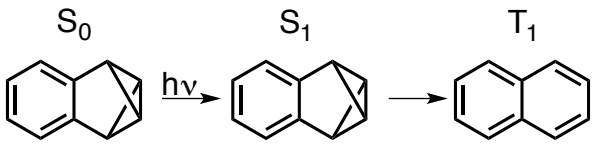

Figure 4. Photo ring-opening of nephthvalene

The two examples above highlight adiabatic photochemical reactions that take place in the excited state. There are also reactions that can occur in the ground state. In hot ground-state reactions, excitation is followed by internal conversion back to the ground state.[2, 9] However, before excess energy can be lost though vibrational energy, it is used to initiate a thermal reaction on the ground state, leading to a new product (Figure 5).[2, 6, 9]

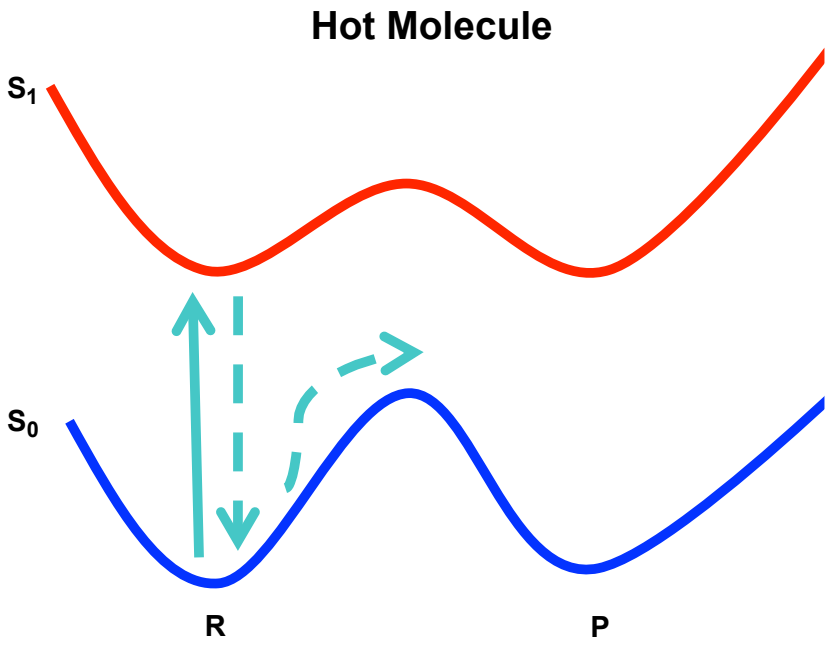

Figure 5. Hot ground-state reaction (**R** is reactant, **P** is product)

Non-adiabatic reactions. When two potential energy surfaces are involved in a photochemical reaction, it is called a non-adiabatic or diabatic reaction.[2, 9, 12] In a non-adiabatic reaction, a molecule is excited from a stable structure on the ground state energy surface $\mathbf{S_0}$ to an unstable structure on the excited state energy surface $\mathbf{S_1}$.[2] In the excited state, the molecule relaxes to a more stable structure on the excited-state energy surface, which is the minimum (or near minimum) on the $\mathbf{S_1}$ surface.[2, 9] When the minimum of the $\mathbf{S_1}$ surface is close in energy to the maximum of the $\mathbf{S_0}$ surface, favorable photochemistry can occur.[24] The small energy gap between these two surfaces allows for crossing from one surface to another, so the molecule is able to 'hop' from the minimum of the excited state $\mathbf{S_1}$ surface to the maximum of the ground state surface $\mathbf{S_0}$ (**CI** in Figure 6).[2, 12]

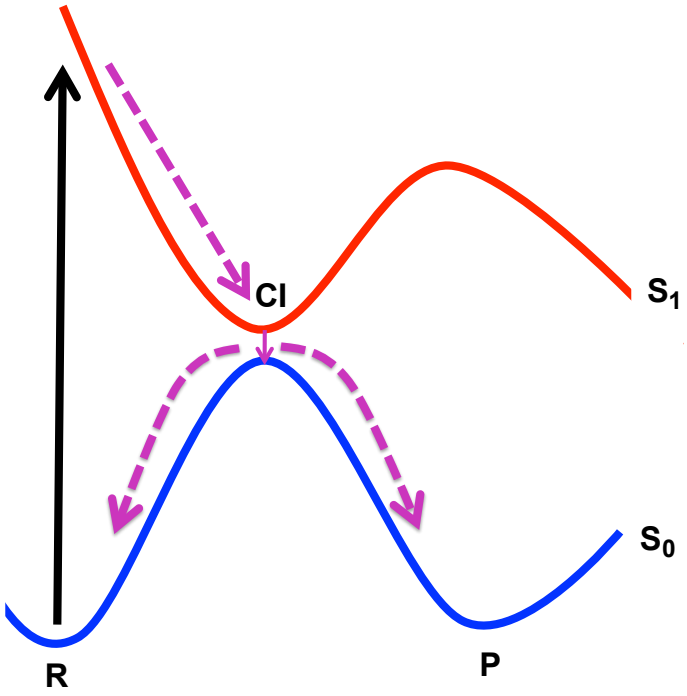

Figure 6. Non-adiabatic photoreaction (**R** is reactant, **P** is product, and **CI** is conical intersection)

When the molecule 'hops' from the excited state to the ground state, either a new product (**P** in Figure 6) can form or the molecule is returned to its original reactant structure (**R** in Figure 6).[25] If the molecule returns to the reactant structure, no photochemistry occurs, which is identical to internal conversion on the Jablonski diagram (Figure 1), however, if the molecule forms a new product, photochemistry occurs. Due to the shape of where the excited state and the ground state surfaces approach one another, or become degenerate, this region is called either a funnel or a conical intersection (**CI** in Figure 6).[6, 11, 14, 17, 26] The degeneracy between the potential energy surfaces leads to a break down of the Born-Oppenheimer approximation,

allowing for non-adiabatic processes to occur.[9, 18, 27, 28] Figure 7 is a one-dimensional representation of the adiabatic and non-adiabatic reactions paths discussed thus far.

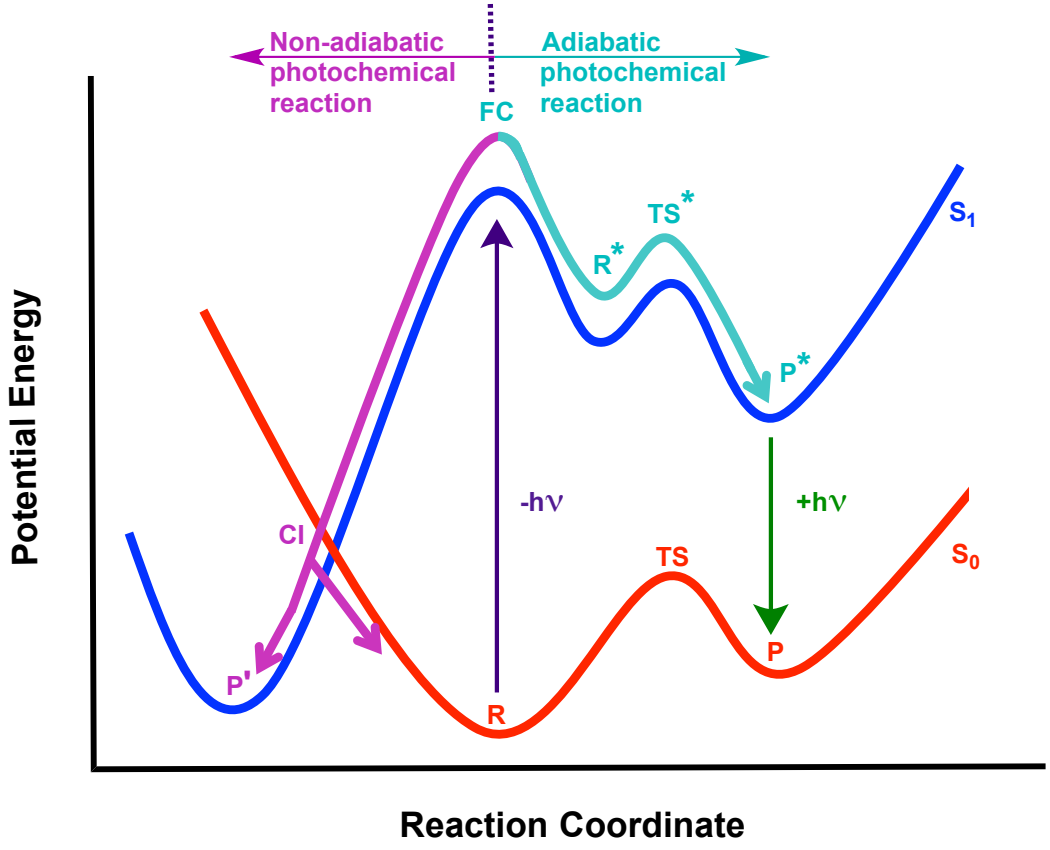

Figure 7. One-dimensional depiction of adiabatic and non-adiabatic reaction paths. (**R** is reactants, **P** is products, **CI** is a conical intersection, **TS** is a transition state, and **FC** is the Franck-Condon region)

Conical intersections and avoided crossings. Conical intersections are crucial to photochemistry, since they provide an efficient route from the excited state to the ground state in polyatomic molecules (Figure 7).[2, 24, 25, 29-31] The closer in energy the gap between the excited state surface and the ground state surface is, the faster and more

efficient this route will be.[2, 6, 9, 14] If a molecule has a minimum on the excited-state surface near a maximum on the ground state surface, there will likely be a conical intersection.[2, 32] It should be noted that diatomic molecules are unable to form conical intersections, but may experience avoided crossings.[27] Because the number of vibrational degrees of freedom in a diatomic molecule is 1, there are not the two dimensions that are required to form the cone shape.[27] Instead, diatomic molecule potential energy surfaces experience avoided crossings. [27, 33, 34]

It was mentioned earlier that unsubstituted styrylpyrene undergoes an adiabatic cis-to-trans isomerization in nonpolar solvents, but that polar substituents on the styryl ring and polar solvents lead to cis-to-trans isomerization via a non-adiabatic route (Figure 8).[20, 22] Tokumaru et al believe that the polar solvents and substituents change the mode of isomerization from an adiabatic isomerization ($\mathbf{S_{1\ Cis}}$ to $\mathbf{S_{1\ Trans}}$) to a non-adiabatic process ($\mathbf{S_{1\ Cis}}$ to $\mathbf{S_{1\ Perpendicular}}$).[22] The authors suggest that there is a perpendicular biradical-like geometry adopted in the excited state that is stabilized by the polar solvents.[2, 22] This stabilization of the excited-state perpendicular geometry decreases the energy gap between $\mathbf{S_1}$ and $\mathbf{S_0}$ enough to allow for funneling back to the ground state (Figure 9).[22]

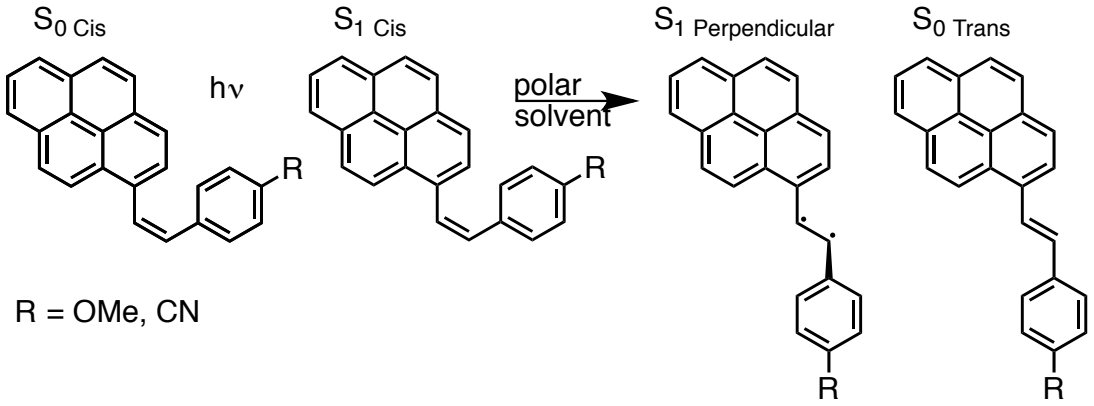

Figure 8. Styrylpyrene non-adiabatic cis-to-trans isomerization

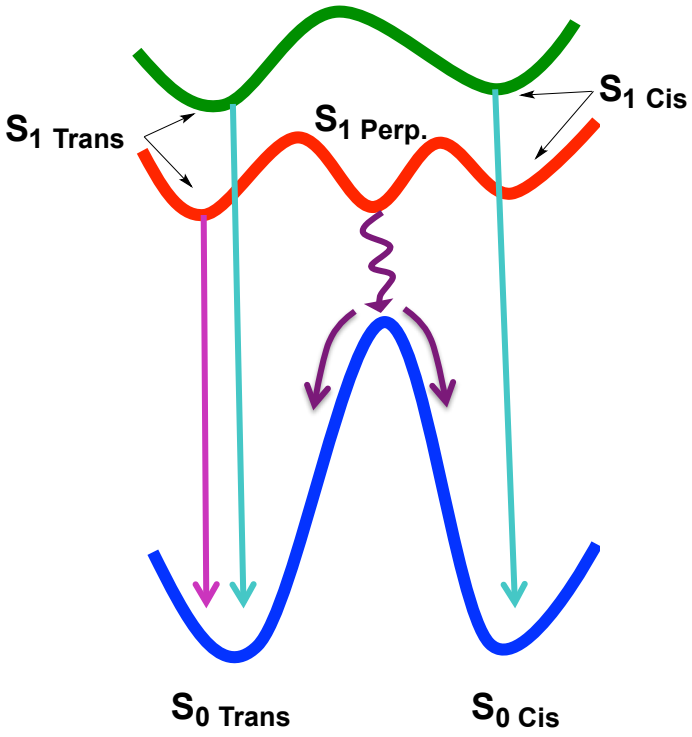

Figure 9. Styrylpyrene non-adiabatic cis-to-trans isomerization. (Red surface is in polar solvent, green surface is in nonpolar solvent)

Sensitizers. Adding a sensitizer to a reaction to generate an excited-state triplet biradical can lead to productive conical intersection formation.[32] Biradical and biradical-like structures are often unstable in $\mathbf{S_0}$, and these biradical-like molecules tend to have a low energy excited state.[2, 35] Recall that Figure 8 showed an example of biradical-like behavior in the excited-state of the cis-to-trans isomerization of styrylpyrene in polar solvents, and Figure 9 showed the low energy excited-state of this biradical-like structure.[22] Biradicals can either be spin-paired ($\mathbf{S_1}$) or spin unpaired ($\mathbf{T_1}$).[2] We learned earlier that spin angular momentum must be conserved in ISC, which is why it is a spin-forbidden process unless there is spin-orbit coupling (El-Sayed's Rule).[2, 36] One way to conserve spin and still generate a triplet is by adding a sensitizer (Figure 10).[2]

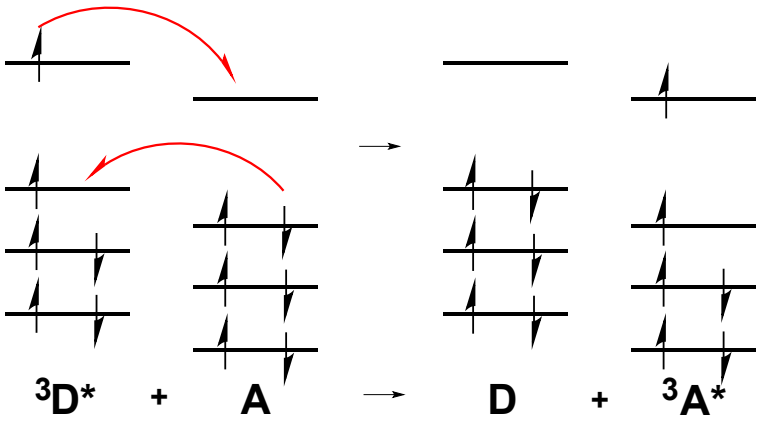

Figure 10. Sensitization

Sensitizers can be used to generate a biradical triplet excited-state by conserving spin, therefore lowering the energy of the excited state.[2, 33] In Figure 10, there is an energy transfer between $^3\mathbf{D}^*$ and **A** which conserves spin while generating $^3\mathbf{A}^*$.[2]

Common sensitizers are those that have efficient ISC, like benzophenone, anthraquinone, and acetophenone.[2]

***Meta*-effect.** Aside from using a sensitizer, a meta-effect trend has been discovered (and disputed among scientists) to help determine whether or not a molecule is likely to have a stable excited state and therefore a favorable conical intersection.[6, 37, 38] In 1956 Havinga et al noticed that hydrolysis of *ortho*-, *meta*,- and *para*-nitrophenyl phosphates occurred at very different rates, with the *meta*-nitrophenyl phosphate having the fastest rate of hydrolysis when exposed to sunlight (Figure 11).[37, 38] The study was repeated with *ortho*-, *meta*-, and *para*-nitrophenyl sulfates, with the same observed trend.[37]

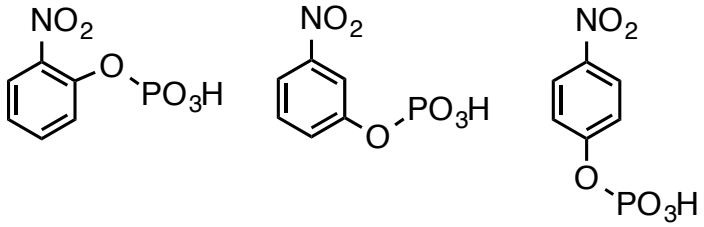

Figure 11. *Ortho*-, *meta*-, and *para*-nitrophenyl phosphates

Havinga rationalized that the observed increased hydrolysis rate for the *meta* derivative was due to the excited-state resonance forms (Figure 12).[37] These resonance forms showed that the carbon *meta* to the nitro group becomes more positive, and therefore more susceptible to nucleophilic attack in the excited state compared to the ground state.[37] This increased reactivity of the *meta* isomer in the excited state is opposite to what is observed in the ground state.[38]

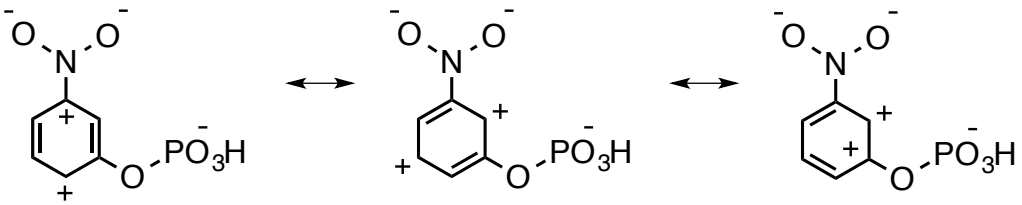

Figure 12. Resonance structures of *meta*-nitrophenyl phosphate in its excited state

In 1963, Zimmerman's group studied the *meta*-effect theoretically (LCAO MO calculations with neglect of orbital overlap) and experimentally on 3- and 4-methoxybenzyl acetates, which supported the experimental observations by Havinga.[39] Thirty years later, however, Zimmerman's widely accepted *meta*-effect theoretical studies were questioned by Pincock, who criticized that Zimmerman failed to look at homolytic cleavage to form radical pairs, but rather only looked at heterolytic cleavage ion pair formation.[38-42] Furthermore, Pincock stated that ion pair formation through heterolytic cleavage was of minimal importance and that the major pathway was through radical pair formation through homolytic cleavage.[5, 41] Regardless of the type of cleavage, there was no denying by Pincock that the benzyl derivatives had inverted substituent effects in the excited state.[40]

In 1995, Zimmerman refuted the claims by Pincock and did more advanced theoretical calculations [CASSCF with (4,4) active space] to support his original claim.[38, 43] He concluded that primary excited state heterolysis was indeed preferred over homolysis for *m*-methoxy substituted benzylic acetates.[38, 43] Many other groups have studied the *meta*-effect on different molecules,[44, 45] and some have even used the *meta*-effect to help with the design of photocages.[46-48]

PHOTOCHEMISTRY OF CAGED COMPOUNDS

Photocages. Numerous photosensitive moieties, or photoremovable protecting groups, have been synthesized that 'cage' or mask a key functional group of a target agent for biochemical or biological studies.[49] There have been many uses of caged molecules in biology including caged ATP, DNA, nucleic acids, etc.[50] The caging of nucleic acids, DNA, etc. temporarily renders the masked functionalities inactive, which allows biologists to study various processes such as translation, transcription, etc.[50]

Nitrobenzyl and coumarinyl analogues are commonly used caging groups with absorbances typically in the range of 250-330 nm and 325-400 nm respectively (Figure 13A and B).[50, 51] Wavelengths of up to 387 nm have been reported for some nitrobenzyl moeities.[51] The recently studied fluorescein analogues have a maximum absorbance (λ_{max}) of up to 520 nm in their enolate form, which makes them possible visible-light cleavable protecting groups (Figure 13C).[52] However, undesirable protonation and tautomerization equilibria lead to messy UV-vis spectra. [52]

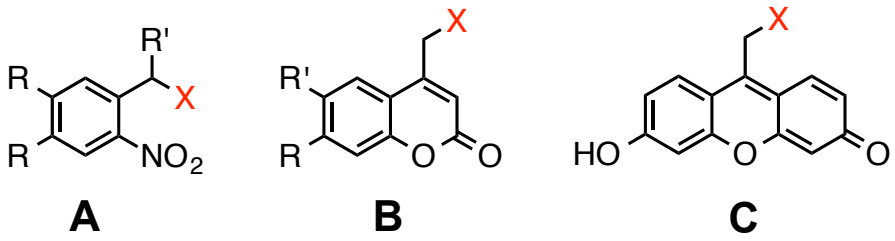

Figure 13. Common photocage backbones

There are several drawbacks to using nitrobenzyl photocages, even though they are widely used. It was already mentioned that their typical λ_{max} is in the UV-vis range,

which can lead to cell damage in biological systems.[48] Electron donating R groups do tend to increase the λ_{max}, but this effect is not great enough to make these cages visible-light cleavable.[50] Incorporating an R' group in the benzylic position leads to chirality of the photocage, which is a drawback if chiral molecules are to be protected (Figure 13A).[48] However, adding a methyl group to the benzylic position does increase quantum yield.[48] Also, photolysis of nitrobenzyl cages forms potentially toxic byproducts that can absorb strongly, like nitrosobenzaldehyde (Figure 14, if R = H).[48]

Various coumarinyl cages have been developed that offer attractive alternatives to the nitrobenzyl cages (Figures 13 and 14).[48] First generation alkoxycoumarinyl cages lacked water solubility, but the incorporation of carboxylates and an aniline moiety has helped overcome that barrier.[48]

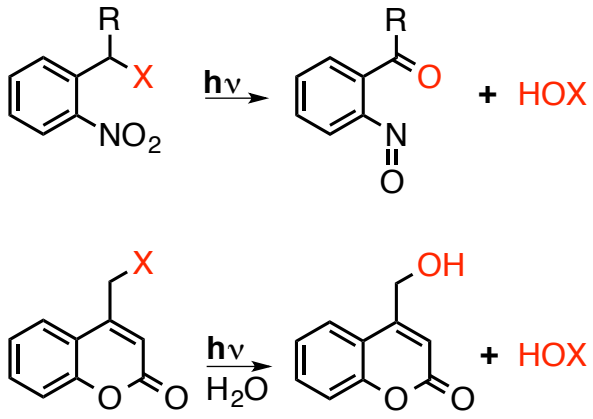

Figure 14. Photo cleavage

One drawback of coumarinyl cages is that it has a strong fluorescence emission, and a low uncaging efficiency.[50] That means that the rate of fluorescence is much faster than the competing photochemical uncaging rate.[2] The mechanism of photorelease is as

follows: after initial absorption, there is relaxation to the lowest π, π* singlet excited state.[48] At this point, there can be radiationless decay, fluorescence, or productive heterolytic C-X bond cleavage (through a conical intersection).[48] The coumarinylmethyl cation formed through heterolytic cleavage can then react with nucleophiles or solvent to form a new stable coumarinyl product (Figure 14).[48]

Recently, Goncalves and co-workers synthesized and studied wavelength-selective cleavage of various photolabile protecting groups by attaching two families of photocages with distinct absorbances to alanine and investigating the photolysis rates in buffered aqueous methanol solutions.[53] Each compound contained a nitrobenzyl-caged alanine that was masked with **A**, **B**, or **C** from Figure 15.[53] The compounds were then irradiated with either 254 nm light to cleave the nitrobenzyl cage, 350 nm light to cleave **A** or **B,** or 419 nm light to cleave **C**.[53] They found that with 350 nm light, cages **A** and **B** cleaved within 18 and 60 minutes respectively.[53] With 419 nm light, cage **C** cleaved within 17 minutes.[53] At both 350 nm and 419 nm, they found that the nitrobenzyl group did photolyze approximately ten percent.[53] Unfortunately, they found that with the 254 nm light, the nitrobenzyl group took 150 minutes to cleave and cages **A**, **B**, and **C** unexpectedly underwent photolysis at times of 25, 48, and 12 minutes respectively. These studies showed that Goncalves et al were able to synthesize wavelength-selective conjugates, but that a specific irradiation sequence was required for success.[53]

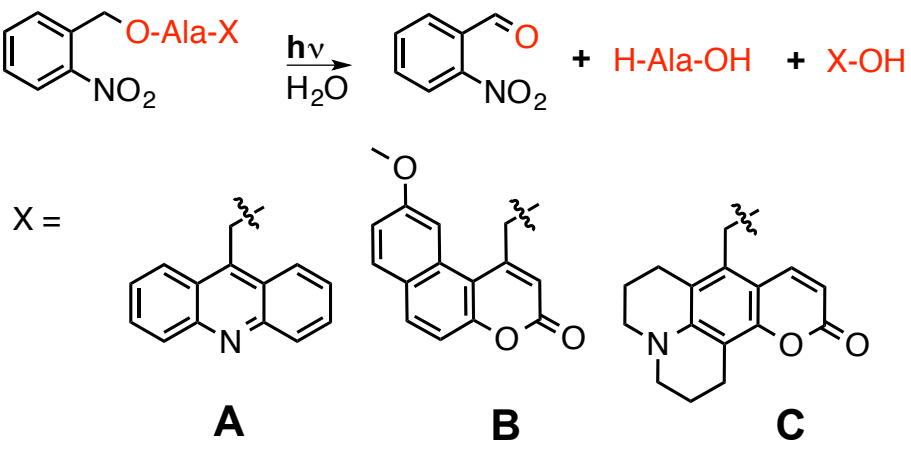

Figure 15. Wavelength-selective cleavage

From the above examples, it is clear that photocages play an important role in biology and chemistry, but it is difficult to rationally design cages that will have an efficient uncaging pathway versus fluorescence pathway. Currently, the structure-reactivity relationship for these photoremovable protecting groups, or photocages, have been discovered serendipitously or through empirical investigations, and the lack of a model for these structure-reactivity relationships hinders the rational design of new structures that undergo photoheterolysis.

REFERENCES

1. G. Ciamician, *Science (New York, N.Y.)*, 1912, **36**, 385-394.
2. E. V. Anslyn and D. A. Dougherty, *Modern Physical Organic Chemistry*, University Science Books, Sausalito, CA, 2006.
3. V. Ramamurthy and K. S. Schanze, *Organic Photochemistry*, 1997.
4. A. G. Griesbeck and J. Mattay, *Synthetic Organic Photochemistry*, 2005.
5. Ramamurthy, V. Ramamurthy and K. S. Schanze, *Optical Sensors and Switches*, 2001.
6. J. Michl, *Electronic Aspects of Organic Photochemistry*, 1990.
7. A. Jablonski, *Nature*, 1933, **131**, 839-840.
8. B. Lasorne, G. A. Worth and M. A. Robb, *Wiley Interdisciplinary Reviews-Computational Molecular Science*, 2011, **1**, 460-475.
9. N. Turro, *Modern Molecular Photochemistry* 1978.
10. N. J. Turro, V. Ramamurthy and J. C. Scaiano, *Modern molecular photochemistry of organic molecules* / University Science Books, 2010.
11. J. Michl, *Molecular Photochemistry*, 1972, **4**, 243.
12. F. Bernardi, M. Olivucci and M. Robb, *Isr. J. Chem.*, 1993, **33**, 265-276.
13. M. A. Robb, F. Bernardi and M. Olivucci, *Pure Appl. Chem.*, 1995, **67**, 783-789.
14. M. Robb, *Advanced Series in Physical Chemistry*, 2011, **17**, 3.
15. F. Bernardi, M. Olivucci and M. A. Robb, *Chem. Soc. Rev.*, 1996, **25**, 321-328.
16. S. Maeda, K. Ohno and K. Morokuma, *Advances in Physical Chemistry*, 2012, **2012**, 13.
17. D. Yarkony, *Reviews of Modern Physics*, 1996, **68**, 985-1013.
18. D. G. Truhlar, in *Encyclopedia of Physical Science and Technology (Third Edition)*, ed. R. A. Meyers, Academic Press, New York, 2003, pp. 9-17.
19. M. Robb, M. Garavelli, M. Olivucci, F. Bernardi, K. B. Lipkowitz and D. B. Boyd, *A Computational Strategy for Organic Photochemistry*, 2000.

20. Ramamurthy, V. Ramamurthy and K. S. Schanze, *Organic Molecular Photochemistry*, 1999.

21. A. Spalletti, G. Bartocci, U. Mazzucato and G. Galiazzo, *Chem. Phys. Lett.*, 1991, **186**, 297-302.

22. Y. Kikuchi, H. Okamoto, T. Arai and K. Tokumaru, *Chem. Phys. Lett.*, 1994, **229**, 564-570.

23. N. J. Turro, P. Lechtken, A. Lyons, R. R. Hautala, E. Carnahan and T. J. Katz, *J. Am. Chem. Soc.*, 1973, **95**, 2035-2037.

24. H. E. Zimmerman, *J. Am. Chem. Soc.*, 1966, **88**, 1564-1565.

25. M. Boggio Pasqua, *The Spectrum*, 2008, **21**, 28.

26. A. D. McNaught and A. Wilkinson, in *XML on-line corrected version*, eds. M. Nic, J. Jirat and B. Kosata, Blackwell Scientific Publications, Oxford, 2nd edn., 1997, vol. 2014.

27. W. Domcke, D. Yarkony and H. Koppel, *Conical Intersections: Electronic Structure, Dynamics & Spectroscopy*, 2004.

28. R. Bourquin, V. Gradinaru and G. A. Hagedorn, *J. Math. Chem.*, 2012, **50**, 602-619.

29. G. A. Worth and L. S. Cederbaum, *Chem. Phys. Lett.*, 2001, **338**, 219-223.

30. W. Domcke and D. R. Yarkony, *Annual Review of Physical Chemistry, Vol 63*, 2012, **63**, 325-352.

31. A. Nenov, P. Kölle, M. Robb and R. de Vivie-Riedle, *J. Org. Chem.*, 2010, **75**, 123-129.

32. J. Michl, *J. Am. Chem. Soc.*, 1971, **93**, 523-524.

33. D. R. Yarkony, *Chem. Rev.*, 2011, **112**, 481-498.

34. A. Devaquet, A. Sevin and B. Bigot, *J. Am. Chem. Soc.*, 1978, **100**, 2009-2011.

35. S. Gozem, I. Schapiro, N. Ferre and M. Olivucci, *Science*, 2012, **337**, 1225-1228.

36. S. Matsika and D. R. Yarkony, *J. Chem. Phys.*, 2001, **115**, 5066-5075.

37. E. Havinga, R. O. Dejongh and W. Dorst, *Recl. Trav. Chim. Pays-Bas*, 1956, **75**, 378-383.

38. H. E. Zimmerman, *J. Am. Chem. Soc.*, 1995, **117**, 8988-8991.

39. H. E. Zimmerman and V. R. Sandel, *J. Am. Chem. Soc.*, 1963, **85**, 915-922.

40. J. A. Pincock and P. J. Wedge, *J. Org. Chem.*, 1994, **59**, 5587-5595.

41. J. W. Hilborn, E. Macknight, J. A. Pincock and P. J. Wedge, *J. Am. Chem. Soc.*, 1994, **116**, 3337-3346.

42. B. Foster, B. Gaillard, N. Mathur, A. L. Pincock, J. A. Pincock and C. Sehmbey, *Can. J. Chem.*, 1987, **65**, 1599-1607.

43. H. E. Zimmerman, *J. Phys. Chem. A*, 1998, **102**, 7725-7725.

44. F. D. Lewis, L. E. Sinks, W. Weigel, M. C. Sajimon and E. M. Crompton, *J. Phys. Chem. A*, 2005, **109**, 2443-2451.

45. V. Dichiarante, D. Dondi, S. Protti, M. Fagnoni and A. Albini, *J. Am. Chem. Soc.*, 2007, **129**, 5605-5611.

46. G. Bouchoux, M. Sablier, T. Miyakoshi and T. Honda, *J. Mass Spectrom.*, 2012, **47**, 539-546.

47. P. Wang, H. Hu and Y. Wang, *Org. Lett.*, 2007, **9**, 2831-2833.

48. P. Klan, T. Solomek, C. G. Bochet, A. Blanc, R. Givens, M. Rubina, V. Popik, A. Kostikov and J. Wirz, *Chem. Rev.*, 2013, **113**, 119-191.

49. X. Tang, J. Zhang, J. Sun, Y. Wang, J. Wu and L. Zhang, *Org. Biomol. Chem.*, 2013, **11**, 7814-7824.

50. X. Tang, in *Photochemistry, Vol 41*, eds. A. Albini and E. Fasani, 2013, vol. 41, pp. 319-341.

51. D. Groff, F. Wang, S. Jockusch, N. J. Turro and P. G. Schultz, *Angew. Chem. Int. Ed.*, 2010, **49**, 7677-7679.

52. P. Sebej, J. Wintner, P. Mueller, T. Slanina, J. Al Anshori, L. A. P. Antony, P. Klan and J. Wirz, *J. Org. Chem.*, 2013, **78**, 1833-1843.

53. A. M. Piloto, S. P. G. Costa and M. S. T. Goncalves, *Tetrahedron*, 2014, **70**, 650-657.

CHAPTER 3

STUDIES TOWARDS UNDERSTANDING PHOTOCHEMICAL HETEROLYSIS FOR DELIVERING BIOMOLECULES

Taken in part from: Buck, A. T.; Beck, C. L.; Winter, A. H., *J. Am. Chem. Soc.,* 2014. In review

INTRODUCTION

The structures of organic molecules that undergo photoheterolysis to generate carbenium ion pairs defy the chemical intuition developed for thermal heterolysis. Known photoheterolysis reactions frequently generate classic examples of unstable carbenium ions, such as pi-donor unconjugated ions,[1, 2] antiaromatic ions,[3-5] and dicoordinated aryl/vinyl cations.[6-8] Few examples report efficient heterolysis to generate stabilized cations. To date, no model connects structure to reactivity for these photoreactions, and many of the known photoremovable protecting groups,[9] or photocages, have been discovered serendipitously or through empirical investigations. The lack of a structure-reactivity relationship for photoheterolysis reactions has hindered the rational design of new structures that undergo photoheterolysis, which are reactions of applied importance in materials,[10] synthetic,[8, 11] medicinal,[12] and biological chemistry.[13]

Here, we attempt to understand why successful photochemical heterolysis reactions of C-LG bonds frequently generate unstabilized carbocations, which is the opposite of structural preferences for thermal heterolysis reactions. We were inspired by Zimmerman's,[14, 15] Turro's,[16,17] and Michl's[18] early investigations on the importance

of conical intersections in photoreactions, Zimmerman's later investigations into the role of the conical intersection for explaining the '*meta*-effect,'[19] and more recent computational advances in searching for conical intersections in complex chemical systems.[20-24] Therefore, we investigated the hypothesis that these surprising photoreactivities might be linked to conical intersection control,[24] which is the concept that an increasing number of photoreactions are thought to proceed via radiationless, non-adiabatic mechanisms, channeling from the excited-state surface to the ground-state surface via a conical intersection.[25, 26] As a result, the role and importance of the conical intersection for non-adiabatic photoreactions has been likened to that of the transition state for thermal reactions in terms of governing the reaction.[27] For example, the propensity of many photoreactions to generate strained molecules has been attributed in part to conical intersection control,[17] wherein highly strained photoproducts are located at energetic spikes on the ground-state surfaces leading to nearby conical intersections with the excited state, providing a productive channel for the photoreaction to proceed from the excited-state to the strained ground-state minimum.

We hypothesized that generation of certain unstabilized carbenium ions, while disfavored thermally, might be favored photochemically by elevating the ground-state heterolysis reaction coordinate surface at the ion pair geometry. In combination with a stabilized excited-state surface at this geometry, a productive conical intersection may result that provides a channel for the photoreaction to proceed from the excited-state to the ground-state ion pair, making the photoheterolysis reaction pathway for these

structures competitive with unproductive photophysical processes (internal conversion, luminescence, etc). In contrast, heterolysis reactions that generate stable cations necessarily have lowered ground-state surfaces along the heterolysis reaction coordinate, making it less likely for these structures to have a nearby productive conical intersection near the ion pair (Figure 1).

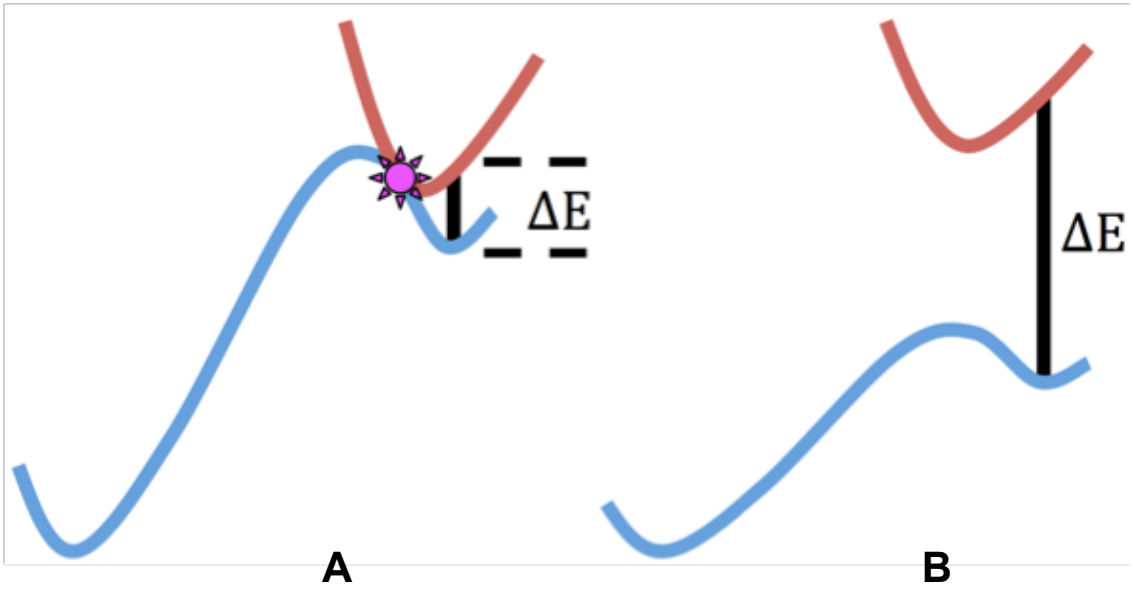

Figure 1. Schematic of hypothesis that a destabilized ground state and a stabilized excited state can lead to a favorable, nearby conical intersection (A), whereas it is unlikely that a stabilized ground state will have a nearby conical intersection (B). The black line indicates how the S_0-S_1 excited-state vertical energy gap for carbocation may act as a convenient, easy-to-calculate probe for a nearby conical intersection.

To test the hypothesis that these unstabilized cation structures have favorable, nearby conical intersections, we performed minimum energy crossing searches (conical intersections) of representative cations in combination with an excited-state vertical energy gap probe approach that allowed us to expand our investigation to a larger number of systems. We find that stable cations, such as those with conjugated pi-donors or aromatic cations, generally have high-energy conical intersections relative to their excited-state minima. In contrast, certain unstabilized or destabilized cations (e.g. non-conjugated donor-substituted cations, antiaromatic cations, substituted aryl cations, etc), have stabilized excited states and low-energy, nearby conical intersections (Figure 2). Our results suggest that the frequent substituent orthogonality between thermal and non-adiabatic photochemical heterolysis reactions may arise from conical intersection control.

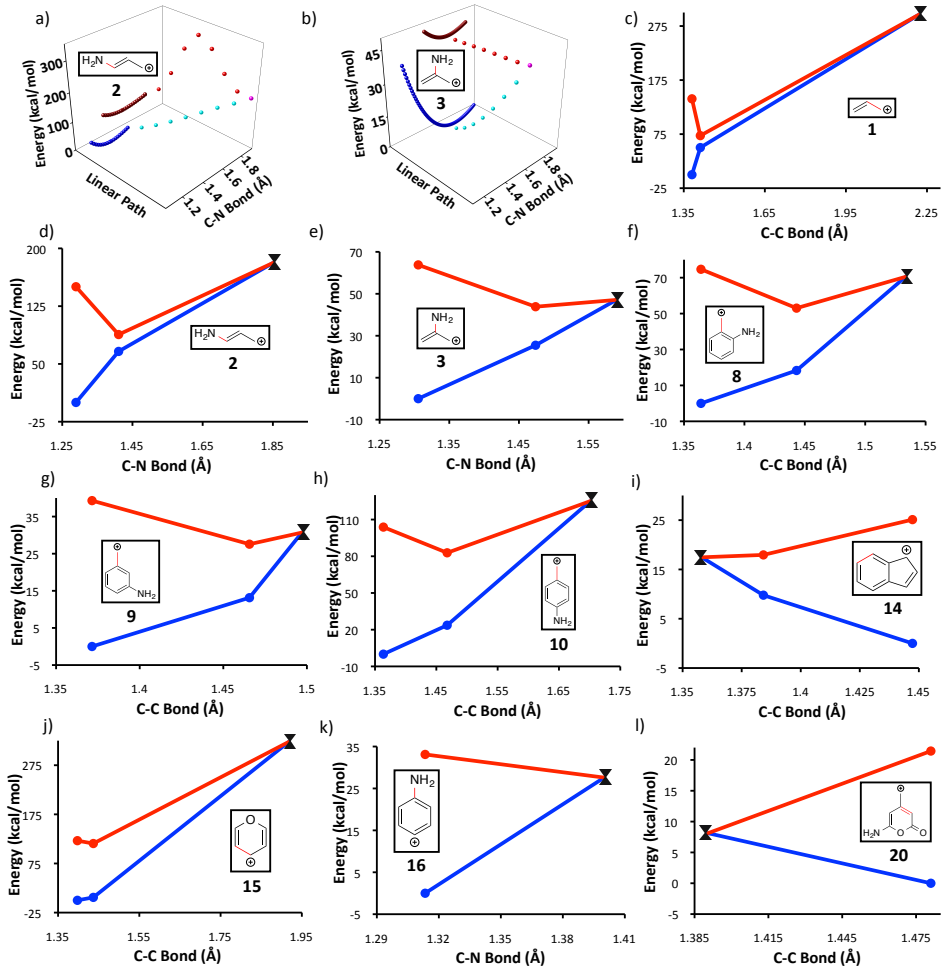

Figure 2. Calculated points on the potential energy surfaces of the cations studied by CASSCF with full pi active space. a, b) 3D graphs of calculated points on S_0 and S_1 surface with linear path to the nearest conical intersection. c - l) graphs of the energies of the potential energy surfaces relative to respective ground states. c) allyl **1**, d) 1-aminoallyl **2**, e) 2-aminoallyl **3**, f) *o*-aminobenzyl **8**, g) *m*-aminobenzyl **9**, h) *p*-aminobenzyl **10**, i) indenium **14**, j) pyrylium **15**, k) *p*-aminophenyl **16**, and l) aminocoumarin analog **20**. Red bond in the inset shows the bond chosen for the geometrical coordinate.

RESULTS AND DISCUSSION

Computational Methods. Minimum energy crossings (conical intersections) were computed using complete pi active spaces for the cations in the gas phase employing the state-averaged CASSCF procedure implemented in GAMESS,[28] using the 6-31G(d) basis set (giving equal weighting to ground state and excited state). For example, the *m*-aminobenzyl cation was computed using a (8,8) active space, consisting of eight π electrons in the eight π orbitals. To ascertain the energy gaps between the ground-state and excited-state surface, we used time-dependent density functional theory (TD-B3LYP/6-311+G(2d,p) at the DFT-optimized geometries (RB3LYP/6-31G(d)) using Gaussian 09.[29] TD-DFT is known to give reasonable results for excited state energy gaps,[30, 31] provided the ground state can be described predominantly by a single reference wavefunction. By computing the conical intersection and excited-state energies of the cation (and neglecting the leaving group) we assume that the photochemistry occurs to the greatest extent on the part of the molecule that becomes the cation moiety and not the leaving group. This approach was employed by Zimmerman for studying the *meta*-effect[14, 15] and appears to be a reasonable assumption, since these excited-state substituent effects appear to be largely independent of the leaving group, experimentally. For example, known photocage structures undergo efficient photoheterolysis with a variety of different leaving groups, suggesting that the photochemistry is largely directed by the structure of the cation than by the leaving group. Typical leaving groups include phosphates (e.g. ATP),[32] carbamates,[33] carbonates,[34] carboxylates,[35] and even 'bad' leaving groups such as $^{-}$OH.

Additionally, by neglecting the leaving group from our calculations we assume that the relative cation ground-state and excited-state energies are not, to a major degree, influenced by ion pairing.

Computational Results. Carbocations that were included in this computational study are shown in Chart 1. Some of these carbocations result from photoheterolysis reactions of known substrates (structures **7-9**, **12-14**, **16**, **21**, **22**, **26-28**, **31-35**),[36] or are simplified structures of known substrates for computational convenience (e.g. cation **15** is a chemically simplified version of the known substrate **21,** while **20** is a chemically simplified version of **26**). Other cations included in our study are those that result from substrates that are emperically known to *not* undergo efficient photoheterolysis (e.g. **10**, **30**). The remaining cations (**1-6**, **11**, **17-19**, **23-25**, **36-39**) were investigated to understand the effect of chemical structure on the ground-state—excited-state vertical energy gap, which we propose may be useful as a simple computational probe for the presence of a nearby conical intersection. Photochemical substrates that do not involve direct heterolytic scission from the excited state, such as the *o*-nitroaromatic caging systems, are not relevant to the present discussion and were omitted from this study.

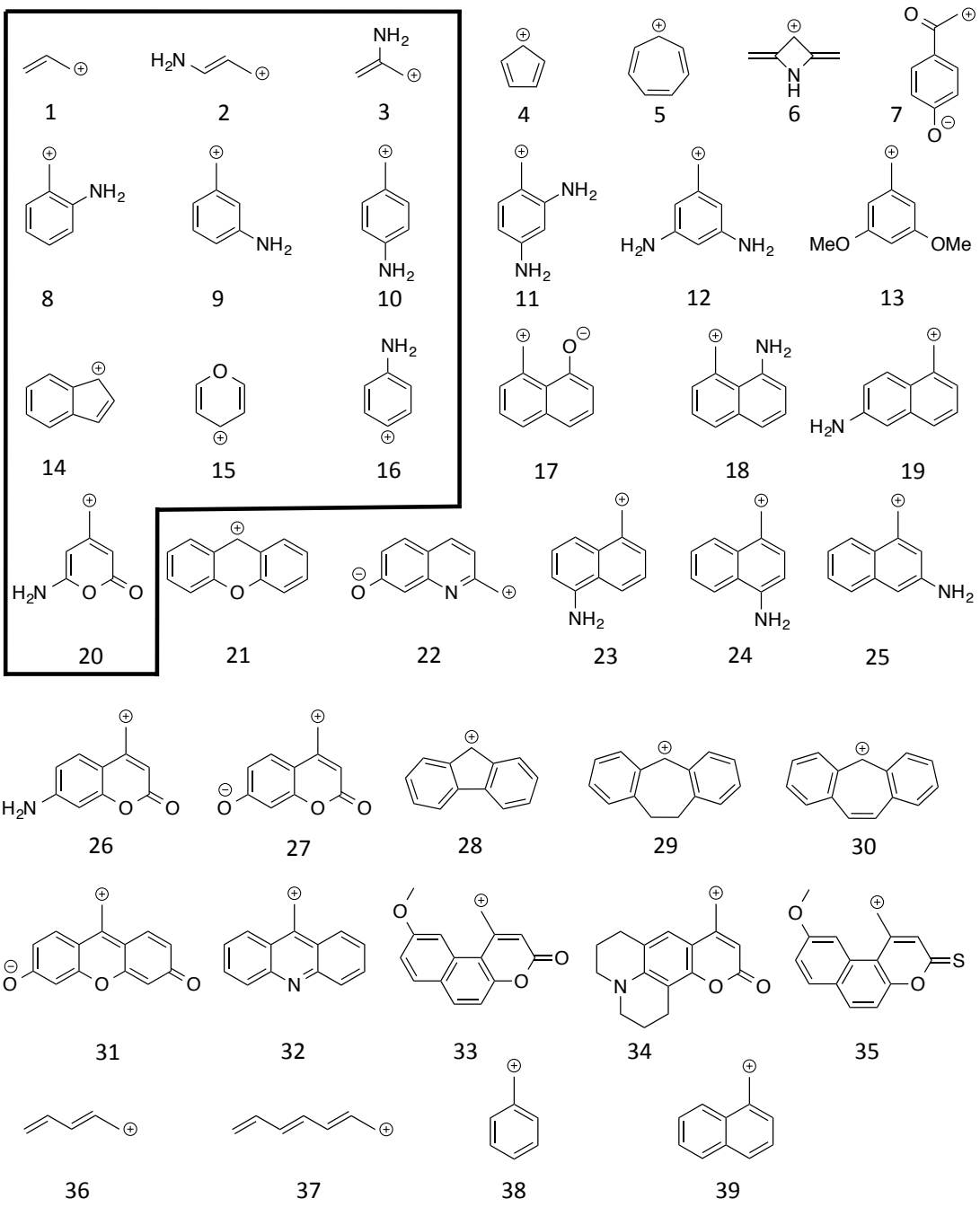

Chart 1. Structures of cations studied. Structures studied by both TD-DFT and CASSCF conical intersection searches are shown within the box while structures studied by TD-DFT alone are shown outside of the box.

Many of the known successful photoheterolysis reactions that generate carbenium ions have cation structures that fall into three main classes: 1) pi-donor unconjugated 'benzylic' cations (e.g. 3,5-dimethoxybenzyl cation[37] **13**, 9-aminocoumaryl cation[9, 38, 39] **26**); 2) Cations that are formally antiaromatic following Hückel's Rule (e.g. fluorenyl[40] **28**, indenyl cation[41] **14**); and 3) Dicoordinated carbocations (e.g. donor-substituted vinyl/aryl cations[6-8] **16**). The unusual nature of these substrates' favor for photoheterolysis has not gone unnoticed. Pincock and Young[41] noted that for photoheterolysis of the indenyl cation that "efficient generation by this photochemical solvolysis is in sharp contrast to the very low reactivity of related ground-state substrates." The original report of the "*meta*-effect" by Havinga[42] noted that rapid heterolysis of *meta*-substituted systems "defies a chemical explanation." In contrast, the scarcity of reports of photoheterolysis in substrates that generate stabilized cations is intriguing. However, two notable cases have been reported as counterpoints to successful photoheterolysis reactions. The precursor to the aromatic ion **5** was reported to not undergo photoheterolysis while the substrate leading to antiaromatic indenyl cation does undergo facile photoheterolysis;[41] additionally, *para*-donor-substituted benzylic systems are reported to not undergo photoheterolysis, in contrast to the *meta*-substitued derivatives,[19] giving rise to the so-called '*meta*-effect.' However, the observation that photochemical heterolyses generally appear to favor the formation of classic examples of unstable carbocations, while few report the formation of stabilized cations, has to our knowledge not been rigorously addressed.

Conical intersection mimimum energy crossing searches for cations *1-3, 8-10, 14-16, 20*. To test the hypothesis that photoheterolysis reactions generate carbocations with favorable conical intersections, we performed conical intersection searches on representative cations that fall within the three major classes of ion favored from photoheterolysis mentioned above as well as the counterpoint substrates that are known to not undergo efficient photoheterolysis. We anticipated that cations resulting from photochemically-favored substrates would have low-energy nearby conical intersections whereas cations resulting from substrates lacking a favored photoheterolysis pathway would have higher energy unfavorable conical intersections. Cations **8-10** were chosen for study since *ortho* and *meta* donor-substituted substrates favor photoheterolysis, whereas a *para* donor substituent does not favor photoheterolysis.[19, 43] Cation **20** was chosen as a simplified model system of the cation resulting from the popular 9-aminocoumaryl photocage **26**, which preserves the unconjugated nature and connectivity of the amine donor substituent but eliminates the benzene ring to yield a system for which a conical intersection search is computationally tractable. Cation **14** is a representative system of the formally antiaromatic cations that are favored from photoheterolysis; pyrilium cation **15** is a simplified version of a known substrate that generates the aromatic ion **21** via an adiabatic photochemical mechanism.[44, 45] Cation **16** is chosen as representative of the dicoordinate carbocations often favored from photoheterolysis. Finally, systems **1-3** were investigated as possible simple new systems that may undergo photoheterolysis.

For each of the carbocations, we computed the CASSCF optimized geometries

and energies for the ground-state minimum, the first singlet excited-state minimum, and the conical intersection between the ground state and the singlet excited state. These energies are plotted versus a geometrical coordinate in Figure 2. As can be seen from Figure 2, cations deriving from photochemically favored substrates **(9**, **14**, **16**, **20)** are found to have low-energy conical intersections relative to the excited-state minimum.

Additionally, cations resulting from photochemically favored substrates have small structural deviations between the excited-state minimum and the conical intersection structures, whereas those unfavored systems with high-energy conical intersections have large structural distortions. There are also large structural distortions between the ground-state minimum and the unfavored high-energy conical intersection structures (Figure 3). Note that in two cases (**16**, **20**) we were unable to locate an excited-state minima, suggesting that there is a direct channel from the Franck-Condon excited state to the conical intersection bypassing a minimum.

These results support the idea that conical intersection control is an important feature of these photoheterolysis reactions. Those unstabilized carbocations that are favored from photoheterolysis (or their model systems) have low-energy, nearby conical intersections to the excited-state minimum. In contrast, the stabilized cations have high-energy, distant conical intersections relative to the excited-state minima.

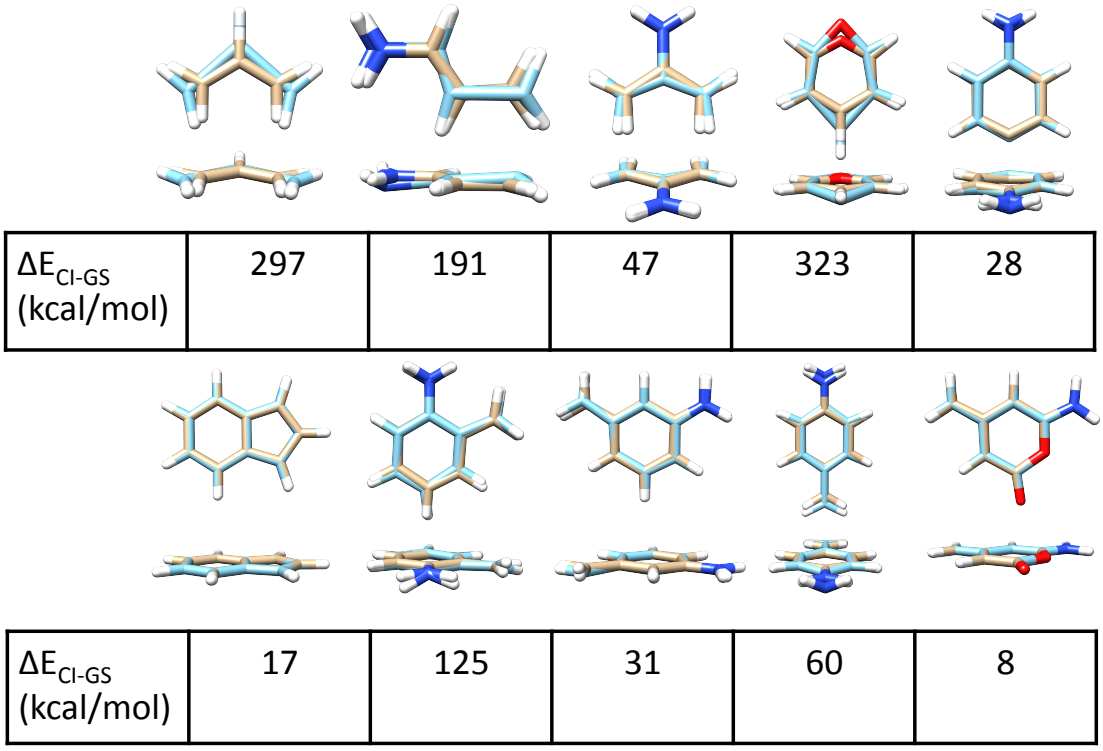

ΔE_{CI-GS} (kcal/mol)	297	191	47	323	28
ΔE_{CI-GS} (kcal/mol)	17	125	31	60	8

CASSCF/6-31G(d) with a full pi active space

Figure 3. Ground-state minimum and conical intersection structures overlayed. When ΔE_{CI-GS} is large (high-energy conical intersection), there are large structural distortions, but when ΔE_{CI-GS} is small, there are small structural distortions.

Stabilized-cation excited states. Conical intersections occur at biradical geometries.[46, 47] Thus, assuming no major structural deviations in the excited state, cations having favorable nearby conical intersections should have low-energy ion diradical forms. For those species belonging to class 1 described on page 118 (donor-unconjugated cations), the excited states resemble stabilized non-Kekule diradical ions (Figure 5). These diradical forms can be envisioned as deriving from promotion of a π

electron on the unconjugated donor substituent to the formally empty cation π* orbital to provide an ion diradical connected by non-disjoint singly occupied molecular orbitals (SOMOs). This view is supported by our time-dependent density functional theory (TD-DFT) computed difference density plots between the ground state and the excited state (Figure 4).

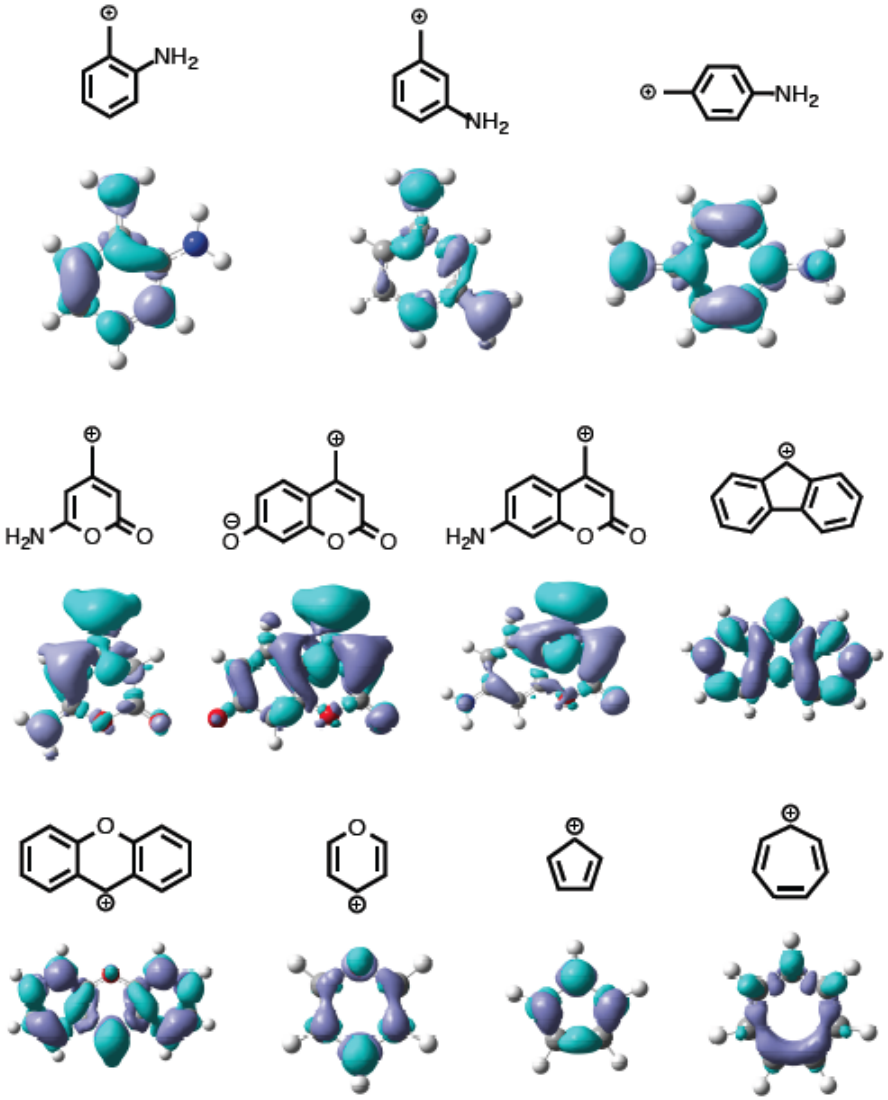

Figure 4. TD-DFT density difference plots between the ground state and the excited state. Electrons travel from lavender in the ground state to aqua in the excited state.

For example, the *meta*-donor substituted systems have an excited singlet ion diradical form that is electronically analogous to the classic *meta* xylylene diradical,[48] with a radical at the "carbenium center" and a cation radical donor substituent. There are numerous examples of cations that fall within this type (**9**, **12**, **13**, **17**, **18**, **19**, **22**, **23**, **24**, **25**, **26**, **27**, **31**). Thus, while the donor group does not act to stabilize the ground-state cation via resonance, it leads to stabilized singlet diradical excited states. For ions belonging to class 2 (antiaromatic cations), the excited state resembles a π,π* cation diradical. These antiaromatic cations are classic examples of cations with low-energy excited states, and Wan has suggested the excited state of these antiaromatic ions may have aromatic character.[5] Examples falling into class 3 (dicoordinated cations, such as aryl/vinyl cations) have excited states resembling open-shell cationic carbenes. These representations can be seen from inspection of the SOMOs and are diagrammed in Figure 5.

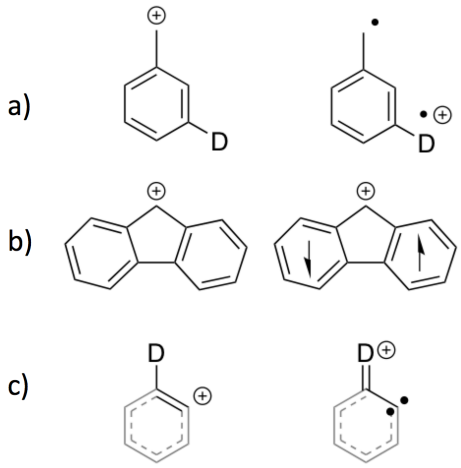

Figure 5. Representations of the different classes of excited-state cations discussed (ground-state cation shown at left, excited state Lewis representation at right). a) donor-unconjugated cations and stabilized non-Kekule ion diradical form (right), b) formally antiaromatic cations, and c) dicoordinated cations.

Excited-state energy gaps as a simple probe for nearby conical intersections. Unfortunately, the practical difficulty and computational expense associated with computing conical intersections makes a complete investigation of all systems unfeasible. Since we are interested in a broad investigation, we tested the possibility of using the ground-state—excited-state vertical energy gap of the cation to probe for a nearby conical intersection. We considered that low vertical energy gaps between the cation ground state to the first excited state, which are easily computable using TD-DFT, would implicate a nearby conical intersection, assuming that there are no major structural deformations in the cation excited-state structure (Figure 1).

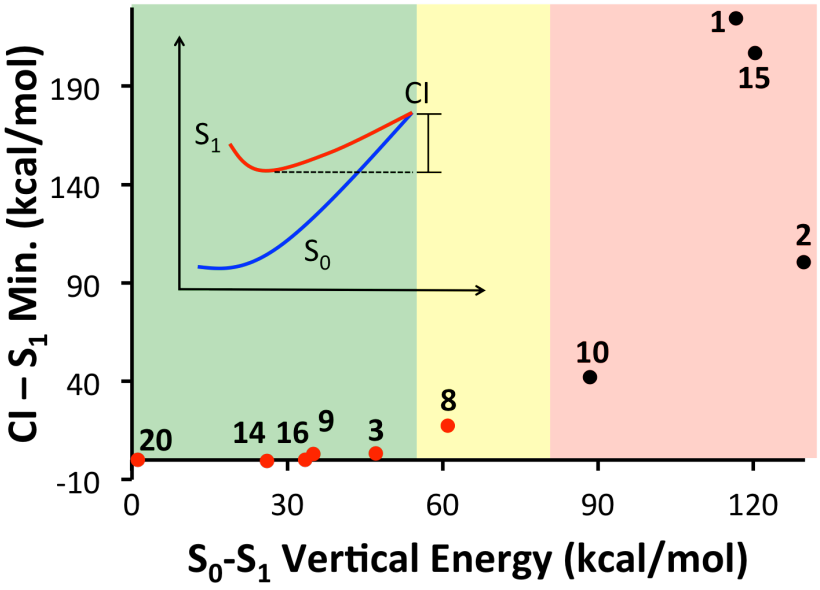

Figure 6. A plot of the difference in conical intersection energy and S_1 minimum energy vs. TD-DFT computed S_0-S_1 Franck-Condon vertical energy gap for the compounds studied. Red points show compounds that are experimentally found to be photoactive or have a nearby conical intersection. Cation **15** is a model system for cation **21** that results from photoheterolysis via an adiabatic mechanism, indicating no nearby conical intersections.

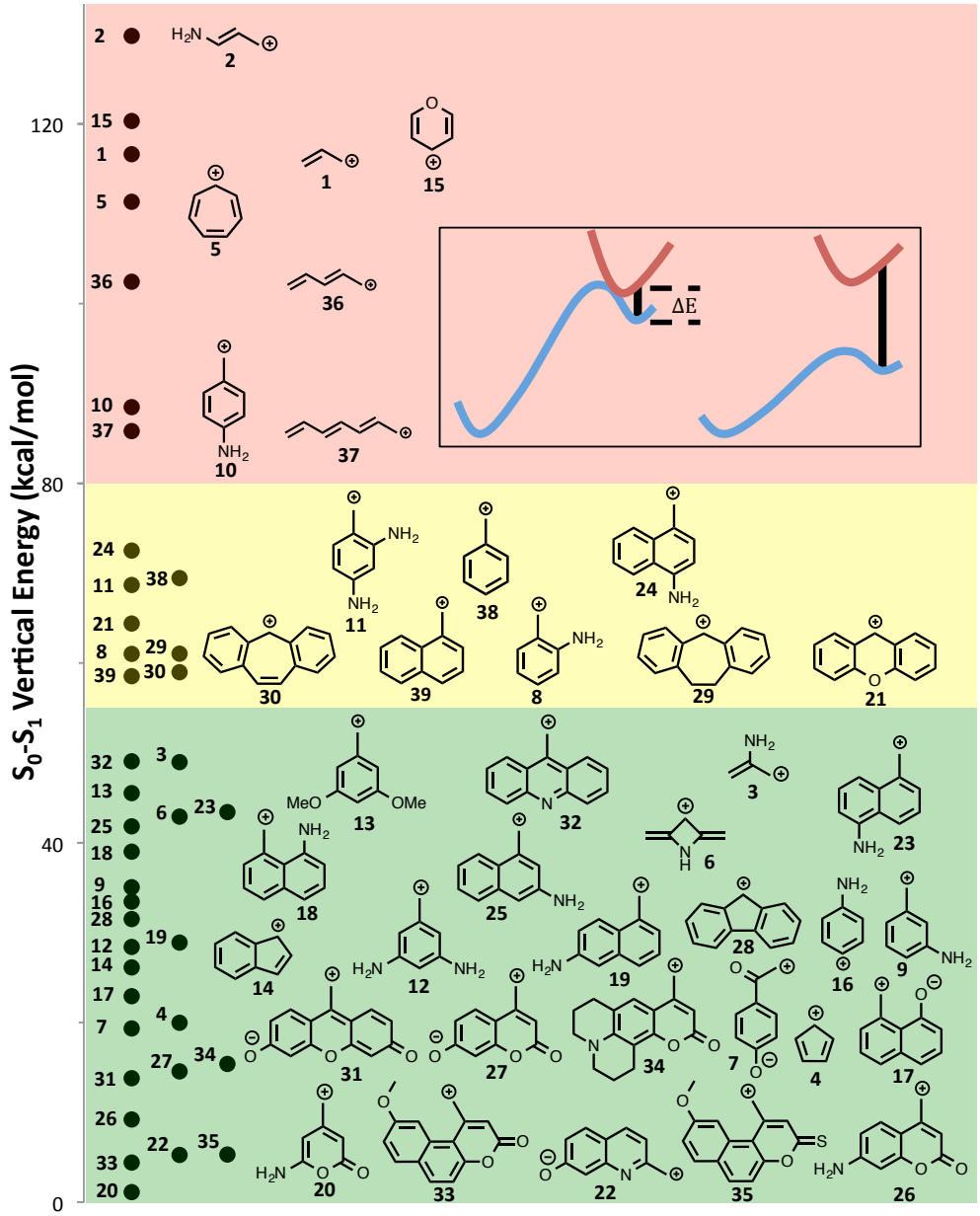

Figure 7. An energy level diagram comparing the Franck-Condon vertical energy gap (TD-B3LYP/6-311+G(2d,p)) of all of the cations studied. Compounds in the green section encompass most of the cations from the photoactive species. The maximum of the green section is where the inflection point is found in Figure 6 for the onset of a significant barrier between the S_1 minimum and the conical intersection. Cations in the

red sections would be expected not to have low-energy conical intersections. Inset: Hypothesis that a small vertical energy gap suggests a nearby conical intersection.

A correlation between the energy of the conical intersections of the cations we computed and their excited-state energy gap computed by TD-DFT appears to provide some evidence to support the validity of this approach (Figure 6), with an apparent inflection point at approximately 60 kcal/mol, where significant barriers between the ground-state minimum and the conical intersection appear. Additionally, the Franck-Condon vertical energy gaps of the unstabilized carbocations that are favored from photoheterolysis are generally lower than for stabilized carbocations (Figure 7). Cations **1** and **36-39** are included to show the vertical gap of "normal" conjugated cations, indicating that these structures do not have a favorable conical intersection in the default case (Figure 7).

Discussion. The preponderance of successful photochemical substrates leading to cations with excited states resembling non-Kekule ion diradicals led us to consider related structures that would have lowered-energy excited states. The simplest non-Kekule diradical is the trimethylene methane diradical. The analogous cation of this structure bearing a donor substituent, 2-aminoallyl cation **3**, would be expected to have a low-energy excited state, while the conjugated 1-aminoallyl cation **2** would not be expected to have this lowered energy excited state. Indeed, the energy from S_0 minimum to S_1 minimum for **2** is 88.2 kcal/mol while the same gap for **3** is 43.8 kcal/mol (Figure 2). Additionally, the energy gap between the conical intersection and

the S_1 minimums for **2** and **3** are 100.7 kcal/mol and 3.2 kcal/mol, respectively, supporting the idea that the 2-aminoallyl cation may have access to a productive conical intersection during photoheterolysis, in contrast to the 1-aminoallyl system. These systems would represent a simple but spectacular demonstration of the substituent orthogonality between thermal and photochemical substrate preferences for heterolysis.

It should be noted that alternative mechanisms are available for photoheterolysis other than direct non-adiabatic heterolysis via a conical intersection located on the cation. For instance, the aromatic ion **21**, for which our calculations on the model system **15** indicates has a high-energy, unfavorable conical intersection, is generated efficiently from photolysis, but arises via a less-common adiabatic mechanism, with formation of the singly-excited carbocation that relaxes by fluorescence to yield the ground-state ion pair. Additionally, by neglecting the leaving group, we are also not considering the possibility of a conical intersection between the diradical and zwitterionic forms (e.g. R• LG• and R^+ LG^-), so a mechanism involving homolytic scission followed by electron transfer may be available. This mechanism may give rise to successful photoheterolysis pathways in systems yielding cations that do not have a conical intersection located on the cation moiety (e.g. possibly ortho-substituted benzylic systems). Generation of highly stabilized carbocations may also arise via hot ground-state photoreactions, although these mechanisms are thought to be rare. Thus, the cation conical intersection (or the vertical energy gap probe) may be more useful in suggesting new systems that are likely to have a productive conical intersection along the heterolysis coordinate than in suggesting systems that will be photostable.

Additionally, this hypothesis provides an explanation of why 'bad' leaving groups in the ground state, such as hydroxides or alkoxides, can be 'good' leaving groups in the excited state, because making a high-energy ion pair would elevate the ground-state surface.[49]

Photocage studies. Compounds **31-35** have been shown in literature to function as photolabile protecting groups (mentioned on page 104 in the Introduction section).[50, 51] The computed vertical energy gap for compounds **31-35** was less than 50 kcal/mol (*vide supra*), indicating the possibility of having a nearby, low-energy conical intersection for these compounds. We were interested in comparing the vertical energy gaps of compounds **31-35** to those of BODIPY cations, which are expected to also find function as photolabile protecting groups (Figure 8). The nitrogens in red are pi-donor unconjugated to the cation, leading to the lone pair of electrons' inability to stabilize the ground-state cation via resonance, resulting in an unstabilized ground state. It is also expected that the BODIPY compounds studied will have stabilized singlet diradical excited states represented by Figure 5a.

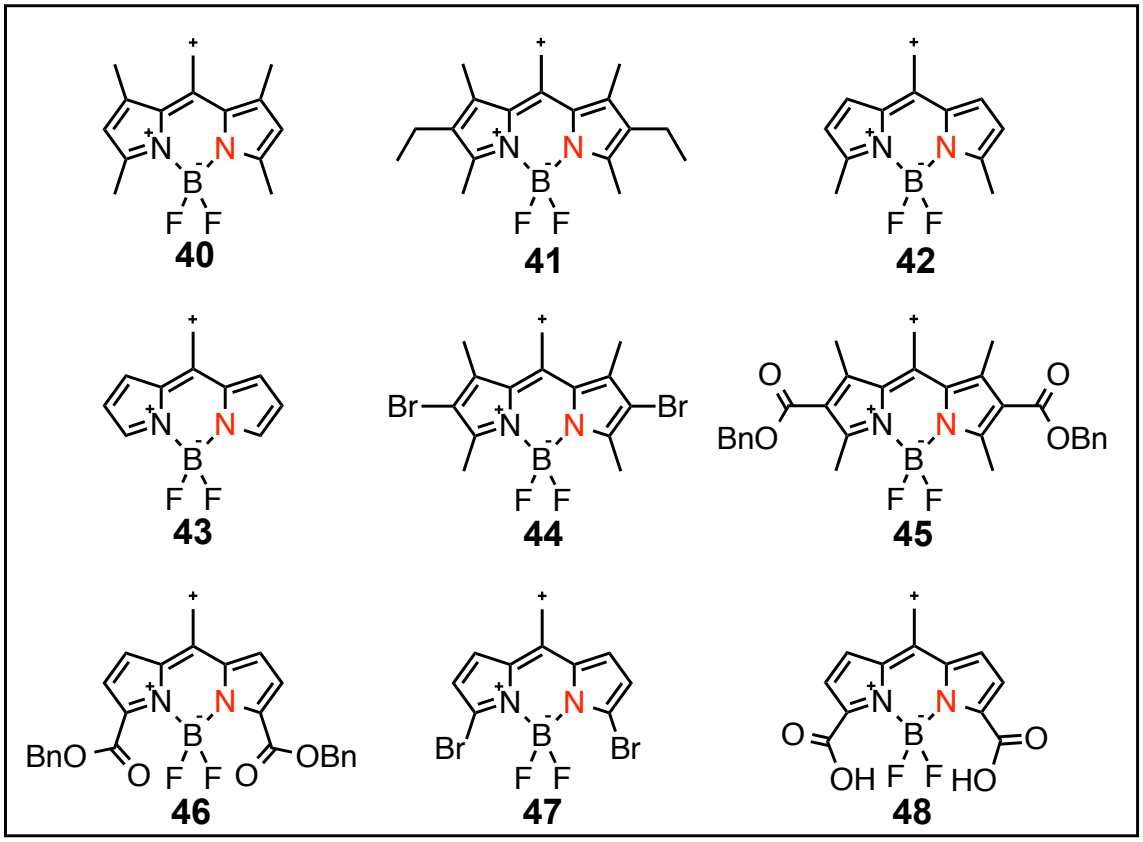

Chart 2. Structures of BODIPY cations studied by TD-DFT computations.

DFT computations (B3LYP/6-31G(d)) were used to compute geometries of cations **40**-**48**. An effort was made to find the lowest-energy rotamer for compounds **41**, **45**, **46**, and **48**. Time-dependent excited-state calculations (TD-B3LYP/6-311+G(2d,p)) were carried out on all of the BODIPY cations in Chart 2.

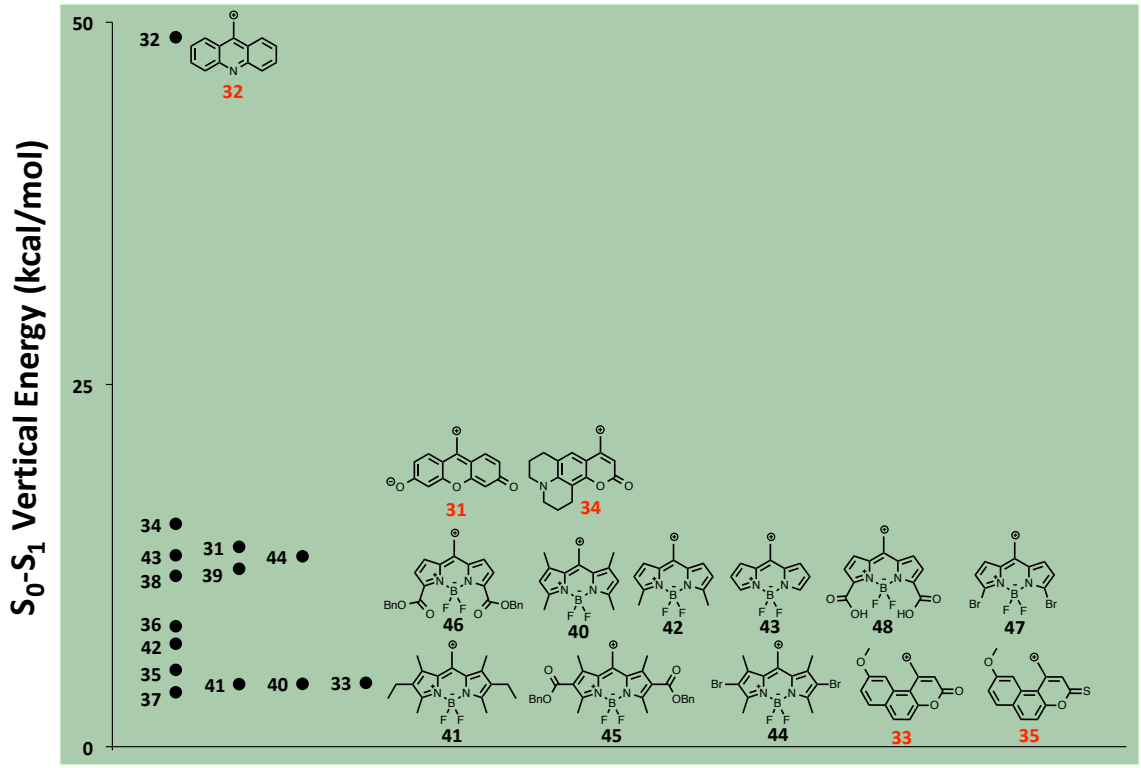

Figure 8. An energy level diagram comparing the Franck-Condon vertical energy gap (TD-B3LYP/6-311+G(2d,p)) of all of the BODIPY cations studied (Black) compared to photolabile protecting groups reported in literature (Red).[50, 51] All compounds lie within the green section, indicating the possibility of having a low-energy, nearby conical intersection.

EXPERIMENTAL

As can be seen in Figure 8, all of the BODIPY cations studied computationally have a vertical energy gap of less than 25 kcal/mol, which indicates the possibility of having a low-energy nearby, conical intersection. We were interested in studying this experimentally, so BODIPY compounds **40a**,[52] **41a**,[52] and **42a**[53] were synthesized

according to known literature procedures (Chart 3). Their spectra matched the reported literature values. A small amount of authentic sample of **40a** was graciously provided by Mark E. Thompson's group from USC, Los Angeles.

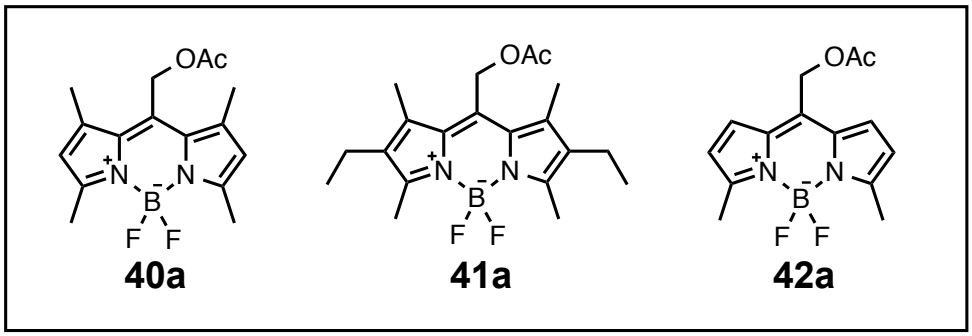

Chart 3. BODIPY compounds studied experimentally

Photolysis studies. Compounds **40a**, **41a**, and **42a** all absorb in the visible region with $\lambda_{max} > 500$ nm. Each sample was dissolved in deuterated methanol, placed in an NMR tube, and irradiated with a xenon lamp for varying time intervals. In all samples, heterolysis of the acetate leaving group followed by solvolysis by the deuterated methanol leads to an increase of an acetic acid peak by NMR (Scheme 1 and Figures 9-11).

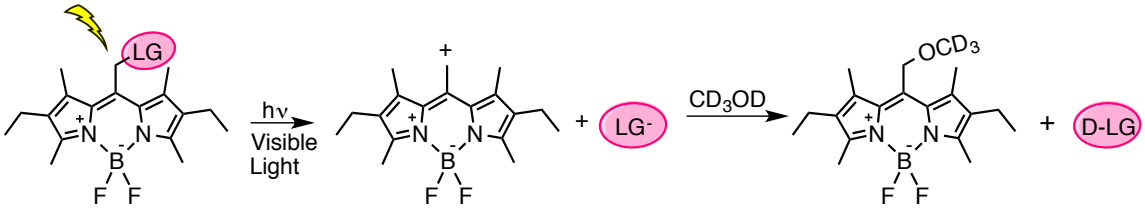

Scheme 1. General scheme for heterolysis followed by solvolysis for all of the dyes studied. It was expected that the growth of the leaving group (acetic acid) would be observed by NMR.

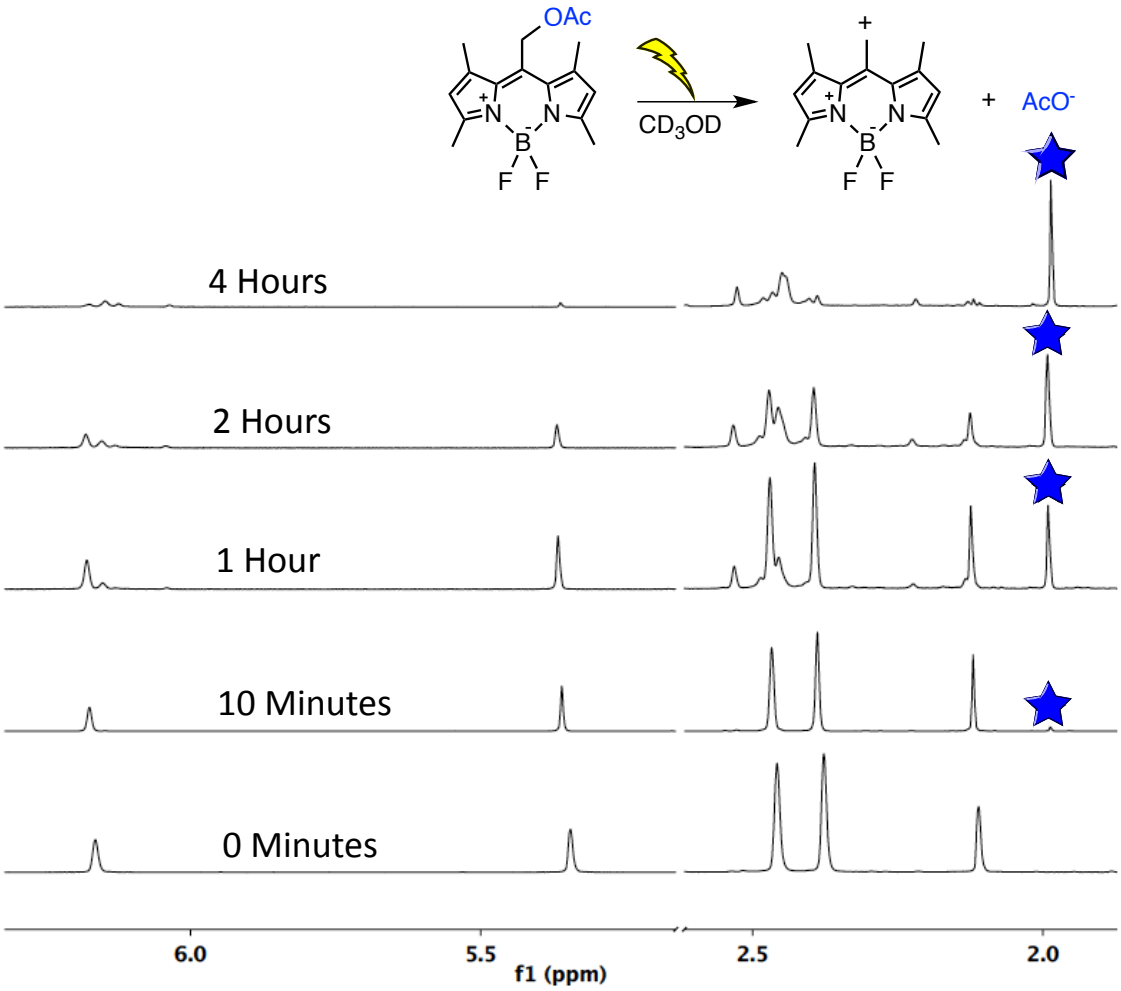

Figure 9. Photolysis of compound **40a** in CD_3OD. ^1H stacked spectra of compound **40a** in CD_3OD-d4 referenced to the water peak (4.87 ppm). The water and methanol peaks have been removed for clarity. Acetic acid (star) begins to appear within ten minutes of irradiation with a xenon lamp (1.99 ppm). Complete heterolysis is seen by 4 hours of irradiation time.

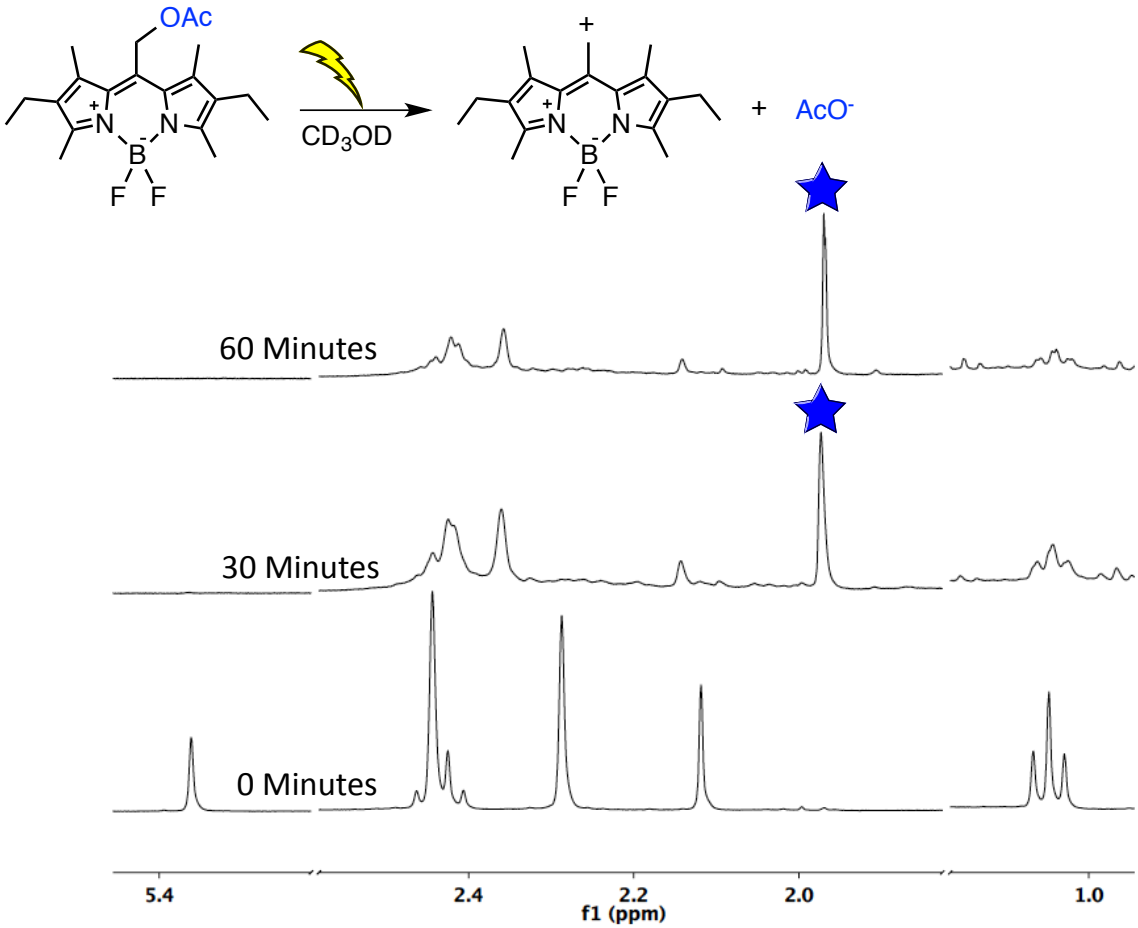

Figure 10. Photolysis of compound **41a** in CD_3OD. ^1H stacked spectra of compound **41a** in CD_3OD-d4 referenced to the water peak (4.87 ppm). The water and methanol peaks have been removed for clarity. Acetic acid (star) begins to appear within thirty minutes of irradiation with a xenon lamp (1.99 ppm). Complete heterolysis is seen within one hour of irradiation time.

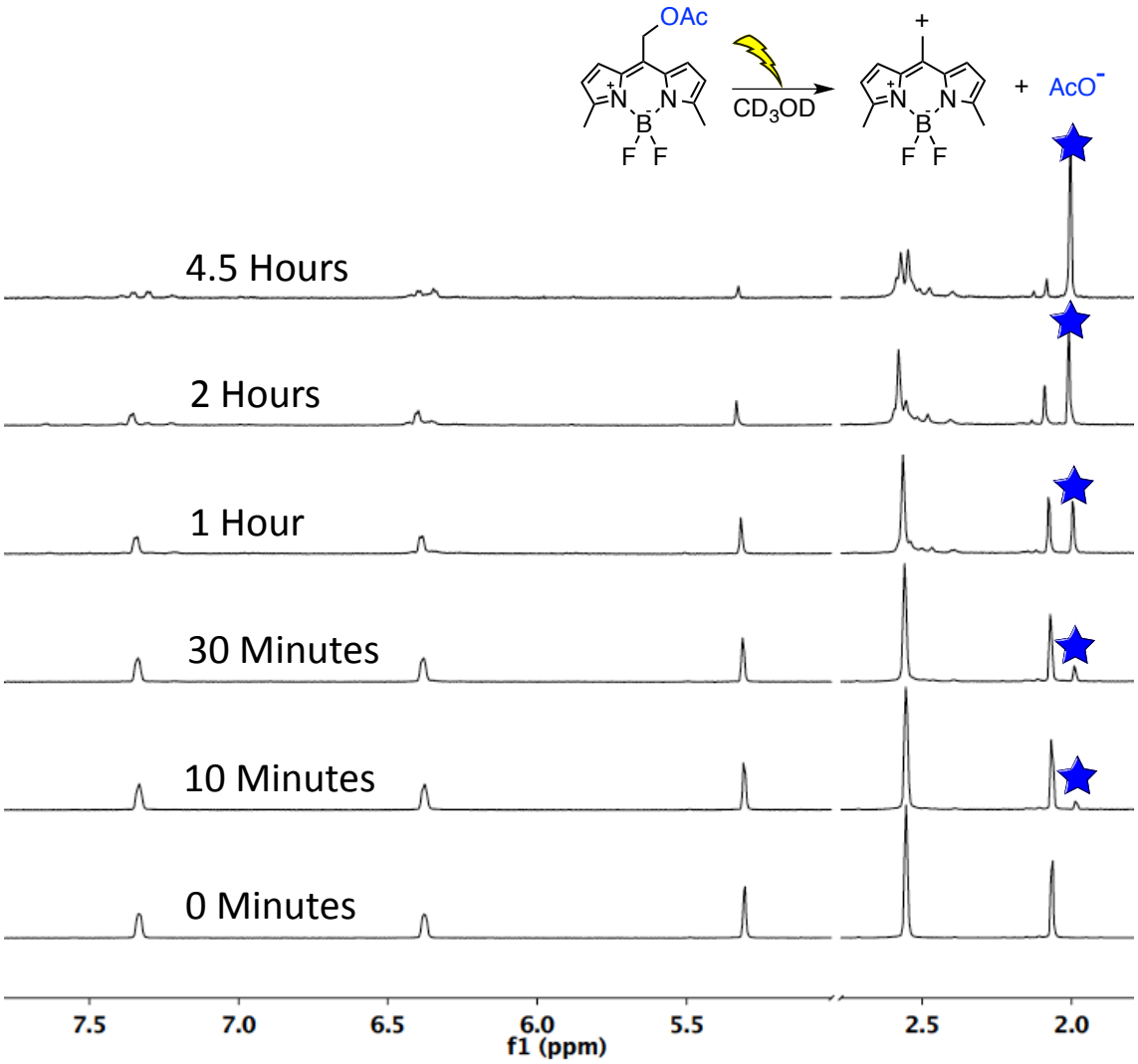

Figure 11. Photolysis of compound **42a** in CD_3OD. ^1H stacked spectra of compound **42a** in CD_3OD-d4 referenced to the water peak (4.87 ppm). The water and methanol peaks have been removed for clarity. Acetic acid (star) begins to appear within ten minutes of irradiation with a xenon lamp (1.99 ppm). Almost complete heterolysis is seen at 4.5 hours of irradiation time.

CONCLUSION

In conclusion, we have shown that carbocations favored from photoheterolysis tend to have nearby, low-energy conical intersections while stable carbocations from thermal heterolysis tend to have high-energy, distant conical intersections. These findings lend support to the idea that conical intersection control leads to the frequent inverted substrate preferences between non-adiabatic photoheterolysis and thermal heterolysis. The idea that these photoheterolysis reactions may be governed by conical intersection control could facilitate the design of new photocages with improved light absorbing properties by searching for substrates leading to carbocations with a favorable built-in conical intersection. We have shown three photocages that undergo heterolysis by visible light photolysis. Time-dependent excited-state vertical energy gap computations of the cations generated through heterolysis show that these photocages have the potential for low-lying, nearby conical intersections. These studies open up the possibility for designing visible-light cleavable photocages that have the potential for numerous applications including drug delivery and biological imaging.

REFERENCES

1. A. H. Winter, D. E. Falvey, C. J. Cramer and B. F. Gherman, *J. Am. Chem. Soc.*, 2007, **129**, 10113-10119.

2. S. Milanesi, M. Fagnoni and A. Albini, *J. Org. Chem.*, 2004, **70**, 603-610.

3. D. Budac and P. Wan, *J. Org. Chem.*, 1992, **57**, 887-894.

4. D. Shukla and P. Wan, *J. Photochem. Photobiol., A*, 1998, **113**, 53-64.

5. P. Wan and E. Krogh, *J. Am. Chem. Soc.*, 1989, **111**, 4887-4895.

6. H. Qrareya, C. Raviola, S. Protti, M. Fagnoni and A. Albini, *J. Org. Chem.*, 2013, **78**, 6016-6024.

7. F. L. Cozens, V. M. Kanagasabapathy, R. A. McClelland and S. Steenken, *Can. J. Chem.*, 1999, **77**, 2069-2082.

8. V. Dichiarante and M. Fagnoni, *Synlett*, 2008, 787-800.

9. P. Klán, T. Šolomek, C. G. Bochet, A. Blanc, R. Givens, M. Rubina, V. Popik, A. Kostikov and J. Wirz, *Chem. Rev.*, 2012, **113**, 119-191.

10. V. Ramamurthy, K. S. Schanze and Editors, *Organic, Physical, and Materials Photochemistry. [In: Mol. Supramol. Photochem., 2000; 6]*, Marcel Dekker, 2000.

11. V. Dichiarante, M. Fagnoni, M. Mella and A. Albini, *Chem. - Eur. J.*, 2006, **12**, 3905-3915.

12. Y. Zhu, C. M. Pavlos, J. P. Toscano and T. M. Dore, *J. Am. Chem. Soc.*, 2006, **128**, 4267-4276.

13. *Dynamic Studies in Biology: Phototriggers, Photoswitches and Caged Biomolecules*, 2005.

14. H. E. Zimmerman, *J. Am. Chem. Soc.*, 1966, **88**, 1564-1565.

15. H. E. Zimmerman, *J. Am. Chem. Soc.*, 1966, **88**, 1566-1567.

16. N. J. Turro, V. Ramamurthy and J. C. Scaiano, *Modern molecular photochemistry of organic molecules* / University Science Books, 2010.

17. N. J. Turro, *Modern Molecular Photochemistry*, Benjamin/Cummings Pub. Co., Menlo Park, California, 1978.

18. J. Michl, *Mol. Photochem.*, 1972, **4**, 243.

19. H. E. Zimmerman, *J. Am. Chem. Soc.*, 1995, **117**, 8988-8991.

20. D. R. Yarkony, *Chem. Rev.*, 2011, **112**, 481-498.

21. W. Domcke and D. R. Yarkony, *Annual Review of Physical Chemistry*, 2012, **63**, 325-352.

22. S. Gozem, I. Schapiro, N. Ferre and M. Olivucci, *Science*, 2012, **337**, 1225-1228.

23. B. Lasorne, G. A. Worth and M. A. Robb, *Wiley Interdisciplinary Reviews: Computational Molecular Science*, 2011, **1**, 460-475.

24. F. Bernardi, M. Olivucci and M. A. Robb, *Chem. Soc. Rev.*, 1996, **25**, 321-328.

25. D. R. Yarkony, *Rev. Mod. Phys.*, 1996, **68**, 985-1013.

26. M. A. Robb, M. Garavelli, M. Olivucci and F. Bernardi, *Rev. Comp. Chem.*, 2000, **15**, 87-146.

27. M. Klessinger, *Angew. Chem., Int. Ed. Engl.*, 1995, **34**, 549-551.

28. M. W. Schmidt, K. K. Baldridge, J. A. Boatz, S. T. Elbert, M. S. Gordon, J. H. Jensen, S. Koseki, N. Matsunaga, K. A. Nguyen, S. J. Su, T. L. Windus, M. Dupuis and J. A. Montgomery, *J. Comput. Chem.*, 1993, **14**, 1347-1363.

29. M. J. Frisch, G. W. Trucks, H. B. Schlegel, G. E. Scuseria, M. A. Robb, J. R. Cheeseman, G. Scalmani, V. Barone, B. Mennucci, G. A. Petersson, H. Nakatsuji, M. Caricato, X. Li, H. P. Hratchian, A. F. Izmaylov, J. Bloino, G. Zheng, J. L. Sonnenberg, M. Hada, M. Ehara, K. Toyota, R. Fukuda, J. Hasegawa, M. Ishida, T. Nakajima, Y. Honda, O. Kitao, H. Nakai, T. Vreven, J. A. M. Jr., J. E. Peralta, F. Ogliaro, M. Bearpark, J. J. Heyd, E. Brothers, K. N. Kudin, V. N. Staroverov, R. Kobayashi, J. Normand, K. Raghavachari, A. Rendell, J. C. Burant, S. S. Iyengar, J. Tomasi, M. Cossi, N. Rega, J. M. Millam, M. Klene, J. E. Knox, J. B. Cross, V. Bakken, C. Adamo, J. Jaramillo, R. Gomperts, R. E. Stratmann, O. Yazyev, A. J. Austin, R. Cammi, C. Pomelli, J. W. Ochterski, R. L. Martin, K. Morokuma, V. G. Zakrzewski, G. A. Voth, P. Salvador, J. J. Dannenberg, S. Dapprich, A. D. Daniels, O. Farkas, J. B. Foresman, J. V. Oritz, J. Cioslowski and D. J. Fox, *Gaussian 09, Revision A.02*, 2009.

30. M. Isegawa and D. G. Truhlar, *J. Chem. Phys.*, 2013, **138**.

31. B. Moore, II and J. Autschbach, *J. Chem. Theory Comput.*, 2013, **9**, 4991-5003.

32. D. Geissler, W. Kresse, B. Wiesner, J. Bendig, H. Kettnemann and V. Hagen, *Chembiochem*, 2003, **4**, 162-170.

33. R. H. Scott, J. Pollock, A. Ayar, N. M. Thatcher and U. Zehavi, *Sphingolipid Metabolism and Cell Signaling, Pt B*, 2000, **312**, 387-400.

34. A. Z. Suzuki, T. Watanabe, M. Kawamoto, K. Nishiyama, H. Yamashita, M. Ishii, M. Iwamura and T. Furuta, *Org. Lett.*, 2003, **5**, 4867-4870.

35. T. Furuta, S. S. H. Wang, J. L. Dantzker, T. M. Dore, W. J. Bybee, E. M. Callaway, W. Denk and R. Y. Tsien, *Proc. Natl. Acad. Sci. U.S.A.*, 1999, **96**, 1193-1200.

36. A. M. Piloto, S. P. G. Costa and M. S. T. Gonçalves, *Tetrahedron*, 2014, **70**, 650-657.

37. D. P. DeCosta, N. Howell, A. L. Pincock, J. A. Pincock and S. Rifai, *J. Org. Chem.*, 2000, **65**, 4698-4705.

38. V. Hagen, B. Dekowski, N. Kotzur, R. Lechler, B. Wiesner, B. Briand and M. Beyermann, *Chem.--Eur. J.*, 2008, **14**, 1621-1627.

39. A. Taniguchi, M. Skwarczynski, Y. Sohma, T. Okada, K. Ikeda, H. Prakash, H. Mukai, Y. Hayashi , T. Kimura, S. Hirota, K. Matsuzaki and Y. Kiso, *ChemBioChem*, 2008, **9**, 3055-3065.

40. M. A. O'Neill, F. L. Cozens and N. P. Schepp, *Tetrahedron*, 2000, **56**, 6969-6977.

41. J. A. Pincock and I. S. Young, *Can. J. Chem.*, 2003, **81**, 1083-1095.

42. R. H. C. H. A. Van, G. Lodder and E. Havinga, *J. Am. Chem. Soc.*, 1981, **103**, 7257-7262.

43. P. Wan, B. Chak and C. Li, *Tetrahedron Lett.*, 1986, **27**, 2937-2940.

44. D. Shukla and P. Wan, *Journal of Photochemistry and Photobiology a-Chemistry*, 1994, **79**, 55-59.

45. P. Wan, K. Yates and M. K. Boyd, *J. Org. Chem.*, 1985, **50**, 2881-2886.

46. L. Salem, W. G. Dauben and N. J. Turro, *J. Chim. Phys. Physicochim. Biol.*, 1973, **70**, 694-696.

47. W. G. Dauben, L. Salem and N. J. Turro, *Acc. Chem. Res.*, 1975, **8**, 41-54.

48. P. Neuhaus, D. Grote and W. Sander, *J. Am. Chem. Soc.*, 2008, **130**, 2993-3000.

49. A. Ouchi, Y. Koga, M. M. Alam and O. Ito, *J. Chem. Soc., Perkin Trans. 2*, 1996, 1705-1709.

50. P. Sebej, J. Wintner, P. Mueller, T. Slanina, J. Al Anshori, L. A. P. Antony, P. Klan and J. Wirz, *J. Org. Chem.*, 2013, **78**, 1833-1843.

51. A. M. Piloto, S. P. G. Costa and M. S. T. Goncalves, *Tetrahedron*, 2014, **70**, 650-657.

52. K. Krumova and G. Cosa, *J. Am. Chem. Soc.*, 2010, **132**, 17560-17569.

53. M. T. Whited, N. M. Patel, S. T. Roberts, K. Allen, P. I. Djurovich, S. E. Bradforth and M. E. Thompson, *Chem. Commun.*, 2012, **48**, 284-286.